

Developing New Methodologies for Electro-Organic Chemistry

A dissertation presented by

Diyuan Li

In partial fulfilment of the requirements for the award of the degree of

DOCTOR OF PHILOSOPHY

at

UNIVERSITY COLLEGE LONDON

Christopher Ingold Building
University College London
20 Gordon Street
WC1H 0AJ

Declaration

I, **Diyuan Li**, confirm that the work presented in this thesis is my own. Where information has been derived from other sources, I confirm that this has been indicated and acknowledged.

Abstract

Electro-Organic Chemistry has great potential to be used extensively in chemical synthesis but remains relatively under-exploited. To help expand this promising field of research, this PhD project was centred around developing new electrochemical methodology for use in organic reactions, particularly through activation of iodide ions and organic iodide compounds. The first research part is related to iodide ions: a dual electrochemical oxidative process in synthesizing the dihydrobenzofuran motif with excellent efficiency has been developed. This allowed for the formation of zinc ions and molecular iodine from a carbon anode in one pot followed by a zinc catalysed iodocyclisation of phenol and alkene. Related mechanistic studies indicate an unusual pathway which explains the selectivity of the reaction without the often-problematic electrophilic aromatic iodination of the aryl ring. Further extension of this newly developed method to aniline has led to a novel aziridine intermediate which ultimately yielded a diaminated product.

The second research part is related to the activation of organic iodide compounds. A newly developed electrochemical approach allows the generation of C-centered radicals for radical addition reaction and cyclisation. The yields and efficiency of the processes are superior in most cases to comparable conditions with tributyltin hydride. The use of air and electricity as the promotor combined with the aqueous reaction media make this a clean and 'green' alternative to these classic C–C bond forming processes. We have described the reaction mechanism in terms of electrogenerated reactive oxygen species which arises from the reduction of molecular oxygen in the aqueous phase. In addition, for easy and cheap access to this area and enable reactions that require for anhydrous conditions, we have successfully applied a supermarket purchased battery and UV light respectively as replacements of the roles of potentiostat equipment and oxygen in the methodology.

Impact Statement

The impact of this work will most likely be felt within academic spheres. The results of this project will be of importance to research chemists working in the field of organic synthesis and wishing to functionalise organic molecules. The emphasis on non-precious metals and use of non-toxic reagents will be of relevance to those concerned with developing sustainable and green synthetic routes. Furthermore, most electrochemistry in the literature has focused on using anodic oxidation reactions to effect synthetic transformations. Very little attention has been given to using reductive potentials to generate reactive oxygen species which then, paradoxically lead to oxidative functionalization of the organic species. We hope that this work may help to encourage more widespread adoption of electrochemistry in synthesis as it is currently an under-exploited area of research. We have also successfully applied the reaction with cheap supermarket purchased battery as replacement of expensive electrochemical equipment. This allows an easy and cheap access to this area for beginners. The work presented in this thesis also encompasses organometallic chemistry and catalysis, as well as biological, material and industrial pollutant treatment relevant contents like the reactive oxygen species. This means that the highly sustainable processes we have developed may also be of interest to these areas of academia and the chemical industry. Other academic impacts include the possibility of future collaborations on related work such as collaboration with biological chemists for protein manipulation and organometallic scientists for site selective C-H functionalisation. Such collaborations help to bridge the gap between the various disciplines and lead to exciting new results.

Outside of academia the impact of this work will most likely be centred around solving environmental issues. The hazards and difficulties of handling elemental halogens can be circumvented through the electrochemical generation of these species *in situ* and 'on-demand' and after reactions they could be reduced back to halides. Our developed metal-coated graphite electrodes and electrochemical metal recovery methodology may be used to minimise the heavy metal pollution of water as well as saving the industrial financial cost. This is because the metal may be released into solution in a specific oxidation state to catalyse a reaction, then recovered simply *via* reduction back onto the graphite rod in an immediately reusable form, saving money on catalyst waste and expensive recovery techniques.

The way in which these impacts may be brought about are primarily through the publication of this work in academic journals, as well as in the presentation of results at national and international conferences. We have already made a good start on this as we were fortunate to be able to publish 4 papers from the work in this thesis (D. Li, P. W. Seavill and J. D. Wilden, *ChemElectroChem*, 2019, **6**, 5829; D. Li, T. Ma, R. J. Scott and J. D. Wilden, *Chem. Sci.*, 2020,

11, 5333-5338; M. Anand *et al.*, *Faraday Discuss.*, **2021**, 29234 and T. Ma, D. Li and J. D. Wilden, *Chem. Commun.*, 2021, paper accepted) and present at several conferences.

Contents

Declaration.....	i
Abstract.....	ii
Impact Statement.....	iii
List of Abbreviations.....	vii
Acknowledgements.....	ix
Chapter 1. Introduction to Electro-Organic Synthesis.....	1
1.1 Electro-Organic Synthesis- Return of The Sustainable Methodology.....	1
1.2 Brief History of Electro-Organic Synthesis.....	1
1.3 The Challenges in Electro-Organic Synthesis.....	6
1.4 Methodology.....	7
Chapter 2. Dihydrobenzofuran Motif: The Start of Electrochemical Methodologies.....	17
2.1 Introduction.....	17
2.2 Electrochemical Iodocyclisation of the Dihydrobenzofuran Motif.....	18
2.3 Electrochemical generation of iodine and zinc ions in one pot.....	21
2.4 Mechanistic studies.....	29
2.4.1 Introduction to traditional iodocyclisation mechanism.....	29
2.4.2 Mechanistic study of iodocyclisation of 2-allylphenol.....	30
2.5 Cyclisation of 2-allylanalines.....	35
Chapter 3. Electrochemical activation of alkyl halides.....	40
3.1 Introduction of Traditional Giese Reaction.....	40
3.2 Traditional Electrochemical Reduction of Alkyl Halides.....	43
3.3 Indium mediated electrochemical indirect reduction of alkyl iodide.....	44
3.4 Electrochemical carbon centred radical formation mediated by arial oxygen ...	46
3.5 Extending the methodology to intramolecular cyclisation.....	51
3.6 Mechanistic study.....	52
3.7 Introduction of superoxide anion.....	54
3.8 Proposed Pathway 1.....	55
3.9 Introduction of Haber-Weiss cycle and Hydroxyl radical.....	60
3.10 Detecting hydroxyl radical by Photolumiscence spectroscopy.....	61
3.11 Electrochemical generation of ozone.....	67
3.12 Evidence for IOH participated in the reaction.....	69
3.13 Other mechanistic aspects.....	70
3.14 Extending the methodology to alkynes.....	72
3.15 Extending the methodology to redox-neutral intramolecular cyclisation.....	74
3.16 Trials with battery and Photo-electrochemistry.....	76
Chapter 4 Conclusions and future work.....	78

Chapter 5 Experimental	81
5.1 General Information (Chapter 2).....	81
5.2 Details of Electrochemical Methods (Chapter 2).....	81
5.3 Experimental Procedures (Chapter 2)	83
5.4 General Information (Chapter 3).....	91
5.5 Details of Electrochemical Methods (Chapter 3).....	92
5.6 Experimental Procedures (Chapter 3)	93
Chapter 6 References	103
Appendix: Associated Publications.....	110

List of Abbreviations

ATRA	Atom Transfer Radical Addition
CE	Counter Electrode
CI	Chemical Ionisation
CV (plot)	Cyclic Voltammetry plot
DCM	Dichloromethane
DMF	Dimethylformamide
DMSO	Dimethyl sulfoxide
EI	Electron Ionisation
EOS	Electro-Organic Synthesis
ESI	Electrospray Ionisation
eq	(Number of) Equivalents
<i>et al.</i>	<i>Et alia</i>
Fc or Fc⁺	Ferrocene or ferrocenium ion
HOMO	Highest Occupied Molecular Orbital
HRMS	High Resolution Mass Spectrometry
IR	Infrared
LRMS	Low Resolution Mass Spectrometry
LUMO	Lowest Unoccupied Molecular Orbital
<i>m</i>	<i>meta</i>
m.p.	Melting Point
NMR	Nuclear Magnetic Resonance
<i>p</i>	<i>para</i>
QRE	Quasi Reference Electrode
RBF	Round-Bottomed Flask
RE	Reference Electrode
REDOX	Reduction/Oxidation
ROS	Reactive Oxygen Species
RT	Room Temperature
SCE	Saturated Calomel Electrode
SET	Single Electron Transfer
THF	Tetrahydrofuran
TLC	Thin-Layer Chromatography
TMS	Trimethylsilyl (group)

UV
WE

Ultraviolet
Working Electrode

Acknowledgements

Firstly, I would like to thank my supervisor Dr Jon Wilden for his support and guidance over the last 3 years. He is such an intelligent, warm-hearted and helpful person that no achievement could be made without his mentorship and inspiration. It has really been a joy to adventure with him together on a completely new area as none of us had any real experience of beforehand. Throughout the journey, we have conquered lots of challenges and I believe the qualities that I learnt from them will also benefit my future life.

Secondly, I would like to thank all the good people that I have shared the lab with over the past years: Marc, Mira, Theo, Thibault, Raul, Chris, Kate, Reuben, Xuanxiao and Freeman. Special thanks to Marc for his patient guidance when I was just starting out; Peter for his longest warm accompany in the lab and the invaluable help that he provided; Theo for sharing his interesting church and football life with me and Reuben and Freeman for lightening the final times of my PhD.

Finally, I would like to thank the strong backing and support from my Family, especially my mom and dad, their love and encouragement leading my way to the light.

Chapter 1. Introduction to Electro-Organic Synthesis

1.1 Electro-Organic Synthesis- Return of The Sustainable Methodology

A rising awareness of 21st century challenges is revealed by current social media.¹ Accompanied by the increasing news of global natural catastrophe, discussions about climate change, limitations of fossil fuels and finite resources and the need for urgent changes are gradually gaining attention.¹ Such issues have already been identified by the scientific community who have been reconsidering chemical synthesis and are looking to establish sustainable techniques to contribute to the restriction of carbon emissions.¹

Amongst several other state of the art techniques, electro-organic synthesis is rising in popularity.¹ Electrochemistry represents one of the most direct and closest ways in which chemists can interact with molecules since the most fundamental forces in chemistry are the electrostatic attractions between electrons and nuclei.² Electrochemistry is naturally redox chemistry as it entails the addition or removal of electrons from such interactions through the direct application of an electrical potential.² Such ability has endowed it with the honour as one of the oldest explored forms of reaction setups in the laboratory.² After being neglected for several decades, this inherently sustainable methodology is now back, re-emerged for synthetic organic chemists, although this approach was already commonly adapted for inorganic transformations including industrial scale basic chemical production such as the using the Hall–Héroult process for chlor-alkali electrolysis and aluminium production.^{1,162}

1.2 Brief History of Electro-Organic Synthesis

The purpose of this part is to deliver the readers a general understanding of this research area including its origin, development and what has been done so far. Thus, here will firstly give a simplified timeline of historic milestones and some recent well known and representative works of electro-organic synthesis (**Figure 1**) which have been adapted from the work of the Baran group^{2,3} with general reaction schemes where necessary, detailed text description is given thereafter.

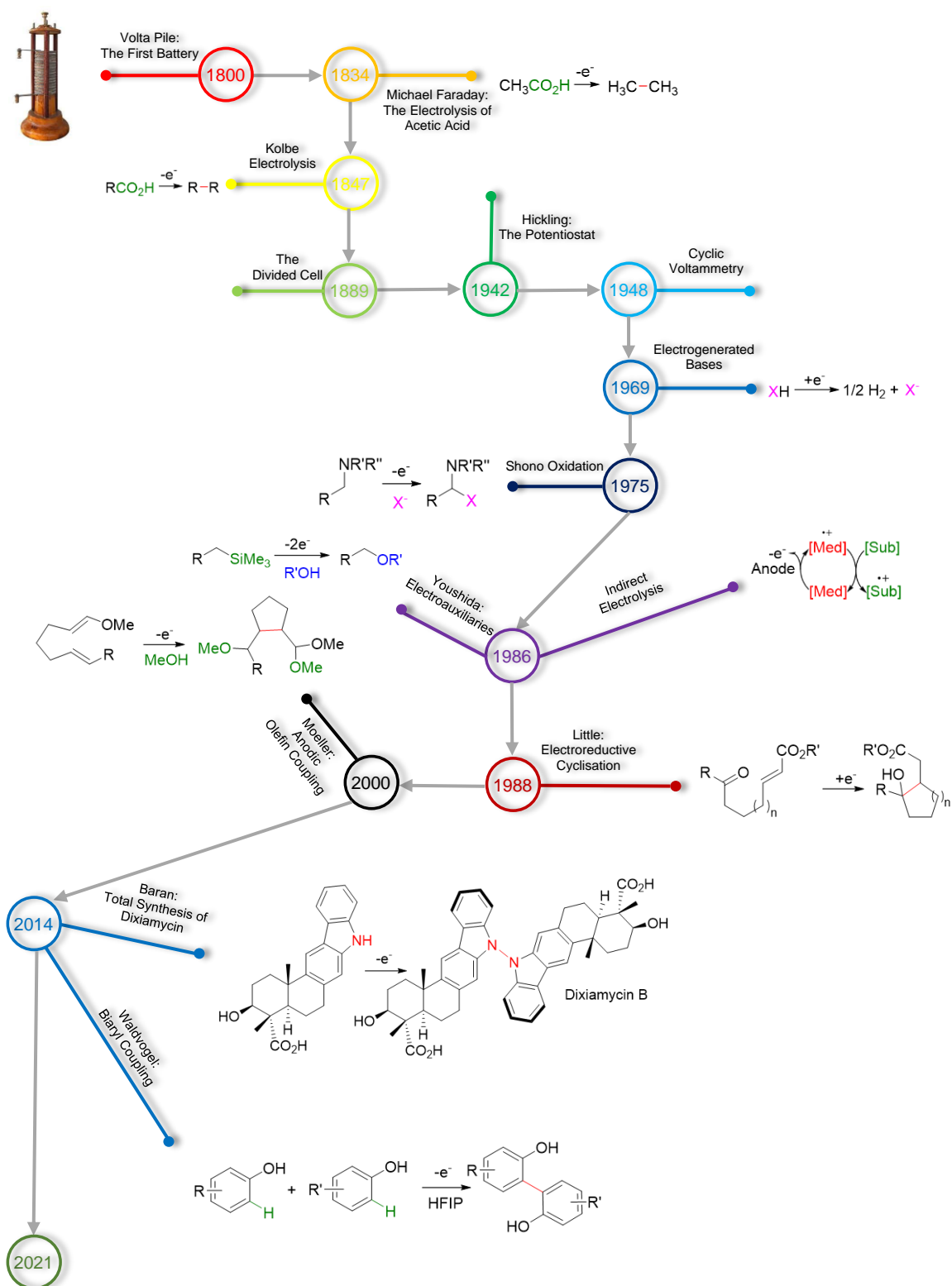


Figure 1: Timeline showing some of the history of Electro-Organic Chemistry from 1800-2021.²⁻¹⁷

The door of Electro-Organic Synthesis was opened in the year 1800 with the invention of the Volta Pile. As the first electric battery, the Volta Pile allowed a continual movement of electrons through a circuit for the first time.^{2,4} After three decades, with the fundamental breakthrough made by Michael Faraday, the world has advanced strides in understanding the nature of electricity. The popularised electrochemical terms such as electrolysis, anode and cathode, the observation of ions moving through electrolyte solutions and the development of Faraday's Laws of Electrolysis (as summarised in **Eq. 1** and has played a crucial role in the work carried out in this project)¹⁹ can all be attributed to Faraday's extensive studies.¹¹

$$n_M = \frac{Q}{zeN_A}$$

n_M = Number of moles of metal species
 Q = Charge passed
 z = Valency number of ions of substrate (**Eq. 1**)
 e = Elementary charge (1.602×10^{-19} C)
 N_A = Avogadro's number (6.022×10^{23} mol⁻¹)

The description of the electrolysis of sodium acetate which would later inspire the invention of the famous Kolbe electrolysis of carboxylic acids to produce alkyl radicals has secured Faraday's position as a pioneer of electro-organic chemistry.^{2,12} The Kolbe electrolysis is so useful that even in modern times there are still processes using Kolbe intermediates such as radical mediated 5-exo-trig type of cyclisation to form five membered rings reported by Lebreux (as shown in **Figure 2**).^{2,19}

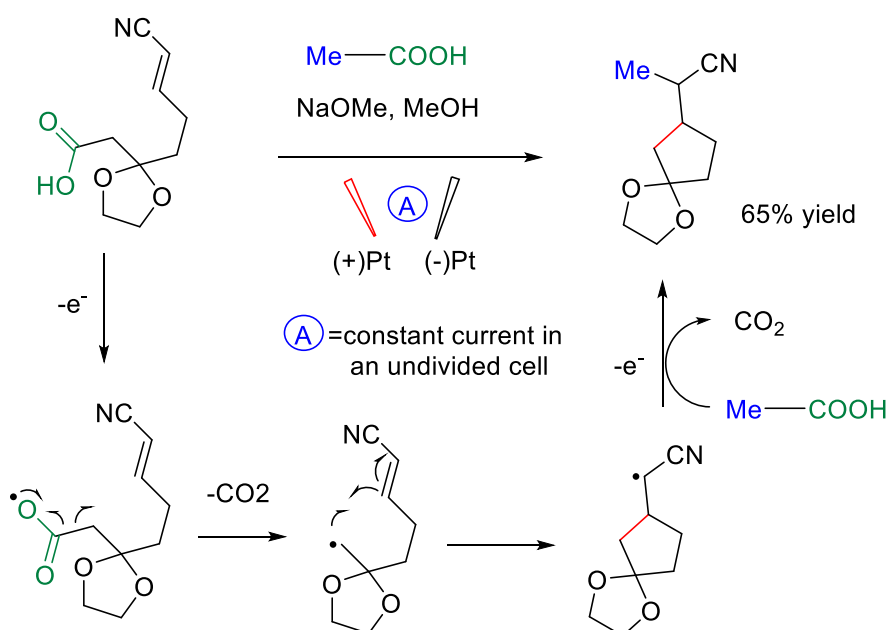


Figure 2. Cyclisation using mixed-Kolbe electrolysis strategy and a plausible mechanism^{2,19}

These early forays were all processed under the simplest prototypes of modern electrochemical setup which is now called 'undivided cell'² (as showing in [Figure 3A](#)): A power source is connected to a reaction mixture through an electrode where functionalisation could be processed when a reactive intermediate was generated through the electrolysis of the substrates. This electrode is known as the working electrode. However, as the circuit is still open, another electrode which is called the counter electrode is needed to add to the reaction and connected with the other end of the power source to complete the circuit.² However, due to the fact that the two electrodes are not separated, the high energy intermediates generated at the working electrode (whether as a cathode or anode) might be oxidized or reduced prematurely at its counterpart.²

This disadvantage was not overcome until 1889, when an early example of membrane electrolysis was described by Maigrot and Stabates, where in their research a divided cell was applied. In a divided cell, with the aid of semipermeable membrane which only allows small ions to pass through it ([Figure 3B](#)).² As such anodic and cathodic reactions could be stopped from interfering with each other.

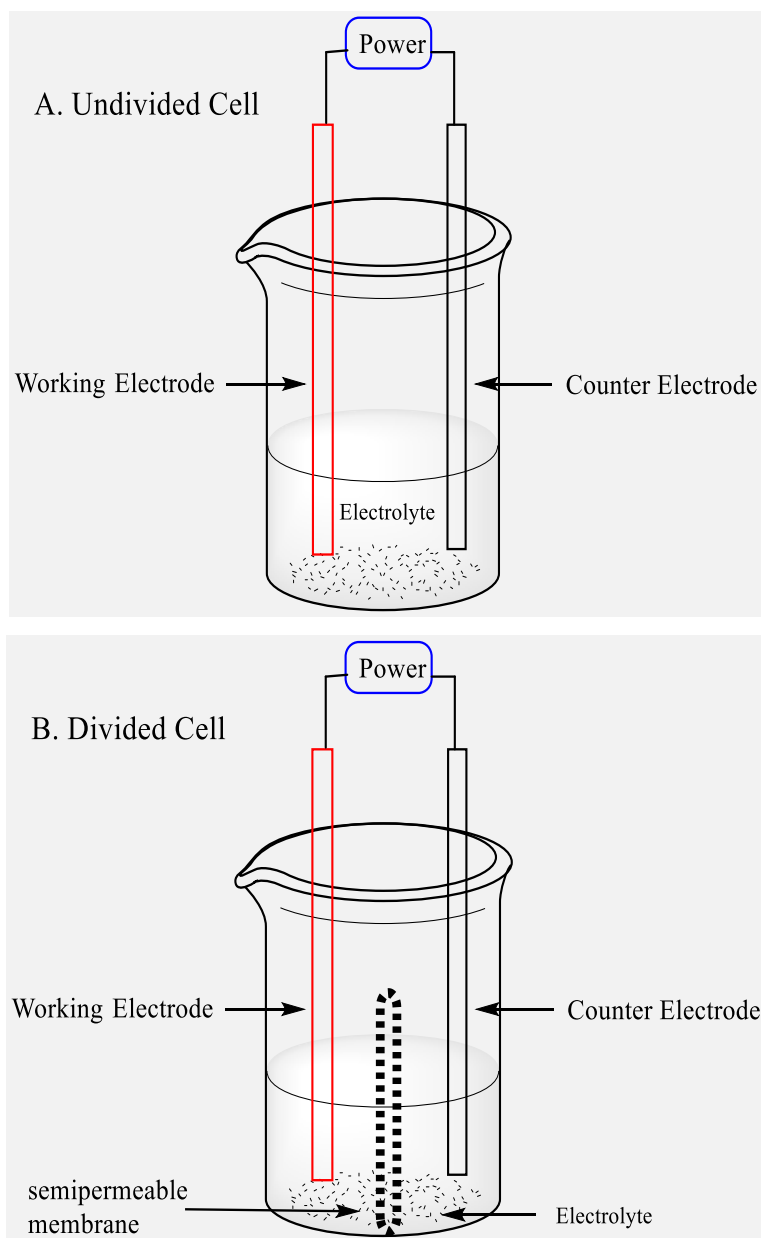


Figure 3. (A) Schematic undivided cell set-up; (B) Schematic divided cell set-up.²

Another ground-breaking stride in the electrochemical apparatus is Hickling's epochal invention in 1942, the potentiostat, which allowed reactions to be carried out under constant potential conditions, achieved by compensatory reduction of current over time.^{2,14} This invention has ended the situation of the 19th century where electrosynthesis could only rely on galvanostatic conditions where the reaction mixture is subjected to a constant stream of current and the potential increases over time.² With further assistance from Randles, who in 1948 reported the world's first cyclic voltammetry experiment which allowed the accurate determination of redox potentials for various specific functional groups and remains to this day

an essential technique in an electrochemist's repertoire.^{2,15} (there are two kind of CV conventions shown below in **Figure 4**,²⁰ the IUPAC convention is used herein), potentiostat, this new dimensional technique of electrochemistry has enabled selective manipulation of functional groups by 'dialing in' these measured properties from cyclic voltammetry.² In potentiostatic setups, Ag/Ag⁺ or saturated calomel electrode is commonly used as a standard electrode to accurately gauge the potential at the working electrode.²

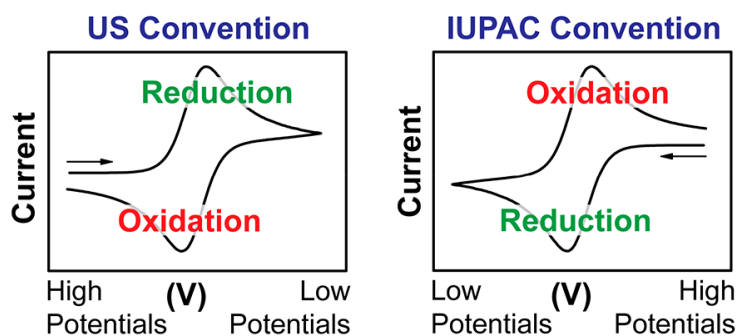


Figure 4. Two CV conventions images from journal of chemistry education.²⁰

Except for these exciting early-aged works in organic-electrosynthesis, many major synthetic developments using electrochemistry have been made within the last 60 years.^{2,3} Notable examples include the electrochemical generation of bases reported by Lund in 1969,¹⁶ the development of the α -functionalisation of alkyl amides in 1975 (which is also called the Shono oxidation)¹⁷ and the promotion of other REDOX reactions using mediators which represented the formalisation of the principles of indirect electrolysis.⁵ Besides, within the last three decades, a series of excellent works in electro-organic synthesis have been reported by names such as electroreductive cyclisation (Little),⁶ anodic olefin coupling (Moeller),⁷ the electroauxiliaries using S and Si (Yoshida),⁸ the total synthesis of dixiamycin (Baran)⁹ and biaryl coupling (Waldvogel),¹⁰ as well as many others. These works have helped to promote the field of electro-organic synthesis and popularise electrochemistry as a strong force in state-of-the-art modern synthesis.

1.3 The Challenges in Electro-Organic Synthesis

Despite these great advantages of electro-organic synthesis introduced before, there are still some barriers obstructing its wide adoption in modern synthetic labs²:

- (1) Lack of standardisation electrochemical equipment with many set-ups been 'home-made'. This introduces a lot of variability between groups and leads to a lack of reproducibility of results. This problem is slowly beginning to be addressed with the development of purpose-built electrochemistry kits that can be used in synthetic laboratories,^{2,21} but it will take some time before such equipment becomes standard issue. This is a significant problem in electro-organic synthesis and thus warrants expression, however the focus of this PhD project was on synthetic methodology rather than mechanical concerns and so that is where the discussion will continue.
- (2) Daunting mathematical treatments applied in the electrochemical literature.²
- (3) Only a limited number of notable transformations have been discovered.²

Although there are still so many difficulties, the significant advantages of widely using electrosynthesis method compared with its traditional counterparts are encouraging us to embrace and conquer these challenges. Electro-organic chemistry is now waiting for a renaissance.²

1.4 Methodology

The experimental work carried out in this project is very often electrochemical in nature, despite the reactions themselves being firmly based in organic chemistry. Hence, various characteristics of the equipment and methods used still need to be further explained.

In general, the work-up and purification parts of reactions described in this report remain 'organic' in nature, in that they do not differ from standard organic chemistry practices and so require no further discussion here. The major difference from a standard organic reaction lies in the use of electrodes and electrolyte solutions. This allows electrons to be given to, or taken away from compounds in solution, thus allowing reactions to take place. In other words, this facilitates REDOX chemistry.

Figure 5 shows the apparatus and example electrodes used to carry out reactions in either an undivided cell or a divided cell. The major components in all setups are: i. an electrolyte solution which is a charged species dissolved in a solvent that shuttle charges between electrodes (e.g. LiClO_4 dissolved in MeCN), ii. electrodes that rest in the electrolyte solution and conduct electrons to or from the potentiostat, iii. a potentiostat, iv. a reaction vessel or cell (divided or undivided).

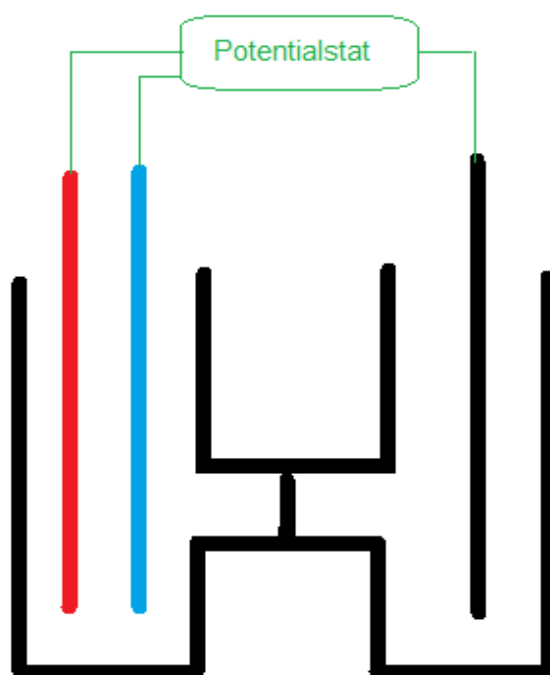


Figure 5a Picture and graphic of divided H cell.

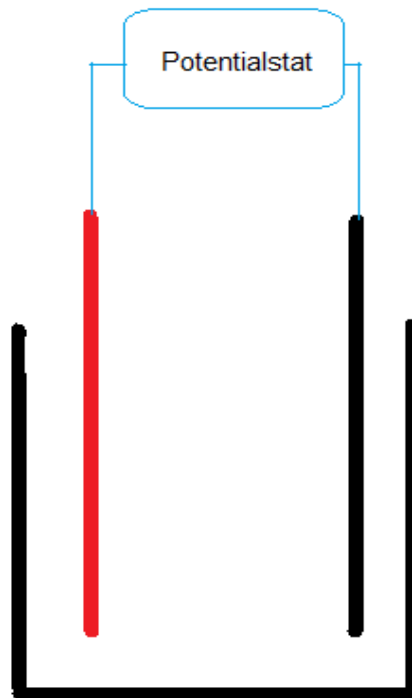


Figure 5b Picture and graphic of undivided two electrode cell

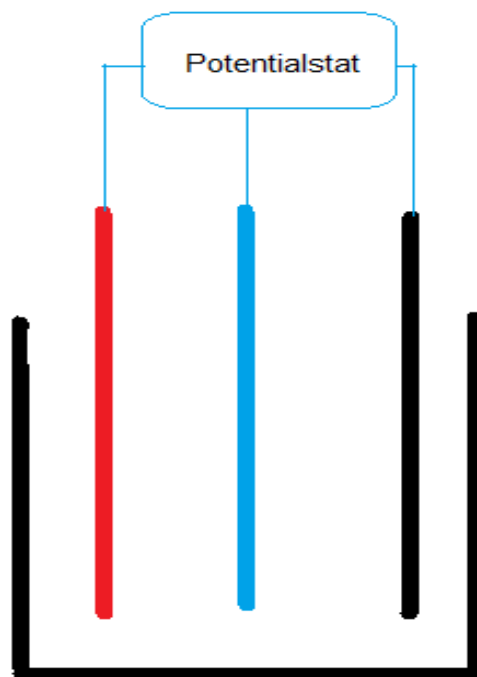


Figure 5c Picture and graphic of cyclic voltammetry setup.

Figure 5a is the real set-up of a divided H cell with a graphic: The red line and blue line in the

left chamber represent the working electrode and reference respectively, the black line is the counter electrode. The heating bowl in the bottom with sand was used for heating the reaction. Similarly, the two pictures in **Figure 5b** are the set-up and its graphic of an undivided reversible two electrode cell: red line is the WE while black line is both RE and CE. The cyclic voltammetry equipment is showing on **Figure 5c**: glassy carbon (red) as the WE, silver (blue) as RE and Pt (black) as CE. Furthermore, the zinc coated electrode that prepared for the reactions in chapter 2 were also produced using the similar setup in **Figure 5c** that only WE and CE need to be replaced with graphite electrode and zinc sacrificial electrode, respectively. **Figure 6** is the outlook of a zinc coated graphite. The difference between the two types of cells is simply whether the working electrode and the counter electrode are separated or not. This separation is easily achieved using an H cell, because it has a chamber either side of a sintered glass semipermeable divider. The semipermeable divider is designed to prevent the mixing of the solutions that are in each chamber, but still allow small ions through to carry charge and complete the circuit.



Figure 6 Zinc coated carbon electrode

Since the undivided cell and coating cell are just normal three necked round bottom flask and beaker, we do not need to introduce its dimensions specifically. For the divided 'H' cell as our reaction vessel (dimensions shown in **Figure 7**) with each chamber having a size B19 ground-glass neck and a total volume of 30 mL. A semiporous sintered glass divider sits between each chamber. Where graphite electrodes were used for the working-electrode and counter electrode, rods of 5 mm diameter were used at a depth of 25 mm giving an effective area of

412 mm². A silver wire, which was 1 mm thick, was used as a quasi-reference electrode and was likewise placed into solution to a depth of 25 mm giving an effective area of 79 mm². One graphite and the silver wire were placed into the same chamber to minimise the potential drop deriving from resistance and kept 10 mm apart. Another graphite was used as the counter-electrode and placed in the other chamber of the H cell. Reactions were run using an Ivium Technologies Vertex model potentiostat operating in chronoamperometry mode. This mode provides real-time charge over time and current over time graphs for measuring the total charges passed over the course of reaction.

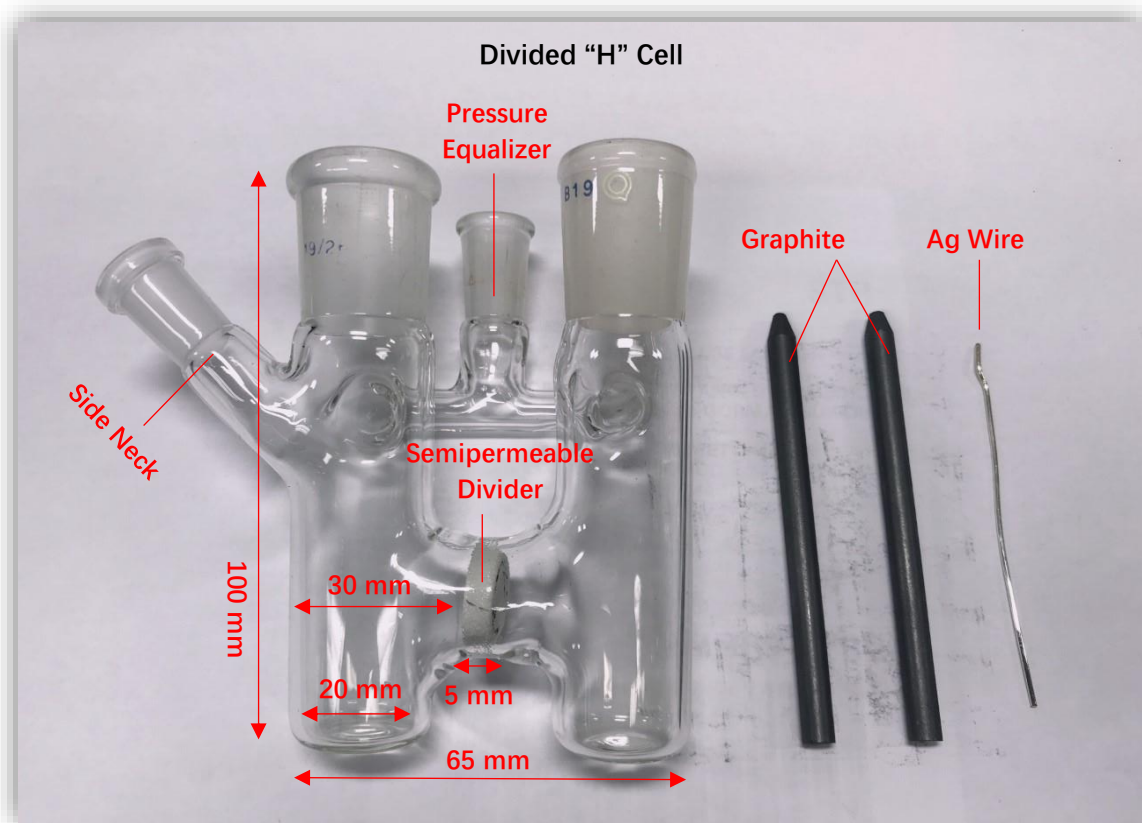


Figure 7 Dimensions of a divided 'H' cell as our reaction vessel

A three-electrode system which involves a working electrode (WE), a reference electrode (RE) and a counter electrode (CE) is typically used for electrochemical experiments to ensure that current only flows between the working electrode and the counter electrode and that the potential of the working electrode is measured relative to that of the reference electrode. Normally, the RE is comprised of species in equilibrium which have a well-defined electrode potential, such as Ag metal and AgCl in an aqueous solution (the AgCl reference electrode). The equilibrium and resulting potential at the interface remain constant as the RE draws negligible current and hence its composition is unchanged during the measurement.

The reference electrode is used as a means of replication of experimentation across different setups and equipment because any applied potential is compared against this reference. In other words, if the potential is set to -1.0 V on the potentiostat, there will be a potential difference of -1.0 V between the WE and the RE. In a divided cell, the potential drop caused by resistance from keeping the electrodes far apart is limited by keeping the working electrode and the reference in the same chamber. During this project we elected to use an Ag wire on its own as a Quasi-Reference Electrode (QRE) instead of using a full reference electrode. This was not only for convenience but also because there are few universal reference electrodes that are suitable for non-aqueous solvents. Ag had the benefit of being a very malleable electrode which did not interfere with other components of our experimental apparatus but had the drawback of not being a rigorously accurate reference, as a well-defined equilibrium may not have existed at its interface during reactions. This meant that the potential of the QRE was sensitive to changes in solution composition and could drift over time. Generally, such QREs maintain a constant potential during a measurement if the solution composition or the area in contact with solution does not change too much. However, their potential can vary between different experiments if carried out on different days. To overcome this, we employed ferrocene as an internal reference to measure potentials in Cyclic Voltammetry (CV) plots as discussed later in this chapter. This is a standard calibration procedure that is commonly carried out for electrochemical measurements in non-aqueous electrolytes.

The working electrode is used to deliver the potential or current the potentiostat is set to. This can be a constant potential, chronoamperometry (also known as bulk electrolysis), or a constant current, chronopotentiometry.²² In this project, chronoamperometry was exclusively used because we believe it allowed for more precise selectivity over which reagents were oxidised and reduced than chronopotentiometry. A constant current experiment will move through a range of potentials, which can allow a range of reactions to take place. The current essentially controls the rate of reaction. Potential is more akin to how much energy is needed to move the electrons. Another method that can be used to perform electrochemical reactions is switching current electrolysis in which pulses of differing currents are applied. This can be useful for switching the polarity of the WE to remove precipitates that may foul the surface of the electrode throughout a reaction. This technique is quite rarely used in the literature compared to chronoamperometry and chronopotentiometry and as such its applications in organic synthesis are limited.²³ The counter electrode opposes the working electrode by maintaining an equal but opposite current to keep charge flowing around the circuit.

A potentiostat can deliver oxidative and reductive potentials to reaction mixtures, which promotes REDOX chemistry. An applied oxidative potential, with enough energy, will remove electrons from the HOMO of certain chemical species such as oxidation, and an applied reductive potential with enough energy will donate electrons into the LUMO such as reduction. Electrons are drawn into the anode and given out from the cathode. Notably, anode/anodic oxidation and cathode/cathodic reduction are often used as nomenclature in the literature. An electrode with an oxidising potential is the anode and an electrode with a reductive potential is the cathode.²⁴⁻²⁸

To determine the potential that will be applied in reactions, a crucial technique that is often employed is to record a CV plot of the reagents in question. This technique involves using a potentiostat to measure changes in current as the potential is altered incrementally. This creates certain peaks when a species is oxidised or reduced as an increase in current accompanies these REDOX processes, and these peaks indicate what potential is best to use in a reaction to achieve REDOX of the reactive species in question. As ferrocene is a kind of species that could produce typical and clear pair of REDOX peaks, here we use ferrocene as an example to illustrate CV plot and **Figure 8** shows a CV plot of ferrocene recorded in the Wilden group.

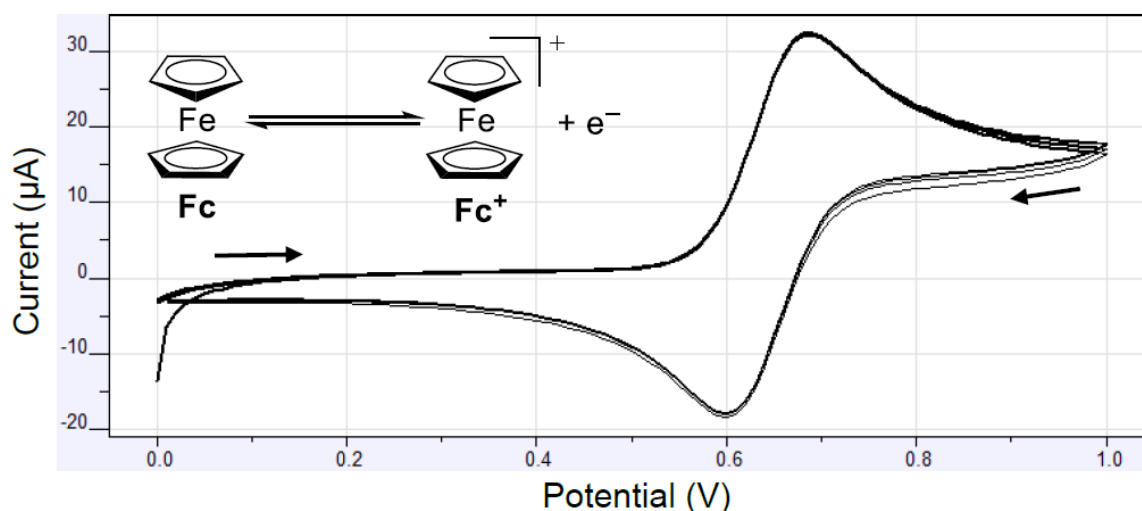
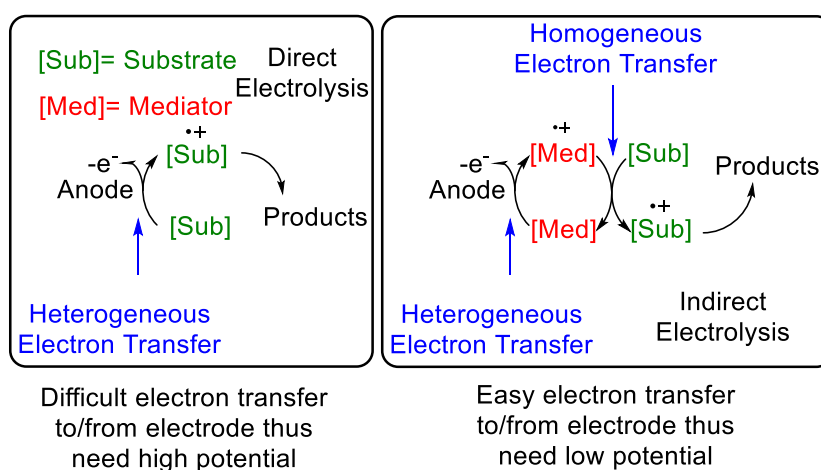


Figure 8: Showing a CV plot of ferrocene recorded in 0.1 M Bu₄NPF₆ / MeCN using a glassy carbon WE, Ag QRE and Pt CE.

It is clear from the CV plot of ferrocene that when the potential is increasing towards a more positive direction from 0 V, a peak was formed which referring to the oxidation of ferrocene (Fc) to the ferrocenium ion (Fc⁺), Fe²⁺ to Fe³⁺. On the reverse scan, when reduction of the

ferrocenium ion back to ferrocene happened, a negative peak appears where this is reversed. The oxidation and reduction peaks appear very similar in magnitude, which indicates a highly reversible process. If only an oxidation or a reduction peak were present, with no REDOX couple, then this would indicate an irreversible process has taken place.

Using CV plots to measure the potential at which oxidation and reduction occurs is very useful and indeed, due to the very clear, characteristic and well-defined nature of the ferrocene REDOX couple, ferrocene is actually used as an internal reference, against which other potentials are measured (as shown in this report and quoted as 'vs Fc/Fc⁺').²⁹⁻³¹ Furthermore, because ferrocene has a stable and highly reversible REDOX couple it is often employed as a mediator in electrochemical reactions (**Scheme 1**). Sometimes, direct electrolysis of a substrate can be very difficult. This is caused by the heterogeneous electron transfer process to/from an electrode having slow kinetics. The activity that organic species adsorbing to the surface of electrodes and forming layers could hinder the conductivity to the bulk solution. In these cases, a mediator that is stable in both oxidation states may be used to help more efficient electron transfer processes with an electrode than the direct electrolysis of the substrate. The mediator can then efficiently, homogeneously transfer electrons to/from the substrate, facilitating the reaction at lower REDOX potentials than would be required for direct electrolysis. A fast, irreversible follow-up reaction for the electrolysed substrate to the desired product is usually necessary to achieve this effect.²³ Again, Ferrocene as well as some other species such as triphenylphosphine and nickel salen can be used as the electron shuttle for indirect electrolysis.



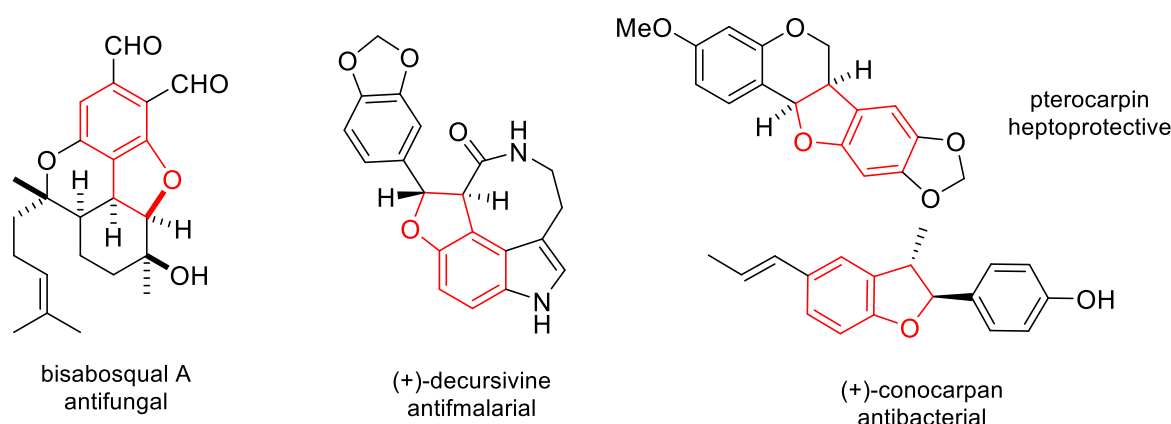
Scheme 1: A situation in which indirect electrolysis facilitated by a mediator may be preferred over direct electrolysis.²³

When carrying out reactions, and producing CV plots, an electrolyte solution must be used. These solutions are very often 'inert' in the sense that the salts used are relatively stable and would require high applied potentials to enable any sort of REDOX. This allows the electrolytes to simply carry charge in solution without interfering with experiments. Sodium triflate or LiClO_4 are two commonly used electrolytes, which are dissolved in standard organic solvents. However, other (non-inert) electrolyte salts can purposefully be used to enable reactions to take place.

Chapter 2. Dihydrobenzofuran Motif: The Start of Electrochemical Methodologies

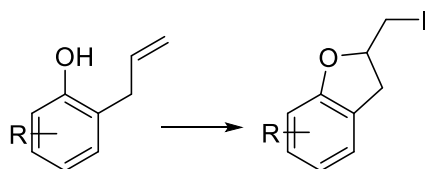
2.1 Introduction

Being new to the area, I wanted to explore some simple but synthetically useful electrochemical transformations in the first instance. Despite its simple structure, the dihydrobenzofuran motif is an important framework in a variety of natural products and drug substances and as such, rapid and efficient processes for the construction of substituted variants *via* the construction of the bicyclic nucleus are synthetically valuable (some examples are given in [Scheme 2](#)).³²



Scheme 2: Examples of natural products containing dihydrobenzofuran motif.³²

Thus, the dihydrobenzofuran motif was chosen as our first synthetic target. Iodocyclisation of alkenes with oxygen nucleophiles is a powerful method of generating dihydrobenzofuran frameworks that maintain the iodine functionality and thereby allow further manipulation.³³⁻³⁷ However, surprisingly, examples of iodocyclisation of phenols onto alkenes are rarely found in the literature at that time. The few known examples are summarised in [Scheme 3](#).^{38,39}



		Catalyst	R	Time	Yield
Wakharkar	0.5 eq. I ₂ , MeOH, reflux	20% w/w EPZ-10	H	35 min	85%
Wakharkar	0.5 eq. I ₂ , MeOH, reflux	0.5 eq. ZnCl ₂	H	35 min	80%
Wakharkar	0.5 eq. I ₂ , MeOH, reflux	20% w/w EPZ-10	4-CH ₃ CO	30 min	86%
Wakharkar	0.5 eq. I ₂ , MeOH, reflux	0.5 eq. ZnCl ₂	4-CH ₃ CO	30 min	85%
Wakharkar	0.5 eq. I ₂ , MeOH, reflux	20% w/w EPZ-10	4-OMe	30 min	84%
Wakharkar	0.5 eq. I ₂ , MeOH, reflux	0.5 eq. ZnCl ₂	4-OMe	30 min	75%
Orito	1.0 eq. I ₂ , CH ₂ Cl ₂ , r.t.	0.5 eq. SnCl ₄	H	24 h	72%

Scheme 3: Examples of iodocyclisation of phenols onto alkenes.^{38,39}

In the above examples, molecular iodine and metal catalyst were used for the iodocyclisation of 2-allylphenols. However, for industrial process development, applying these traditional methods face issues of handling of toxic metal catalysts and stoichiometric amounts of iodine. Thus, the development of a green and sustainable alternative method using electrochemistry would be welcomed by the synthetic chemistry community.

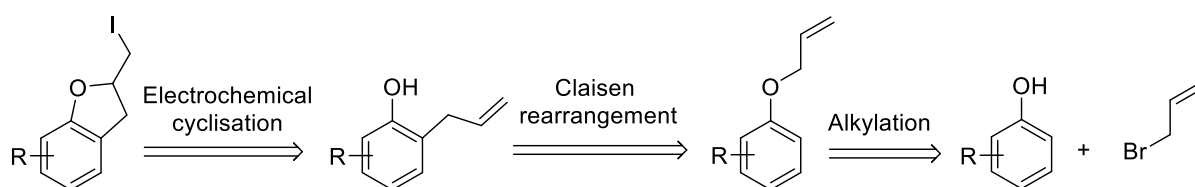
2.2 Electrochemical Iodocyclisation of the Dihydrobenzofuran Motif

Halogens have been widely used in organic synthesis while the hazards and difficulties of handling elemental halogens remain a significant issue. Luckily, this issue can now be circumvented *via* electrochemical generation of these species *in situ*, without a direct operator having to handle stoichiometric quantities of the elemental forms. The electrochemical approach even provides a possibility to reverse the excess of halogen back into halide.

Metal ions also play an important role as catalysts in organic synthesis. However, catalysts containing metal ions, to some extent, are not that environmentally friendly and easily contaminate water (eg. ZnCl₂ is toxic and harmful to aquatic life, its dust is also harmful to the operator. Furthermore, it is notoriously hygroscopic which can cause difficulties in some reactions). Hence, generating metal ions purely without introducing anion counterpart from

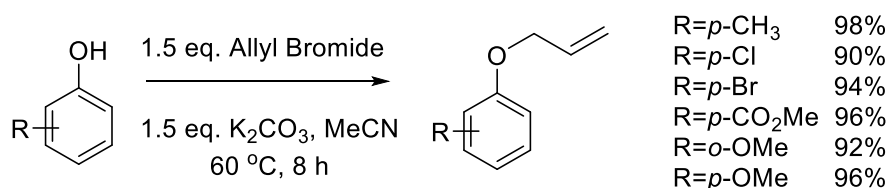
cheap and non-toxic metal with the support of electricity is an attractive promising application of electrochemistry. In addition, electrochemical control can also provide the possibility of controlling the oxidation state of the metal ions released. With former experience of *in situ* recovering metal additives *via* electrochemistry of my group,¹⁸ I aimed to employ zinc and iodine as the reaction reactive species, both generated with the aid of electrochemistry. We reasoned that both zinc ions and molecular iodine could be produced from less toxic zinc metal (as a sacrificial anode) and a simple iodide salt. After the reaction, zinc ions could potentially be recovered and iodine could be reduced to iodide. As such, all toxic and reactive species would be generated *in situ* and avoid handling outside the cell. Based on that, the problems outlined in introduction part could be circumvented.

After retrosynthetic analysis (**Scheme 4**), we then focused on the two steps of synthesising 2-allylphenols from phenols.



Scheme 4: Retrosynthesis of iodocyclised product

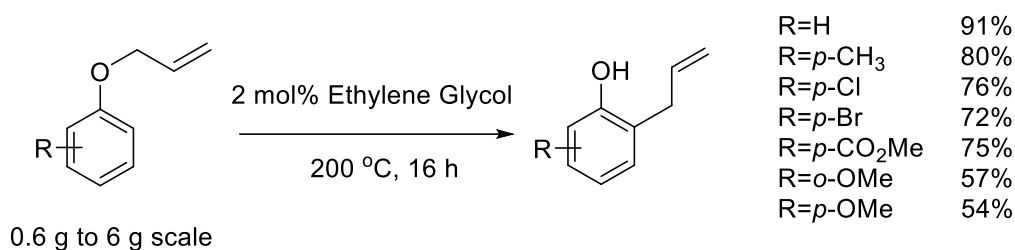
The first step was the alkylation of phenols which is very efficient after 8 hours' reaction. Six examples were prepared from different phenols bearing both EWG and EDGs to broaden the scope. In all cases, high isolated yields were obtained (**Scheme 5**).



Scheme 5: General procedure of producing O-allylphenols

For the second step I firstly turned to the classic Claisen rearrangement to deliver the required 2-allylphenols for our study. Although this reaction is known to proceed in good yields under various conditions at high temperatures (>190 °C), in our hands we found these procedures capricious and often inconvenient (and not amenable to scale up synthesis). We found

however, that the reaction could be promoted smoothly and in good yields at the 'standard' temperature of 200 °C by the addition of a small quantity (2 mol% measured by volume) of ethylene glycol (**Scheme 6**).



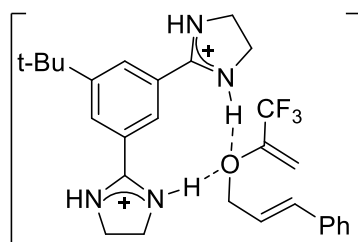
Scheme 6 General procedure of producing 2-allylphenols

Table 1 Control reactions that demonstrate the catalytic ability of ethylene glycol in Claisen rearrangement

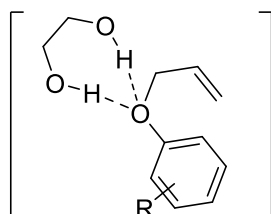
Entry	Starting Material (Scale)	Ethylene Glycol	Temperature (°C)	Reaction Time (h)	2-allylphenol Isolated Yield (%)
1	Allyl phenyl ether (3 g)	0	100	72	0
2	Allyl phenyl ether (3 g)	2 mol%	100	16	33
3	Allyl phenyl ether (3 g)	2 mol%	200	16	91
4	O-allyl guaiacol (4 g)	2 mol%	200	16	57
5	O-allyl guaiacol (4 g)	0	200	72	21

In **Table 1**, entries 1 and 2, 4 and 5 prove that even 2 mol% (measured by volume) of ethylene glycol could catalyse the rearrangement of large quantities of O-allylphenols. Entry 2 and 3 showing that although ethylene glycol did dramatically increase the yield, high temperatures are still required to maintain high yields. Crucially, no solvent is required meaning that the

reaction can be carried out on a multigram scale with relative ease. Such catalysis might be explained by the formation of dual H-bond between the phenol oxygen and the protons of the two OH group in the ethylene glycol. There is already a related report describing the use of hydrogen bond donors such as bisamidinium catalyst to promote this traditional reaction (**Scheme 7**).⁴⁰ Since that report has already described the same role of water and alcohol as hydrogen bond donors in the Claisen rearrangement as well,⁴⁰ it is reasonable to believe that the ethylene glycol might do similar work in my reaction (**Scheme 8**), although the mixture of ethylene glycol and O-allylphenol has not been monitored by NMR.



Scheme 7 Literature discovered bisamidinium catalyst formed intermediate.⁴⁰



Scheme 8 Proposed ethylene glycol formed dual H bond intermediate.

2.3 Electrochemical generation of iodine and zinc ions in one pot

Following successful preparation of allylphenols, in order to develop our process, we first needed to establish the electrochemical conditions required for: (i) oxidative release of Zn^{2+} from the zinc sacrificial anode; (ii) oxidation of NaI to molecular iodine. Since the standard reduction potential of Zn^{2+} is significantly lower than for I_2 (-0.76 V vs +0.54 V vs SHE) we realised that any potential required to oxidise NaI would first oxidise the zinc and would allow us to generate both species in a single reaction vessel using a constant potential. Accordingly,

we examined a solution of NaI using cyclic voltammetry (CV) to determine the potential that would be required to generate the halogen. Glassy carbon was used as working electrode while silver wire and platinum wire were used as reference and counter electrode, respectively. The results are shown in **Figure 9**.

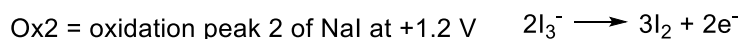
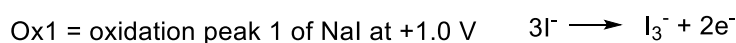
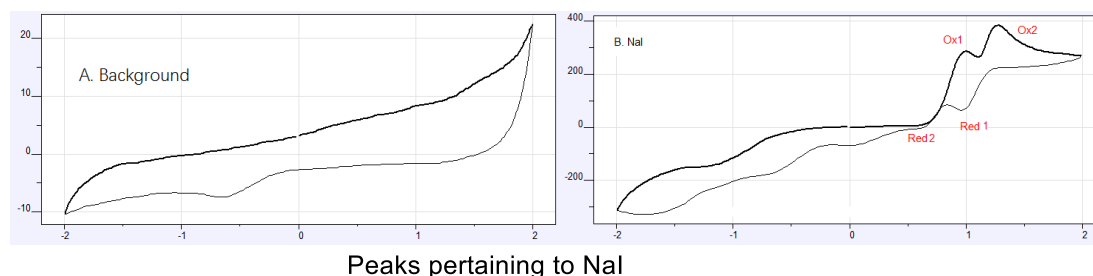


Figure 9 Showing the CV plot of NaI recorded in 0.3 M LiClO₄ in MeCN, X axes = potential (V), Y axes = current (μA).

Figure 9A shows the background with only 0.3 M of LiClO₄ in 10 mL of MeCN. The solvent was degassed for approximately 10 min under argon before the measurement, this is because atmospheric oxygen might be reduced and affect the accuracy of measuring redox peak.

Figure 9B shows the CV plot of NaI added to the background solution. There are several features worthy of note: Firstly, the Ox1 corresponds to Red2 and Ox2 corresponds to Red1, the first pair of redox peaks correspond to the oxidation of three I⁻ to I₃⁻ and the second pair are most likely to be the fully conversion from I₃⁻ to I₂ as shown.

According to the CV plot, +1.2 V was chosen as the setting potential for the reaction of generating iodine in order to limit the transformation stage at I₃⁻. Since I₃⁻ and I₂ / I⁻ are in equilibrium, we reasoned that this would deliver a low concentration of I₂ which would be sufficient to allow the ring formation to occur but not generate unwanted side products, eg. halogenation of the activated aromatic ring.

With the appropriate oxidative potential in hand, we firstly targeted using an undivided cell setup to process our reaction. As described earlier, an undivided cell is the simplest setup of electrolysis, with working and counter electrodes reside in the same chamber. To do that, we use a pure zinc metal plate as the anode, silver wire as reference and graphite as the counter

electrode. However, this setup did not provide us with any iodocyclised product. Instead, we did not believe that iodine was being generated in sufficient quantities to cause the desired reaction to occur. We have attributed the failure to the fact that, zinc metal is not only easier to oxidise than iodide, but molecular iodine could also react directly with the zinc anode.

Following this failure, we came up with the idea of 'reverse electrode electrolysis' to tackle this problem. Although this concept has not been reported before in the literature, it is very simple to apply with the aid of electrochemical equipment. To be more precise, we just to need to switch the role of anode and cathode, with zinc metal plate first acts as the anode for 30 seconds by applying with a positive potential (+1.2 V), then the zinc metal plate will act as the cathode for another 30 seconds when it is hit with a negative potential (-1.2 V). Finally, zinc plate is switched to anode again and such process will be repeated over night. When zinc plate is working as the anode, only zinc ions will be produced and released to the solvent system. However, during the periods that zinc plate as the cathode, iodine could be produced at the graphite electrode, which is unreactive towards the generated iodine. With such strategy, zinc ions and iodine could be produced in one pot (Figure 10).

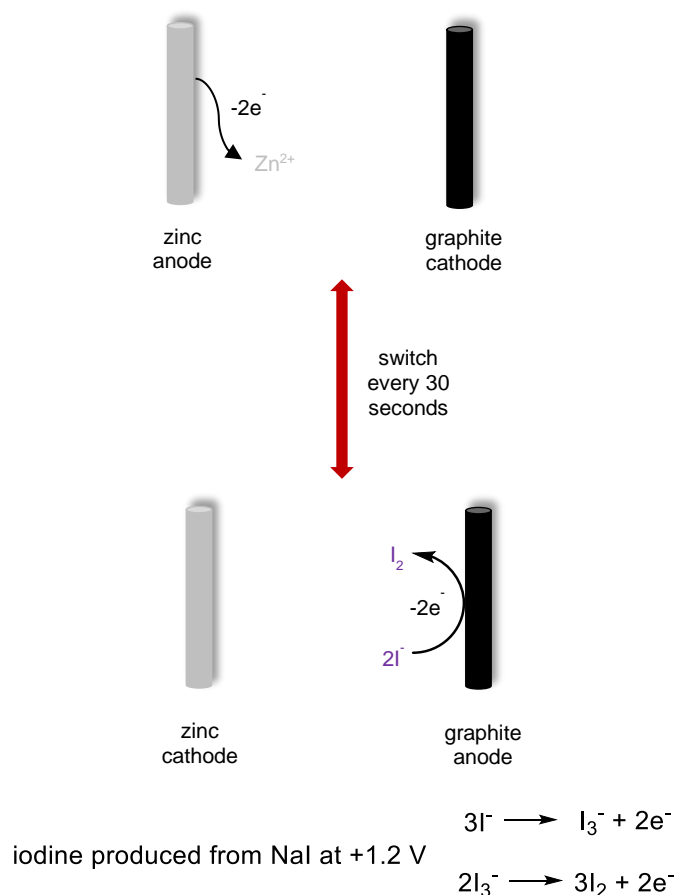


Figure 10 Schematic diagram of 'reverse electrode electrolysis'.

Pleasingly, this setup has successfully provided us with the final iodocyclised dihydrobenzofuran product at 50% isolated yield. However, following optimisation of this method have revealed to us that this setup has a fatal weakness, which is also the typical weakness of undivided cell towards those redox reversible active species. Scenarios can arise where high energy intermediates generated at the working anode are prematurely reduced at the cathode and *vice versa*. Here as zinc metal is in an excess, the iodine generated would be partially reduced by it, competing with the desired cyclised process. After several trials such as adjust the reverse time distributed to the electrode, increase reacting temperature and modification of the distance between the two electrodes, the yield of the product was still fixed at around 50%. We finally decided to abandon this set up, and the idea of using a zinc coated carbon working electrode with a divided “H-cell” was envisaged. A divided cell where anodic and cathodic chambers are segregated by a partially permeable membrane or a salt bridge could overcome the issue of the yield block at the undivided cell, while zinc coated carbon is an alternative to the reverse electrode electrolysis strategy.

The concept of metal coated carbon origins from electroplating, which is the general name for process that uses a reducing current to dissolve metal cations from a metal sacrificial anode followed by form a thin coherent metal coating on an electrode.⁴¹ The current is provided by an external power supply.⁴¹ (Figure 11)

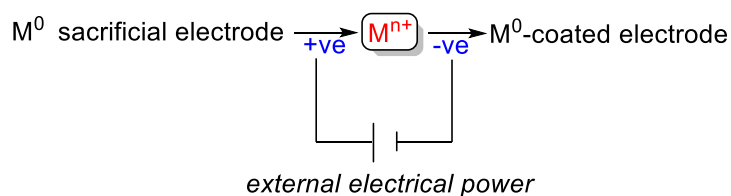
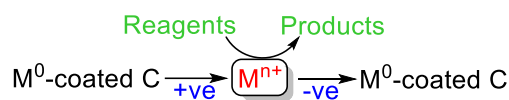


Figure 11 Simplified electroplating process with an external electrical power.⁴¹

Electroplating is widely used in industry and decorative arts to improve the surface qualities of objects.⁴² This includes resistance to abrasion and corrosion, improve plastic performing, electrical conductivity and heat transfer ability.⁴²

However, the electroplating method has not found wild application in organic chemistry (Scheme 9) with literature precedent. Previous research in our group which focused on copper coated graphite (Figure 12)¹⁸ could be a good inspiration for this project where zinc might be used. Here copper metal could be coated onto the graphite electrode from Cu (II) on demand

and selectively released to the reaction system as Cu (I) state only to catalysing organic reactions¹⁸.



Scheme 9 Electroplating in organic chemistry.¹⁸

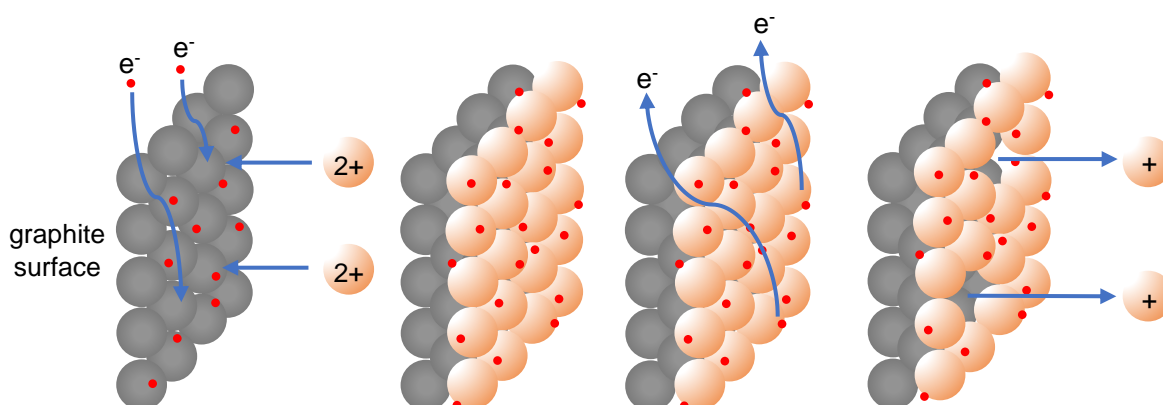


Figure 12 Selective coating and release of copper ions for organic catalysis.¹⁸

The copper coated graphite electrode was then developed for an approach to Glaser–Hay coupling (**Figure 13**) and recovery of the metal catalyst by switching to a reducing potential.¹⁸ During this process, copper(I) could be produced with a pre-calculated potential and current, ensuring only Cu(I) is released and Cu(I) acetylides are formed exclusively.¹⁸ The process is atom efficient as there is no iodide present in the starting copper species; In contrast, by using a traditional method, only around 33% by weight of CuI is copper, not to mention the non-trivial issues surrounding the disposal of iodide waste.¹⁸

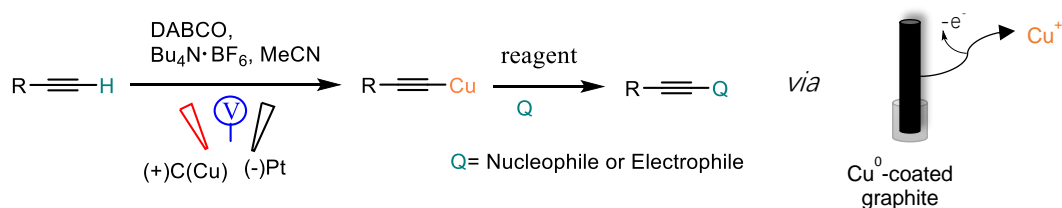

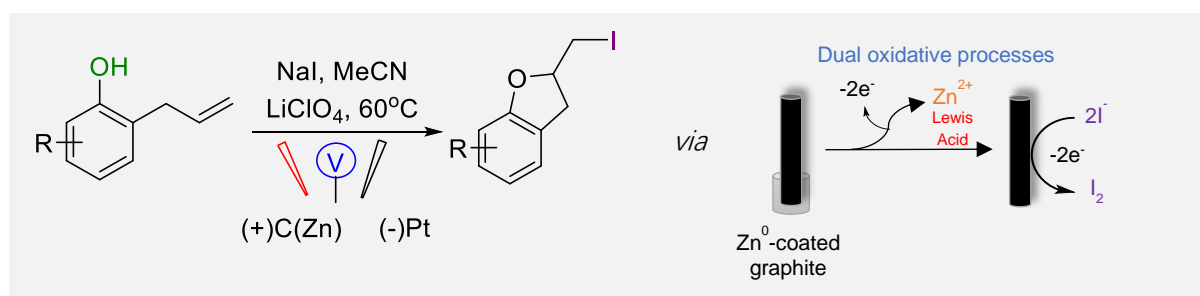


Figure 13. Electrochemical generation of copper acetylides.¹⁸

The advantage of applying this technology introducing zinc coated graphite into the reaction will be that only the required amount of zinc could be coated onto the electrode and once an oxidative potential applied, Zn^{2+} could be released. Once the zinc coating was exhausted, oxidation of I^- to I_2 would then occur from the exposed graphite electrode (**Scheme 10**, The symbol  refers to a divided cell with a constant potential.)



Scheme 10 Generate 2-(iodomethyl)-2,3-dihydro-1-benzofuran electrochemically with Zinc-coated graphite electrode

The coating of graphite electrode with zinc metal is easily achieved by applying a reducing potential to a graphite electrode in a solution of 2 M Na₂CO₃, with a zinc plate as the sacrificial anode. During the reaction, the zinc coat could be observed to fade slowly from the surface of carbon electrode (released into the solution as Zn²⁺). Within this period, no iodine was formed (as could be seen by the lack of red-brown colour developing in the reaction chamber). In addition, the real time potential was around -0.3 V since zinc ions are easily generated and released to the solution, followed by a smooth increasing to +0.5 V by 3 h. After that, iodine could be observed being produced from WE (As illustrated before, the first oxidation peak of NaI was +1.0 V, the oxidation already started from +0.5 V). The charge delivered for the whole cyclisation process in 16 h is shown in **Figure 14**. There was a significant switch in charge at the interface between zinc oxidation and iodine oxidation.

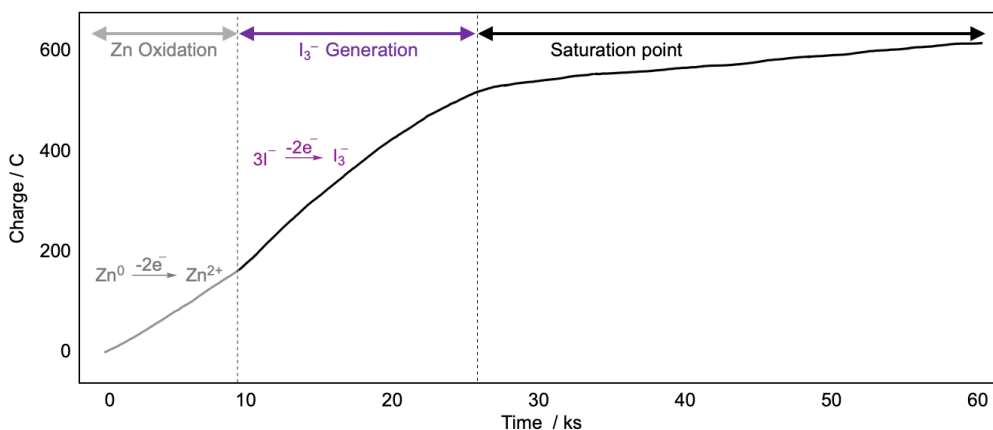


Figure 14 Charge-time profile indicating the generation of Zn^{2+} followed by the oxidation of I^- .

Also, with the aid of Faraday equation: $n=Q/(e \times N_A)$, the number of moles of electrons (n in the equation) passed during the reaction can be easily calculated. Q is the charge read from the figure (eg. here in **Figure 15**, Q for zinc ions is apparently 34 C); N_A is Avogadro's number which equals to 6.02×10^{23} ; e is the charge of single electrons which equals to 1.6×10^{-19} C.

Thus, the amount of zinc has been deposited on the carbon electrode could be calculated with $n/2$ because producing 1 mol zinc ions requires 2 mol electrons.

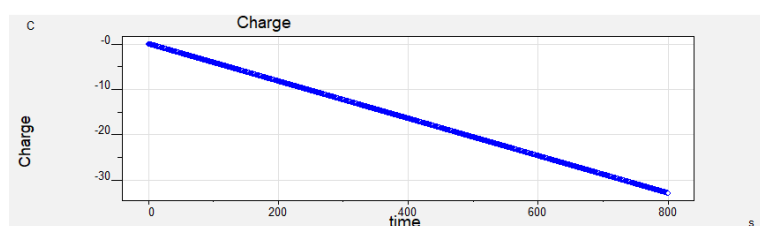

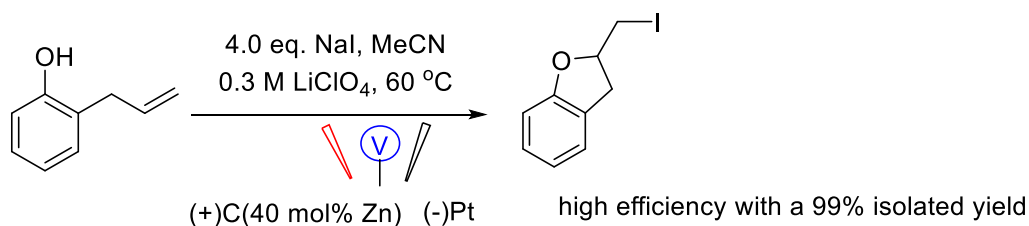


Figure 15 Charge-time profile of zinc coating process

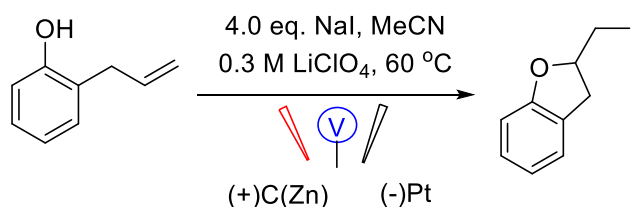
To our delight, when we applied the new set-up to the iodocyclisation of 2-allylphenol, a near quantitative yield of the cyclised product was obtained (**Scheme 11**, The symbol  refers to a divided cell with a constant potential).



Scheme 11 First successful iodocyclisation reaction

Following the first successful iodocyclisation reaction, some optimisation reactions and the cyclisation for different substituted allylphenols are summarized in **Table 2**. Entry 6, 16, 17 reveal the fact that larger amounts of zinc ions lead to a higher yield. Entry 8 and 10 demonstrate zinc and heating is essential. A methyl group in the *para* position gave a very high isolated yield while stronger electron donating groups like OMe only gave a 64% yield (Entry 11 and 14). Weak electron withdrawing groups like Br and Cl gave similar yields with both around 80%, however a moderate electron withdrawing group only yielded approximately 67% (Entry 12, 13, 15). The entries in table 2 show an interesting fact that the closer the electron properties of the substitutions in the aromatic ring to moderate state, the higher yields can be obtained. The stronger EWG makes the lone pair of electrons in OH less reactive, hence lowering the yield. EDG substituted aromatics performed better than those substituted with weak EWGs as this makes the OH more nucleophilic but doesn't decrease its acidity and hence deprotonation is slower. Besides, no aryl dehalogenation product was found for entry 15 after reaction.

Table 2 Yields of electrochemically promoted iodo-cyclisation of 2-allylphenols



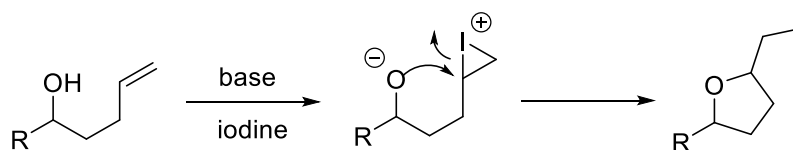
Entry	Electrode	Conditions	R	T / °C	Isolated Yield / %
6	Zn (40 mol%)-coated graphite	+1.2 V	H	60	99

7	Zinc metal	+1.2 V	H	60	0
8	Zn (40 mol%)-coated graphite	+1.2 V	H	RT	0
9	No electrode	No electricity, I ₂ , ZnCl ₂	H	60	>99
10	Graphite	+1.2 V	H	60	0
11	Zn (40 mol%)-coated graphite	+1.2 V	<i>p</i> -CH ₃	60	93
12	Zn (40 mol%)-coated graphite	+1.2 V	<i>p</i> -Cl	60	81
13	Zn (40 mol%)-coated graphite	+1.2 V	<i>p</i> -CO ₂ Me	60	67
14	Zn (40 mol%)-coated graphite	+1.2 V	<i>o</i> -OMe	60	64
15	Zn (40 mol%)-coated graphite	+1.2 V	<i>p</i> -Br	60	83
16	Zn (20 mol%)-coated graphite	+1.2 V	H	60	60
17	Zn (10 mol%)-coated graphite	+1.2 V	H	60	Trace
18	Graphite	No electricity	H	60	0
19	Zn (40 mol%)-coated graphite	No electricity	H	60	0

2.4 Mechanistic studies

2.4.1 Introduction to traditional iodocyclisation mechanism

For classical non-phenolic iodocyclisation of alcohols and alkenes, the traditional mechanistic pathway suggest it is via a nucleophilic attack from the oxygen to the iodonium intermediate, where base is normally used in such reactions to deprotonate alcohol. ([Scheme 12](#)).



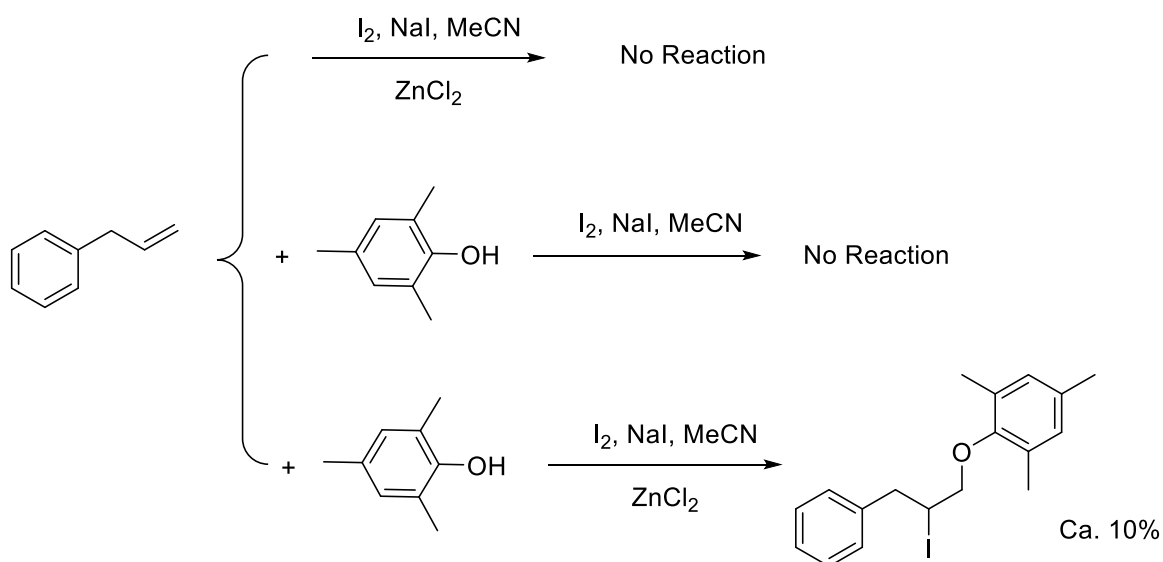
Scheme 12 Non-phenolic iodocyclisation mechanism.

However, for the aromatic phenol iodocyclisation, we were surprised to find that few mechanistic studies could be found in the literature. After assessing the conditions from existing papers, it was found that the reaction conditions used for phenol iodocyclisation are usually very different from the non-phenolic analogues, with no base included. These findings might therefore imply a different mechanistic pathway for such phenol iodocyclisation reactions. Consequently, we decided to investigate our system in more detail.


2.4.2 Mechanistic study of iodocyclisation of 2-allylphenol

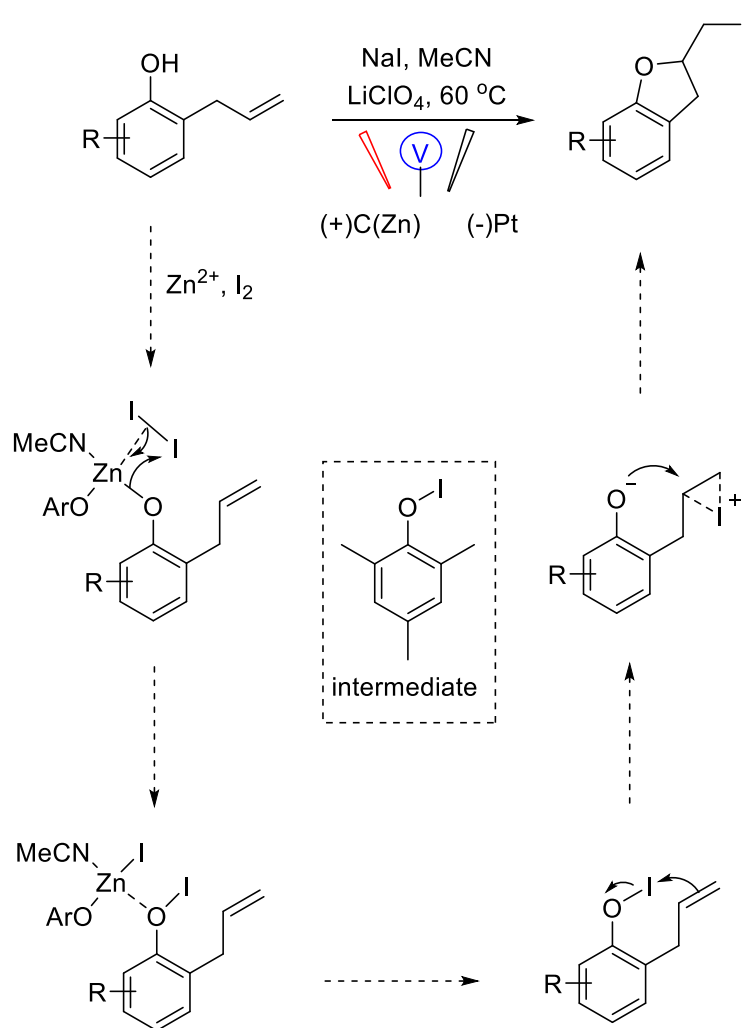
To test if it is really a different mechanistic pathway, we firstly needed to test whether base will influence the reaction. If it is *via* a traditional pathway, then it would be expected that the addition of a base would accelerate the reaction by facilitating the formation of a zinc-phenol complex. In order to reduce the influence from electricity and make a proper comparison with the traditional pathway, all of these tests were processed under non-electrochemical conditions. When we attempted the reaction outlined in Table 2, entry 9 with one equivalent of added K_2CO_3 , no acceleration in rate was observed and rather than cleanly isolating the cycloiodinated product, only a small amount of the cyclised material was produced. The majority of the isolated material comprised products of arene iodination. Similarly, when the reaction was performed in the presence of K_2CO_3 and the absence of a zinc Lewis acid, only iodinated arenes were observed. This suggests that although a cycloiodinium ion may form under these conditions, an alternative pathway is required to give the clean cyclised products. It also suggests that a process that 'protects' the activated aromatic ring from iodination is also in operation.

As shown in [Figure 14](#), the predominant active iodine species in the reaction mixture will be triiodide given that at any one point, only low concentrations of iodine will be present compared to that of iodide. At this point, we could not rule out the possibility that an active iodine species was reversibly generating a cycloiodonium ion (in low concentrations) which was then interacting with the zinc salt of the phenol to yield the product observed in [Scheme 11](#).



Scheme 13 A discovery of possible interaction between the Lewis acid and molecular iodine.

We therefore performed a set of experiments (outlined in **Scheme 13**) to determine which were the key factors in this mechanistic pathway. The results rule out the possible interaction between the Lewis acid and molecular iodine in generating the reactive iodinating species and instead suggests that a transient iodosylaryl species (outlined in **Scheme 14**) is responsible. Accordingly, this would suggest a reaction pathway for cyclisation of 2-allylphenols to be that shown in **Scheme 14**: The reaction is promoted *via* a sub-stoichiometric amount of zinc ions being released into solution. A zinc bis(aryloxy) complex is generated following iodide undergoing anodic oxidation. Coordination of I_2 , metathesis of the I-I and Zn-O bonds then leads to the reactive iodophenoxy intermediate (possibly still coordinated to the Lewis acid providing further activation). After that, the newly formed iodosylaryl species would lead to a phenoxide iodonium intermediate. Finally, the phenoxide attacks the iodonium to yield the terminal iodo-cyclized product. (The symbol  refers to a divided cell under constant potential.)

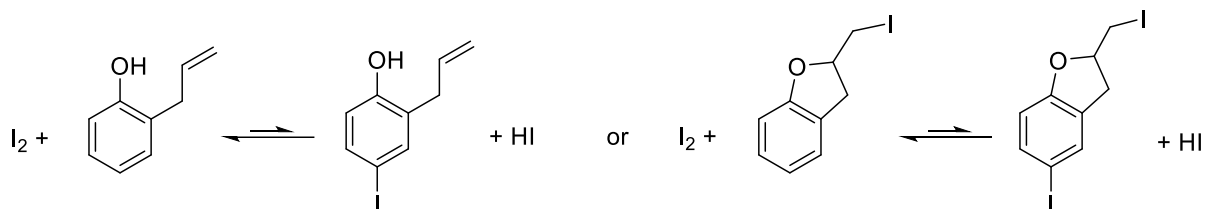


Scheme 14 Proposed mechanistic pathway.

Our proposed mechanism is therefore several steps more complex than the traditional accepted direct iodonium process. However, it is reasonable given that Zn (II) is a hard Lewis acid and molecular iodine is a soft electrophile and therefore unlikely to efficiently interact with Zn^{2+} . Furthermore, a consultation of the literature reveals that zinc-phenoxy complexes, (particularly zinc bis(aryloxy) compounds) have been prepared by reaction of a Zn (II) salt with the deprotonated phenol and are stable in aprotic solvents.⁴³

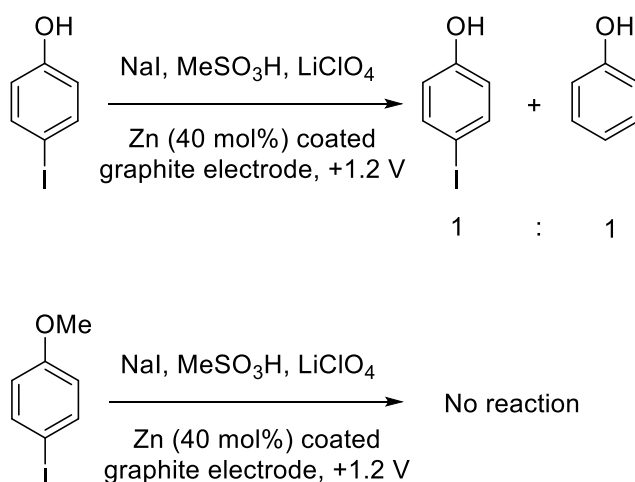
We were curious as to why only rarely we observed iodination of the arene, a reaction that might be expected to be more pronounced when given an active iodine species is generated (and in similar reaction mixtures leads to ring iodination).^{44,45} In order to explain this phenomenon, a hypothesis was proposed: In the absence of base, it is the *in situ* formed HI which reversed the iodinated aromatic product. But the question still remains: does the

iodination of the aromatic ring and its reverse processes occur before or after the cyclisation has taken place (or on both)? (See [scheme 15](#)).



Scheme 15 Possible aromatic ring iodination in equilibrium with HI.

To test this hypothesis, the reactions outlined in [Scheme 16](#) were designed by using MeSO_3H (2 eq.) as a strong acid to mimic the presence of HI which is necessarily produced in the observed cyclisation. The reason for choosing MeSO_3H as the source of H^+ was that MeSO_3H is a strong acid with a pK_a of -1.9 and it normally does not contain water. 4-iodophenol and 4-iodoanisole were chosen as model systems because their electron properties are similar to our starting phenol and iodocyclised product respectively. The purpose is to examine the model systems under our reaction conditions to see if the iodine atom in those species was labile.

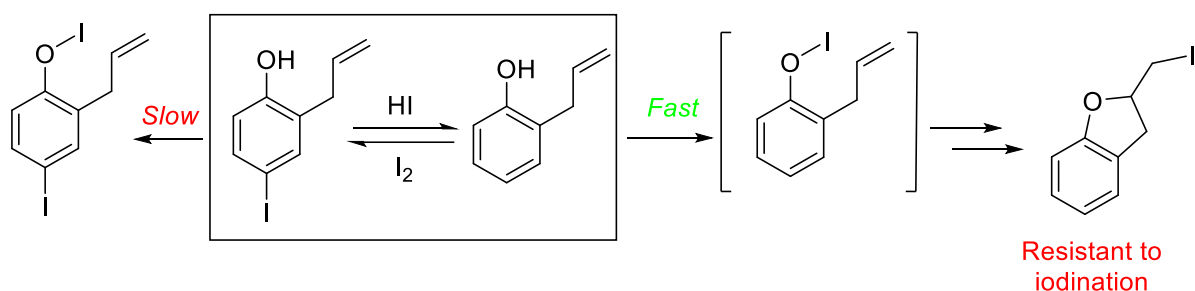


Scheme 16 Test of aromatic ring iodination in the presence of an HI mimic, MeSO_3H .

By performing the experiments under electrochemical conditions (generating Zn^{2+} from a zinc-

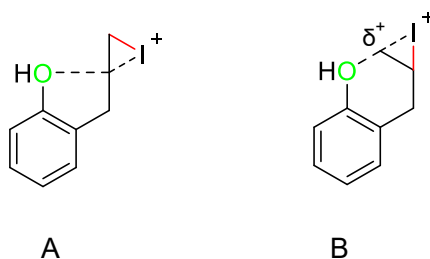
coated graphite electrode and I_2 via oxidation of NaI as outlined in [Scheme 10](#)) we could be sure that the Lewis acid was dry (zinc halides are notoriously hygroscopic) so that we could conclude that water was not involved in the process. Similarly, the electrochemical generation of I_2 would allow us to determine that this was the initial reactive iodine species formed and not more powerful iodinating agents such as ICl generated from the zinc salt counterion.

The results outlined in [Scheme 16](#) show that in the phenolic system, the iodine is labile, however in the alkylated variant the iodine atom is resistant to reductive exchange. This suggests that an equilibrium between iodinated and unsubstituted 2-allylphenol is established prior to cyclisation. Of these two compounds, the iodinated species is more resistant to the formation of the required reactive intermediate due to the electron-withdrawing nature of the iodine atom attached to the aromatic ring.⁴⁶ Consequently, cyclisation occurs most rapidly via the unsubstituted system leading to the dihydrobenzofuran which (like 4-iodoanisole) is then impervious to iodination under these reaction conditions ([Scheme 17](#)).



Scheme 17 Proposed rationale for the absence of iodinated aromatic products.

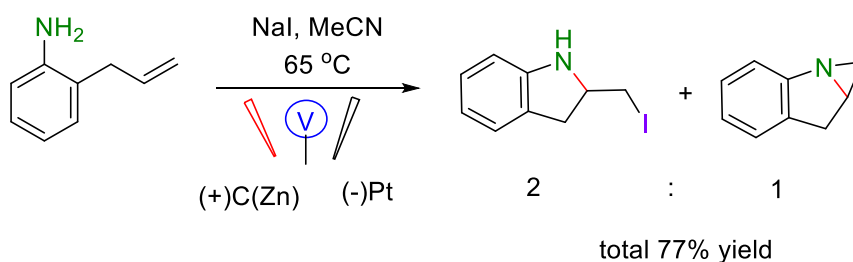
Additionally, no six-membered ring product was observed among all the iodo-cyclisation cases. Although according to Baldwin's rule, both 5-*exo-tet* and 6-*exo-tet* are favored for ring closures, the selectivity of this reaction might be explained as shown below: A is the intermediate of forming five-membered ring and B is the intermediate of forming six-membered ring. There will be a relative δ^+ charge in the carbon that attacked by the oxygen lone pair of electrons.



The five-membered intermediate was preferred because the δ^+ in A is more stable compared with B (since it is a Pseudo-secondary cation). Most importantly, the reacting rate of forming a five membered ring is faster than forming a six membered ring. All these factors lead to the selectivity of the five membered ring formations rather than six membered rings.

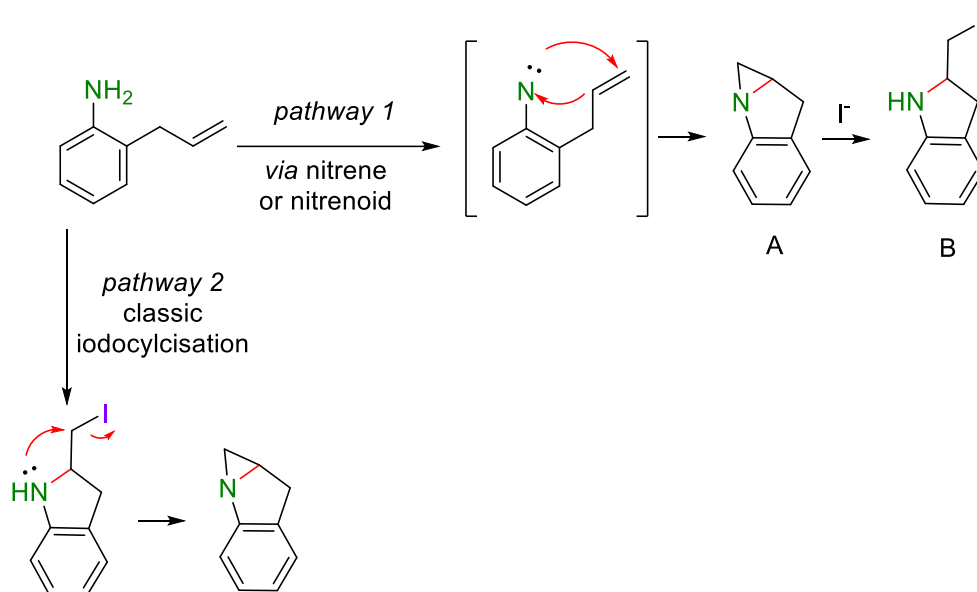
2.5 Cyclisation of 2-allylanalines

We were interested in seeing if similar methodology could be applied to the iodocyclisation of anilines. Iodo-cyclisation reactions involving nitrogen as the nucleophile are much less common than those utilizing oxygen and so we decided to examine the anilines in more detail. Surprisingly, when the same conditions were employed, a mixture of indoline and aziridine products were obtained rather than pure product 2 (**Scheme 18**)



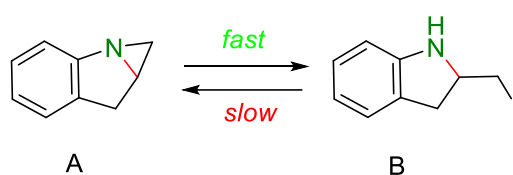
Scheme 18 Electrochemical generation of a mixture of indoline and aziridine

To explain this result, we have firstly proposed two possible mechanistic pathways (**Scheme 19**). Pathway 1 involves the formation of a nitrene or nitrenoid intermediate which undergoes a concerted insertion into the pendant alkene to yield the aziridine. This strained system is then opened by nucleophilic attack of iodide. Alternatively, pathway 2 involves iodocyclisation directly undergoes to the phenolic systems followed by a ring closure to give the aziridine.

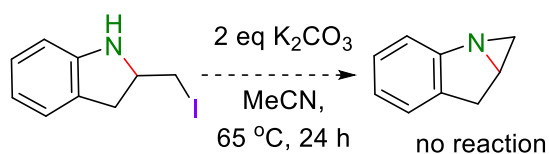


Scheme 19 Two possible mechanistic pathways

I reasoned that the rate of formation of A from B is expected to be slow as the structure of B is too rigid to produce A (**Scheme 20**). To further prove this assumption, I applied a control experiment by treating B with amount of base to see if it will ultimately converted to A (**Scheme 21**). As expected, no product A was detected. This suggests that A is probably produced in a single step and that nucleophilic attack of I^- facilitated by Zn^{2+} then yields the iodide product B.

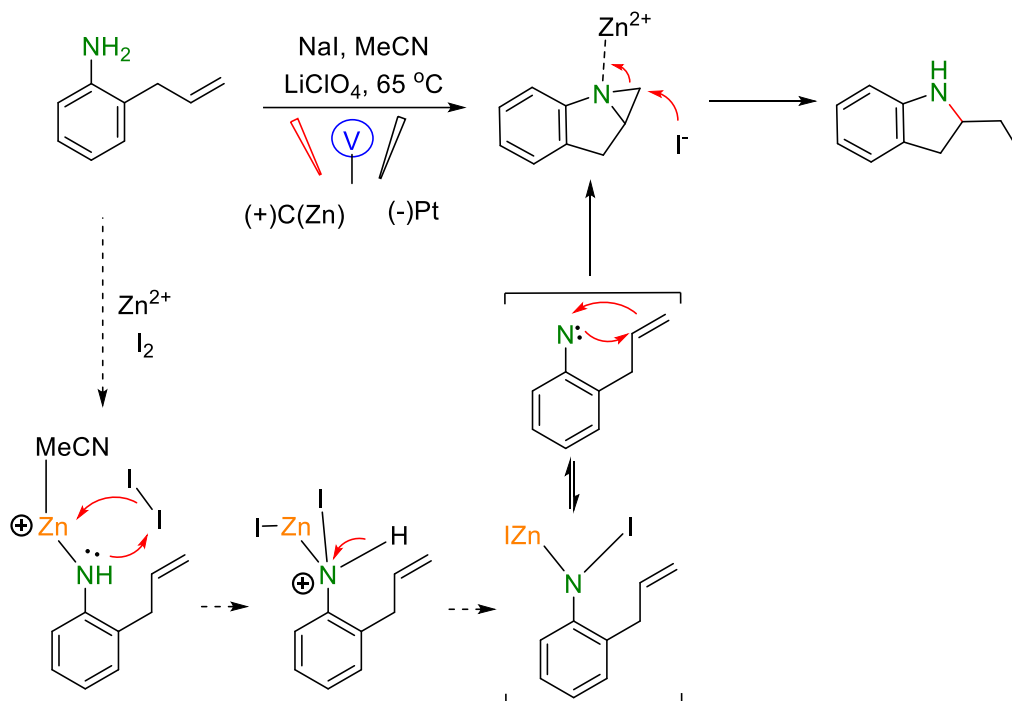


Scheme 20 Transformation speed between A and B



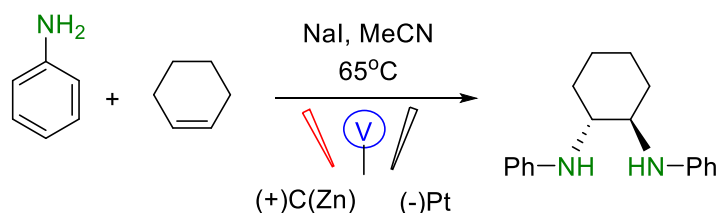
Scheme 21 Base control experiment from B to A

Based on the discussion above, a proposed mechanism is outlined in **Scheme 22**.



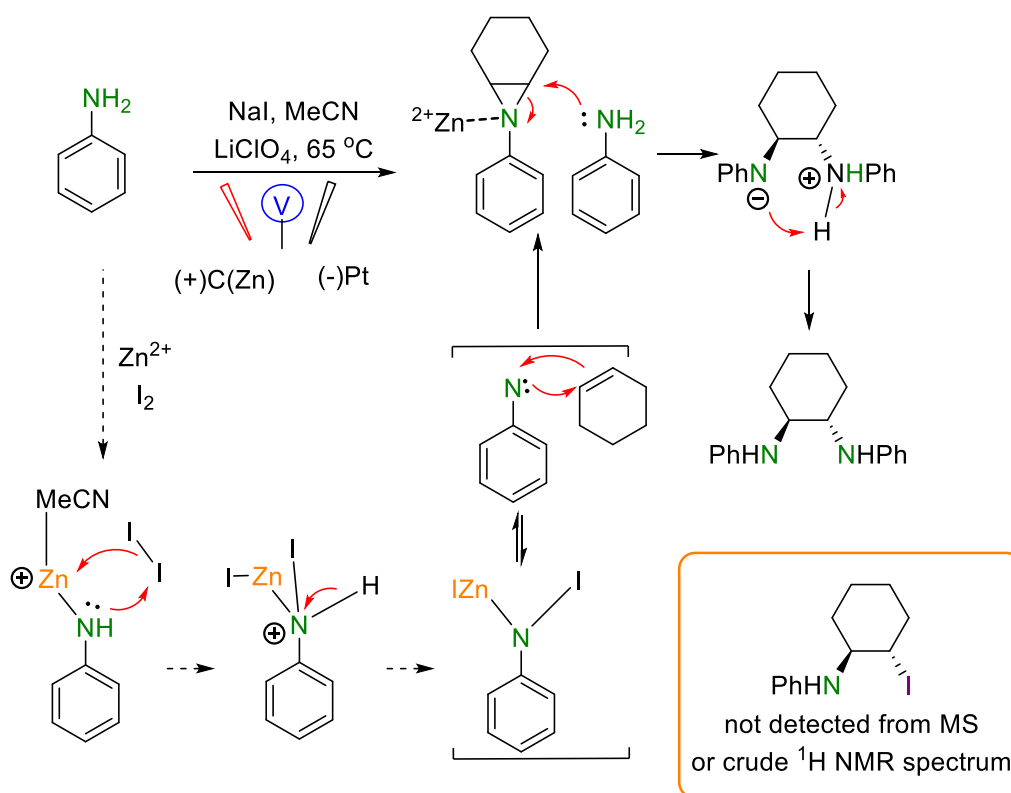
Scheme 22 proposed mechanism of aniline reaction

Following the proposal of this mechanism, a reaction between aniline and cyclohexene was designed in order to find if pure aziridines could be obtained in an intermolecular manner. However, to our surprise, a diaminated product was formed in 70% isolated yield (**Scheme 23**), as a single diastereoisomer. At the meantime, no aziridine stuff has been detected.



Scheme 23 Diamination of cyclohexene

A similar mechanism has been proposed and is outlined in **Scheme 24**.



Scheme 24 Proposed mechanism of diamination

Such protocol for diamination is particularly interesting as there currently has no method of converting an alkene to a diamine in a single operation. While it is an interesting process, work is required to extend the limited scope of the reaction, such as using amide as a replacement to aniline. Besides, one important part of the future mechanistic study will be located on whether it is *via* a radical process. Thus, a TEMPO control experiment might be involved. Nevertheless, a one-step diamination of an inactivated alkene is an unprecedented and exciting development and would be synthetically very useful.

In conclusion, in this chapter, a newly developed dual electrochemical oxidative process in synthesizing the dihydrobenzofuran motif with excellent efficiency has been described. This allowed for the formation of zinc ions and molecular iodine from a carbon anode in one pot followed by a zinc catalysed iodocyclisation of phenol and alkene. During the whole process, the hazards and difficulties of handling elemental I₂ and metal ions can be circumvented through the electrochemical generation of these species in situ and 'on-demand'. Related

mechanistic studies indicate an unusual pathway which explains the selectivity of the reaction without the often-problematic electrophilic aromatic iodination of the aryl ring. Further extension of this newly developed method to aniline has led to a novel aziridine intermediate which ultimately yielded a diaminated product.

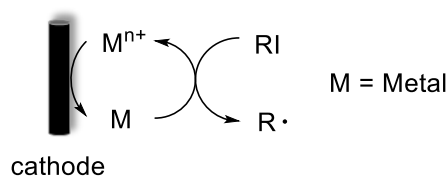
Chapter 3. Electrochemical activation of alkyl halides

The use of radical reactions for the construction of complex organic molecules are now almost ubiquitous in synthetic chemistry.⁴⁷ Historically however, organic chemistry has relied on tributyltin hydride (and similar reagents) to mediate such processes.⁴⁸ Organotin reagents have proved remarkably efficient for the generation and mediation of carbon-centred radicals. Their drawbacks however are significant; the reagents are extremely toxic, expensive and the side-products are often difficult to remove from the reaction medium post reaction. As such, recent years have seen intense interest in alternatives to these extremely useful reagents.⁴⁹ Almost without exception however, none have matched the efficiency, generality, and functional group tolerance of tin-based reagents. The result of this is that many chemists, particularly those in industry, have shunned tin reagents. However, in doing so they necessarily preclude the advantages that this class of radical reactions can offer in terms of the construction of complex organic architectures.

Encouraged by the new methodology established above in iodocyclisation, we were then keen to know if a metal and an organic iodide could be used to do some more exciting radical reactions electrochemically.

3.1 Introduction of Traditional Giese Reaction

We envisaged that a putative radical reaction which uses a stoichiometric amount of a metal mediator might be a perfect candidate for improvement by metal recycling *via* a reductive electrode (**Scheme 25**).

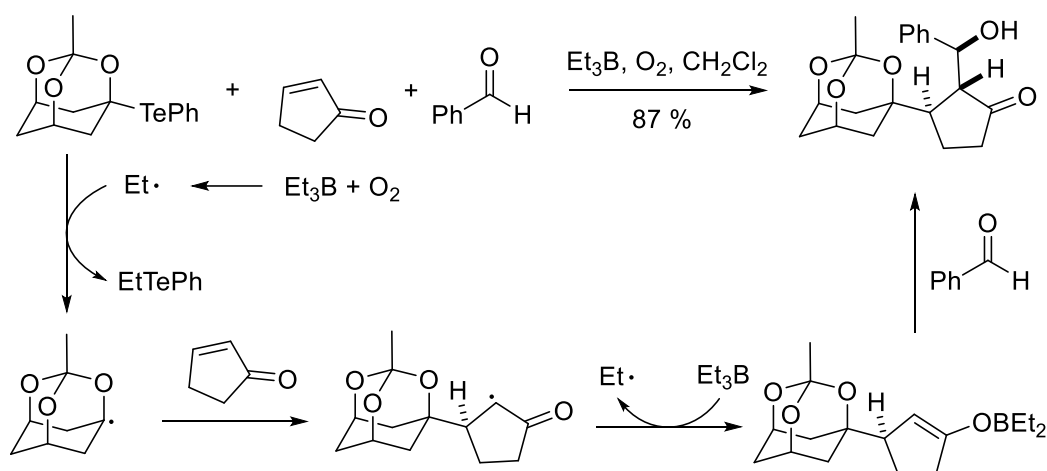


Scheme 25 *Ideal target radical reaction working type*

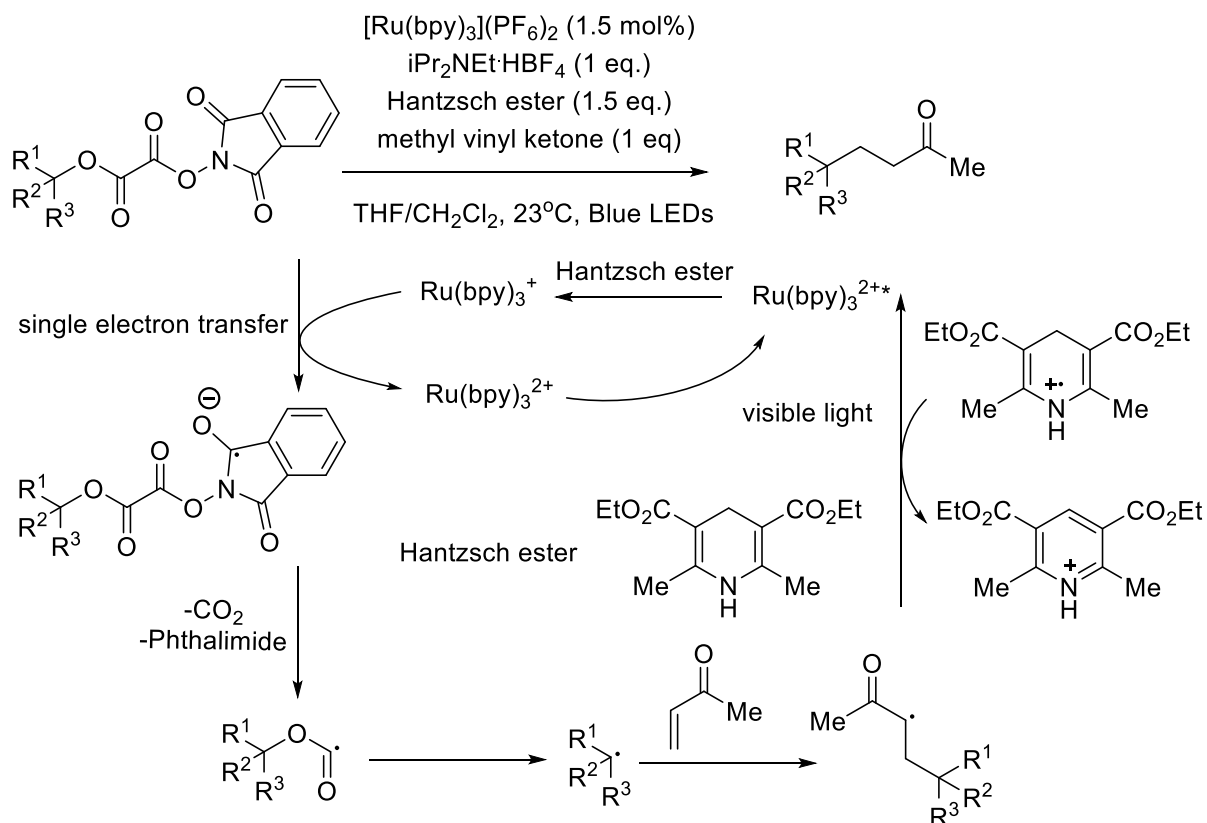
Thus, the Giese reaction was chosen as our target. Nucleophilic carbon centred radicals can

be trapped with various electrophiles.⁵⁰⁻⁵³ Particularly, the process of forming carbon-carbon bonds *via* trapping of free-radicals with electron-deficient alkenes is called the Giese reaction.⁵⁰⁻⁵³ The newly formed α -carbon radicals can also be reacted further with the second electrophiles in tandem fashion.⁵⁰⁻⁵³ It is also commonly seen the application of this reaction in intramolecular cyclization in natural product synthesis.⁵⁰⁻⁵³

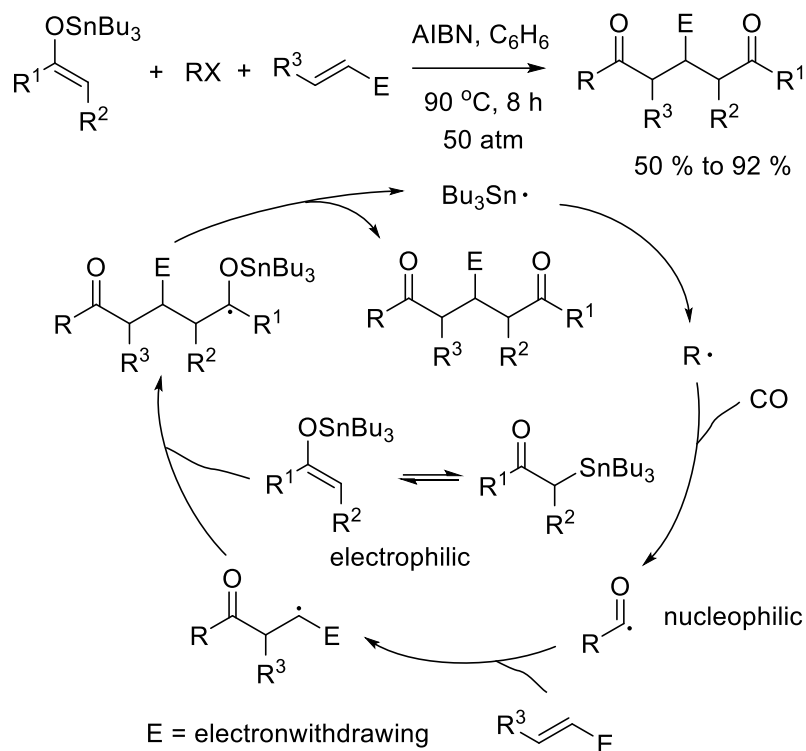
Since the first paper named formation of C-C bonds by addition of free radicals to alkene was published by Bernd Giese in 1983,⁵¹ the Giese reaction started to be known and widely used by chemists. Initially reported with only Tin reagent (eg. tributyl tin hydride), till recent times, development in Giese reaction has undergone significant progress.^{52,53} Various new methods and applications have been developed, such as the tandem Giese reaction using organic tellurium reagents (**Scheme 25**)⁵⁴, the photoredox synthesis of sterically congested carbon-carbon bonds (**Scheme 26**)⁵⁵ and Giese reaction with a carbonyl group inserted under CO atmosphere (**Scheme 27**).⁵⁶



Scheme 25 Tandem Giese reaction using organic tellurium reagents.⁵⁴



Scheme 26 The photoredox synthesis of sterically congested carbon-carbon bonds.⁵⁵



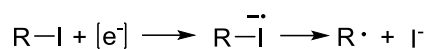
Scheme 27 Carbonyl insertion Giese reaction under CO atmosphere, E= electron withdrawing group.⁵⁶

The drawbacks of these methods engaged with organic tin reagents are significant: the agents are extremely toxic, expensive and the side-products are often difficult to remove from the reaction medium post reaction. As such, recent years have seen intense interest in alternatives to these extremely useful reagents. However, almost without exception, none have matched the generality, functional group tolerance and efficiency of tin-based reagents.

Photoredox catalysis has already, in a short amount of time, proved to be a powerful tool for the activation of organic molecules.^{57,58} Similarly, synthetic organic electrochemistry is becoming an increasingly popular alternative way to activate organic molecules *via* direct addition or removal of electrons to generate reactive radical species.²

3.2 Traditional Electrochemical Reduction of Alkyl Halides

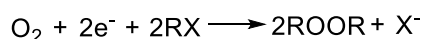
As the most used source for alkyl radical of Giese reaction is alkyl iodide, in this project we have targeted on electrochemical reduction of alkyl iodide, with a view to generating an alkyl radical *via* single electron transfer (SET) and subsequent fragmentation (**Scheme 28**):



Scheme 28 *Generating an alkyl radical via single electron transfer (SET)*

In the 1980s, the electrochemical reduction of alkyl halides was mainly reported processed at mercury cathodes, while only rare studies are published dealing with carbon cathodes, which include the isolation, characterization, and quantitation of products derived from electrolysis of alkyl halides at carbon.⁵⁹ The relationship between the cathode material and reduction pathway of 1-bromobutane was demonstrated by Wagenknecht.⁶⁰ When a mercury cathode was applied, 1-bromobutane will go through reduction *via* a radical intermediate pathway, whereas when graphite was employed, the butyl carbanion will be formed *via* a two electron process.⁶⁰ Coincidentally, Bard and Merz also established that the elementary reaction of allyl halides at a reticulated vitreous carbon cathode is a two electron process.⁶¹

Unfortunately, the direct electrochemical reduction of alkyl halides requires highly reducing potentials and as such has not found general application because of the incompatibility of these extreme potentials with various functional groups.^{59,62} There are also some examples of indirect reduction of alkyl halides with the aid of superoxide ions generated from oxygen, however, such reaction will lead to the di-organic peroxide as the main product and will not be expected to form alkyl radicals. (**Scheme 29**)⁶³

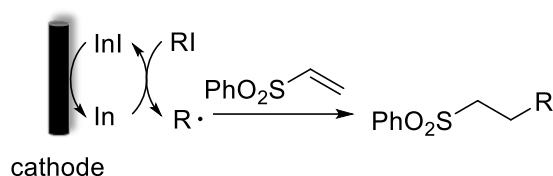


Scheme 29 *Superoxide ions mediated indirect reduction of alkyl halides.*⁶³

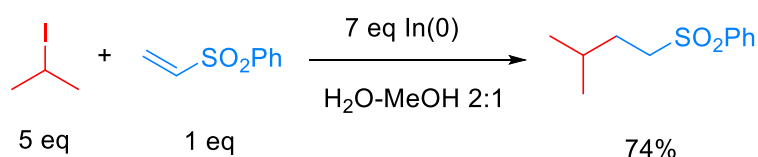
3.3 Indium mediated electrochemical indirect reduction of alkyl iodide

Since the drawbacks of direct reduction of alkyl iodide discussed above, we firstly designed to use indium as the reduction mediator for alkyl iodide as showing below in **Scheme 30**. In the Giese method using indium metal (**Scheme 31**), super-stoichiometric amount of indium and alkyl iodide were used.⁶⁴ In contrast, our newly designed electrochemical indium mediated Giese reaction, if successful, will significantly improve this situation, with only 1.2 eq of alkyl iodide and a catalytic amount of indium trichloride needed as the low valent In could be recycled at the electrode. For the solvent system of such reaction, water and methanol mixture

was used. The literature explanations for using such solvent system is that indium reactions have been shown to be most efficient in aqueous and alcohol solvent. In addition to this, the case for employing aqueous solvents for organic transfer reaction is strong in both economic and environmental considerations.⁶⁴ Based on that, we planned to keep using organic aqueous solvent system for our reaction.

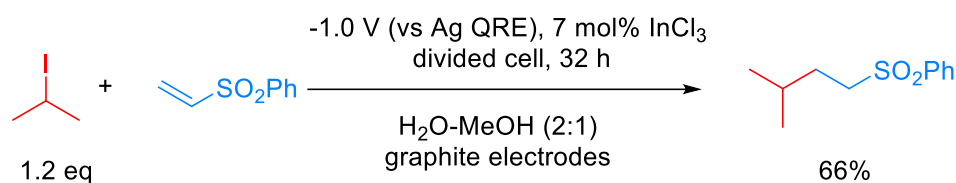


Scheme 30 Anticipated electro-indium mediated Giese reaction



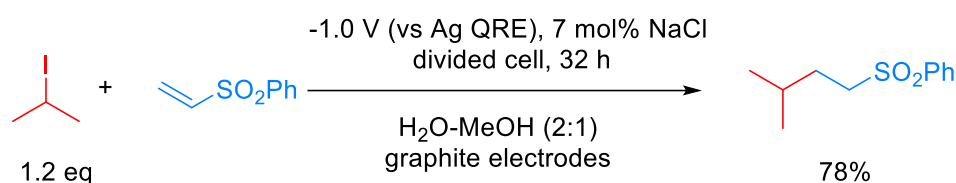
Scheme 31 Indium mediated Giese reaction.⁶⁴

To establish our new method, a suitable reducing potential of indium ions will first be needed to be determined. Although the standard reducing potential of indium ions to indium metal is only -0.34 V vs. SHE, when we are doing zinc coating experiment before in the iodocyclisation part, it has been found that higher reducing potential could make the reducing process of zinc ions with more efficiency. Besides, combined with the fact that the reduction window of water is around -1.5 V, we chose -1.0 V as the setting potential of the reaction. Under such potential, the reduction of indium ions should be very efficient while water in the solvent system will remain intact rather than been reduced to hydrogen gas and hydroxyl ions. To our delight, the trials between isopropyl iodide and phenyl vinyl sulfone using 7 mol% of indium trichloride with an applied potential of -1.0 V gave the Giese product in a good yield of 66 % (**Scheme 32**).



Scheme 32

Encouraged by this result we then sought to undertake the necessary control experiments by excluding indium trichloride. To our amazement, rather than observing a decrease in yield, the efficiency of the reaction actually improved (**Scheme 33**).

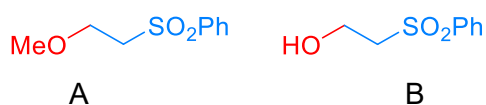


Scheme 33

The control experiment has shown that indium is not necessary and such reaction could directly be processed with no additional catalyst. Given the factors discussed above, it did not seem likely that this reaction was the result of direct reduction of the alkyl iodide at the electrode. We therefore decided to examine the reaction mechanism. This is discussed in section 3.6 below.

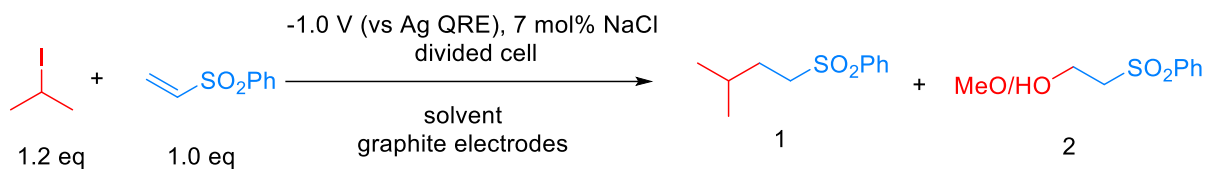
3.4 Electrochemical carbon centred radical formation mediated by arial oxygen

It was noted that, side product A and B were also detected during the reaction.



Thus, the first task of this research would be design and process optimisation experiments of this new method. **Table 3** shows the optimisation for the reaction outlined in **Scheme 33**.

Table 3 Optimisation experiments



[a] Isolated yield. [b] pH adjusted with NaOH. [c] pH adjusted with HCl. [d] PBS 7.4 buffer.

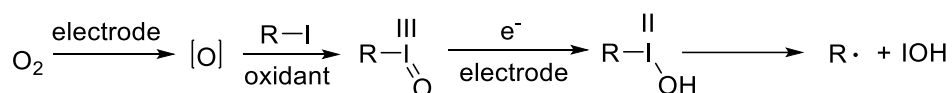
Entry	Solvent	Atmos.	Time, h	pH	1% ^[a]	2% ^[a]
1	MeOH	Air	32	7	0	70
2	H ₂ O-MeOH (2:1)	Air	32	7	78	9
3	MeCN	Air	32	7	Trace	0
4	H ₂ O-MeCN (1:3)	Air	32	7	Trace	Trace
5	H ₂ O-MeCN (1:1)	Air	32	7	68	Trace
6	H ₂ O-MeCN (2:1)	Air	32	7	90	Trace
7	H ₂ O-MeCN (2:1)	Ar degassed	32	7	0	0

8	H ₂ O-MeCN (2:1)	Stream of O ₂	32	7	Trace	Trace
9	H ₂ O-MeCN (2:1)	Air	20	9 ^[b]	47	53
10	H ₂ O-DMF (2:1)	Air	20	2 ^[c]	74	0
11	H ₂ O-MeCN (2:1)	Air	20	7.4 ^[d]	86	14
12	H ₂ O-MeCN (2:1)	Air	20	5 ^[c]	82	18
13	H ₂ O-MeCN (2:1)	Air	20	2 ^[c]	100	0

Several observations are noteworthy. Firstly, water is essential for the success of the reaction, without water, nearly no terminal product was detected (Entry 1, 3). Secondly, it was noted that the pH of the solution slowly rises as the reaction proceeds, and as such, the formation of the undesired hydroxy addition product accelerates. Lowering the pH from the outset, therefore, minimises this undesired side-reaction. Based on that, side product B was successfully removed by modifying the pH value of the solvent system, with a series of control experiments at different pH value (Entry 9, 10, 11, 12, 13). Meanwhile, as side product A is supposed to be most likely produced from methoxy anion, which arises from the reduction of methanol at the cathode. The use of different organic solvent in place of methanol in the solvent system should therefore remove this side product. Acetonitrile was found to be the best solvent in this respect. We also noted that, the ratio between water and MeCN is also very important for the yield of the addition product 1 (Entry 4, 5, 6).

Finally, as demonstrated in entry 7, oxygen is required for the reaction to proceed, however entry 8 demonstrates that there is no advantage to performing the reaction in an oxygen

atmosphere. In fact, such an approach is actually negative and almost completely attenuates the reaction. After this reaction, only traces of products were detected, and almost quantitative starting materials were recovered. This gave us the first inclination that oxygen may be required only in sub-stoichiometric quantities for the putative radical reaction. With these observations, we have proposed a hypothesis to explain such phenomenon: We believe that the reaction is probably *via* an oxidation-reduction process. (**Scheme 34**)



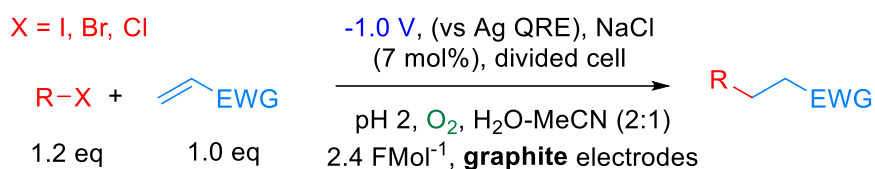
Scheme 34 oxidation-reduction process

After iodide was oxidised by the powerful oxidant produced by initial electrochemical reduction of aerial O₂, the oxidised intermediate will be further reduced at the cathode to liberate the alkyl radical. Most importantly, the reduction window of this intermediate might be between -1.0 V and the reduction peak of oxygen. In other words, oxygen is easier to be reduced than the oxidised intermediate. Thus, before all the oxygen been exhausted, the oxidised intermediate cannot be reduced. There will be further evidence which proved our hypothesis in the detailed mechanistic study part below later.

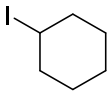
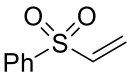
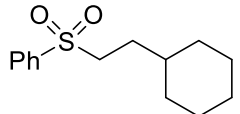
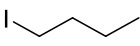
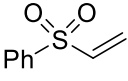
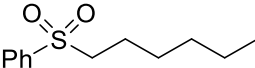
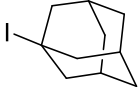
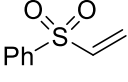
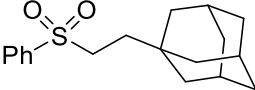
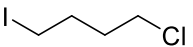
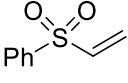
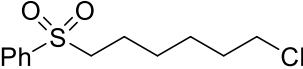
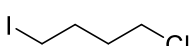
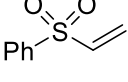
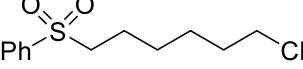
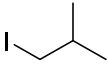
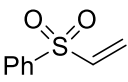
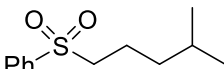
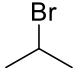
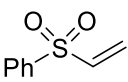
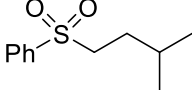
Having established a robust set of conditions that resulted in high yields of the desired product 1, we were then keen to establish the scope of the reaction with a more diverse set of alkyl halides and acceptors. The results are outlined in **Table 4**. It is noteworthy that, in terms of the amount of the alkyl iodide employed, the efficiency of the reactions outlined in **Table 4** is generally higher than with other radical chain carriers such as tributyltin hydride where, in order to circumvent competing reduction by Bu₃SnH, multiple equivalents of the alkyl halide are typically employed. Tertiary iodides are also applicable (e.g. Entry 3) however the high reactivity and poor solubility of accessible tertiary-iodides prevented a more diverse screen at this point. For entry 4, the primary reaction with 1.2 eq iodide only yielded 62% product. This might be caused by the existence of the chloride on the other side of the chain which decreased the stability of the produced alkyl radical. The increasing of the equivalent of the iodide from 1.2 to 3.0 has provided more chance for the alkyl radical to attack the alkene thus has dramatically increased the yield of the desired product from the original 62% to 95%.

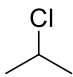
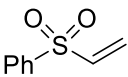
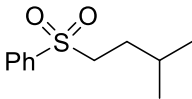
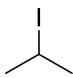
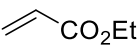
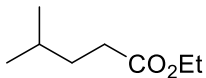
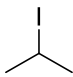
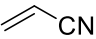
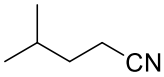
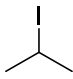
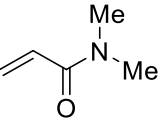
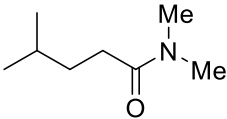
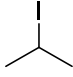
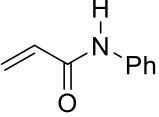
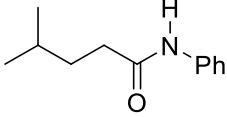
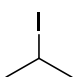
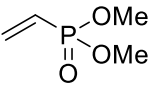
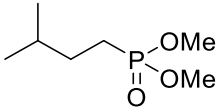
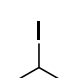
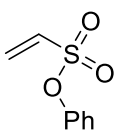
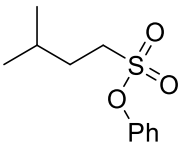
Surprisingly, even some alkyl bromides proved reasonably effective (Entry 7) although admittedly, this is far from optimised, while when the alkyl was connected with a more electron negative chloride, no product was detected. **Table 4** demonstrates that a wide range of alkyl iodides could be coupled with various electron-deficient acceptors in generally excellent yields. We were also encouraged by entry 10 where an amide with a free N–H can be employed in excellent yields. The conditions employed are more amenable to our future ambitions to manipulate biological molecules than classical tin-mediated radical methods and illustrate a further advantage of the mild electrochemical technique. The alkyl might also tolerance to other functional groups and will be discovered in the future work.

Table 4 Exploring the reaction scope.



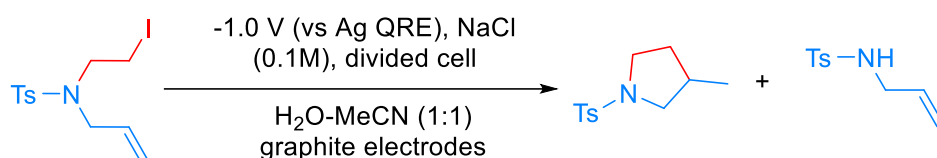
[a] Isolated yield. [b] 3.0 equivalents of iodide employed [c] unoptimized.

Entry	Halide	Acceptor.	Product	Yield % ^[a]
1				100
2				82
3				60
4				62
5				95 ^[b]
6				98
7				21 ^[c]

8				0
9				90
10				98
11				96
12				98
13				95
14				99

3.5 Extending the methodology to intramolecular cyclisation

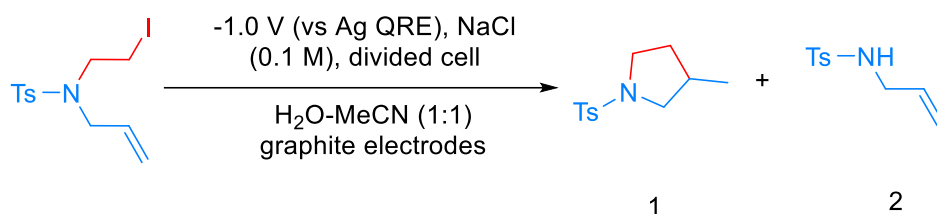
Encouraged by the excellent performance of our approach in intermolecular radical addition reactions, we want to test if such methodology also applies to reductive intramolecular cyclisation. Interestingly, the different ratio mixtures of MeCN-H₂O have not found any obvious effect on the yield of the intramolecular cyclisation reactions of *N*-allyl-*N*-(2-iodoethyl)-4-methylbenzenesulfonamide. Thus, a 1:1 MeCN-H₂O mixture was applied here for a better solubility of this iodide. When such iodide was subjected to -1.0 V in an acidified MeCN-H₂O (1 : 1, pH 1) solution, it was reductively cyclised into the corresponding pyrrolidine with *N*-allyltosylamide as a by-product (**Scheme 35** and **Table 5**, entry 1). *N*-allyltosylamide is likely to be produced *via* β -elimination from an anionic intermediate, terminated by the abstraction of the hydrogen atom from the solvent.⁶⁵



Scheme 35 Reductive intramolecular cyclisation

The effect of pH was also examined by adjusting the pH of the solvent with various buffer solutions. It was found that optimal conversion occurred (**Table 5**, entry 2) at pH 3.6 and no reaction occurred at pH 7.

Table 5 Optimisation of reductive intramolecular cyclisation



[a] Isolated yield. [b] pH Adjusted with HCl. [c] pH Adjusted with acetate buffer. [d] pH Adjusted with phosphate buffer. [e] Alkyl iodide was fully recovered.

Entry	Solvent	pH	Time, h	1% ^[a]	2% ^[a]
1	MeCN-H ₂ O (1:1)	1 ^[b]	24	31	23
2	MeCN-H ₂ O (1:1)	3.6 ^[c]	6	40	37
3	MeCN-H ₂ O (1:1)	5.7 ^[c]	24	Trace	33
4	MeCN-H ₂ O (1:1)	7 ^[d]	24	N/R ^[e]	N/R ^[e]

3.6 Mechanistic study

With these results in hand, we were keen to undertake some preliminary mechanistic investigations into this reaction and to see if our hypothesised mechanism was accurate. We

first turned to cyclic voltammetry of the various reactants present in the solution. We discovered that the only species that was redox active at the potentials employed was molecular oxygen which was reduced between -0.7 and -0.8 V (vs. QRE in our system). (Figure 17 and Figure 18)

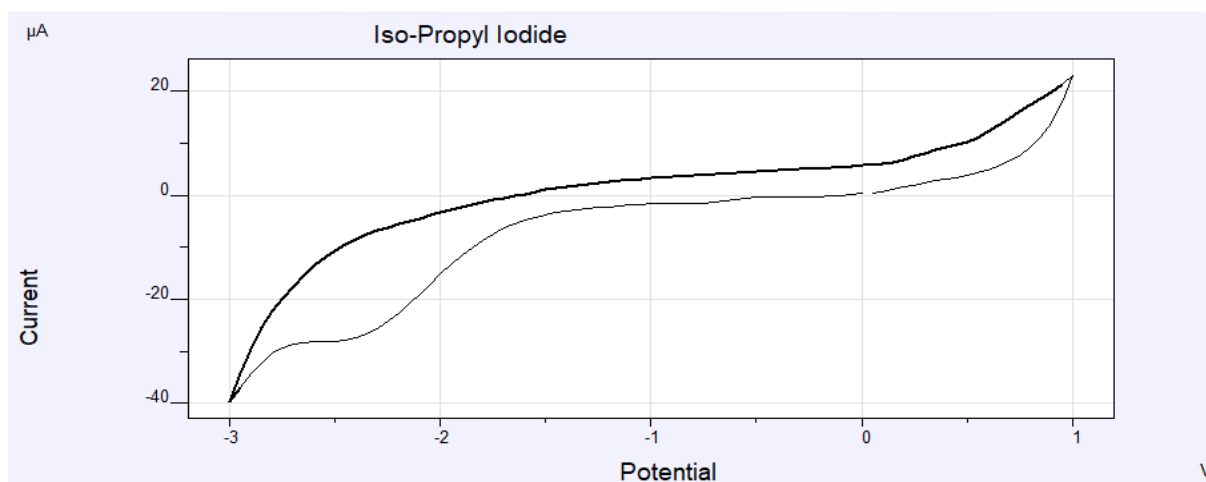


Figure 17 Cyclic Voltammetry of Isopropyl Iodide

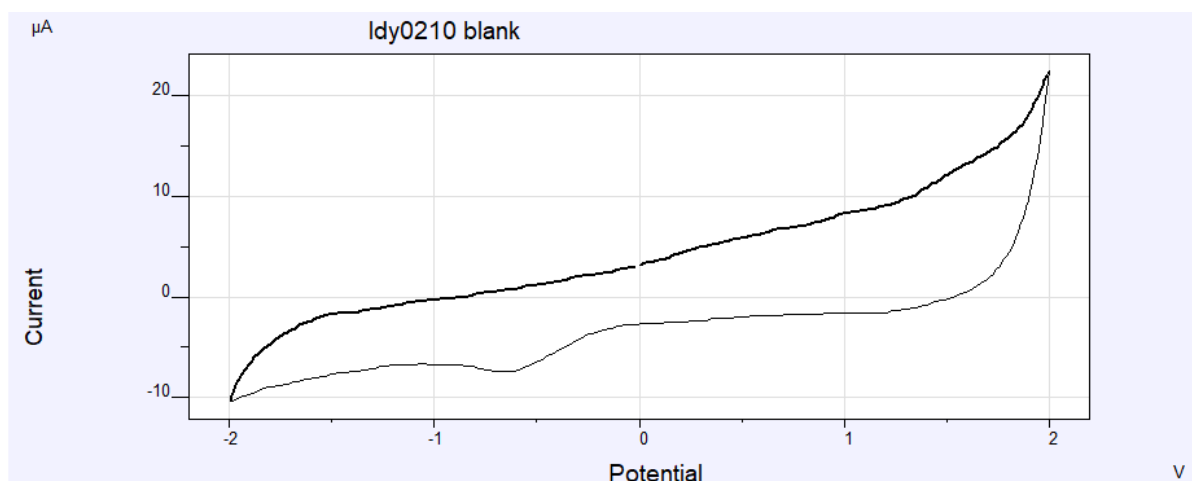
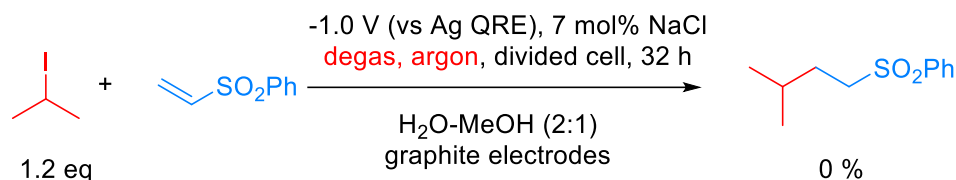


Figure 18 Cyclic Voltammetry of Molecular Oxygen

Since the reduction potential of isopropyl iodide is much larger than -1.0 V and oxygen was found to be the only redox active species under the potentials we applied, it is likely that the reaction was not processed by direct reduction of the isopropyl iodide at cathode. To be more

precise, the argon control experiment (**Scheme 36**) further demonstrated this judgement. I realised therefore that activation of molecular oxygen was a key step in the process and I decided to examine the redox chemistry of oxygen more closely.

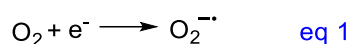


Scheme 36 The argon control experiment

3.7 Introduction of superoxide anion

Ordinary O_2 often reacts poorly with many other organic molecules. However, it can be activated after transformed into reactive oxygen species (ROS) by adding naturally or artificially derived energy.⁶⁶ Reactive oxygen species (ROS), according to their own name, derive and present higher reactivity than molecular oxygen with redox activity.⁶⁶ The ROS designation comprehends not only reactive oxygen radicals, such as superoxide radical ($O_2^{\bullet-}$), hydroperoxyl radical (HO_2^{\bullet}), hydroxyl radical (HO^{\bullet}), peroxy radical (ROO^{\bullet}) and alkoxy radical (RO^{\bullet}), but also non-radical derivatives of oxygen, namely hydrogen peroxide (H_2O_2), singlet oxygen (1O_2), and hypochlorous acid ($HOCl$).⁶⁷

Although maintaining $O_2^{\bullet-}$ in a stable state for a long duration is difficult, $O_2^{\bullet-}$ has attracted considerable attention.⁶⁶ The monovalent reduction of O_2 gives $O_2^{\bullet-}$, which is a radical anion with both the radical sign (\bullet) and a charge of -1 (**eq 1**).⁶⁶



Unpaired electrons make free radicals highly reactive.⁶⁶ $O_2^{\bullet-}$ is one of the isolable paramagnetic main-group ions and one of the many intermediates at oxygen reduction reactions.^{66,72} With the term “superoxide”, $O_2^{\bullet-}$ has prompted several scientists to presume that it is a powerful oxidizing agent and an initiator of radical reactions due to its exceptionally high reactivity.^{66,74-76} Indeed, $O_2^{\bullet-}$ has already been reported to be relatively reactive by few studies.⁶⁸⁻⁷⁰ However, a previous study showed that $O_2^{\bullet-}$ is not highly reactive despite being a free radical.⁷¹ In addition, $O_2^{\bullet-}$ is stable only up to 348 K.^{66,73} Consequently, only a few measurement techniques such as chemical reactions, spin trapping, and direct detection can

be used.⁶⁶

Technically, the major generation methods of $O_2^{\cdot-}$ from O_2 include electrochemical, chemical, photocatalytic and generation at oxide surfaces.⁷⁷ Here, as electrochemical method was used in our reaction, we only need to focus on the electrochemical approaches. $O_2^{\cdot-}$ is normally produced by the electrolytic reduction of molecular oxygen.⁷⁷ This method allows the generation of pure $O_2^{\cdot-}$ to be controlled at low concentrations ($<10^{-2}$ M) and is well suited for mechanistic studies.⁷⁷ The electrochemical reduction of O_2 in aprotic solvents typically occurs at $E = \pm (-1.0)$ V vs. SCE in the absence of protonic species or H_2O .^{66,76,78-80}

Although $O_2^{\cdot-}$ is considered as a superior nucleophile in aprotic solvents, due to the strong solvation and spontaneous disproportionation, there is no such reactivity exhibited in H_2O .^{74,81,82}

The organic chemistry of $O_2^{\cdot-}$ has been reported by numerous studies and many of these studies are related to the interaction of $O_2^{\cdot-}$ with various organic substances.^{77,83-92} It is now clear that $O_2^{\cdot-}$ displays four basic modes of action including deprotonation, H-atom abstraction, nucleophilic attack and single electron transfer.^{66,93}

3.8 Proposed Pathway 1

We first examined the total amount of charge passed for the reaction of isopropyl iodide with phenyl vinyl sulfone under the optimal conditions in **Table 3** (Entry 13). The charge–time graph is shown in **Figure 19** and shows a relatively smooth transfer of charge from the start of the reaction to the point where no more sulfone was observed. We have calculated that for a 1.2 mmol reaction scale (1.44 mmol of alkyl iodide), around 300 C of charge was passed which corresponds to no more than two moles of electrons per mole of alkyl iodide. This is extraordinarily efficient in terms of the amount of electricity used.

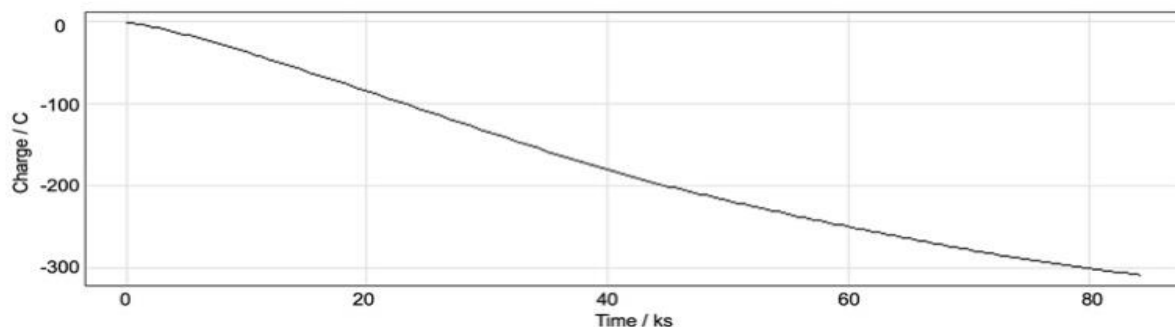
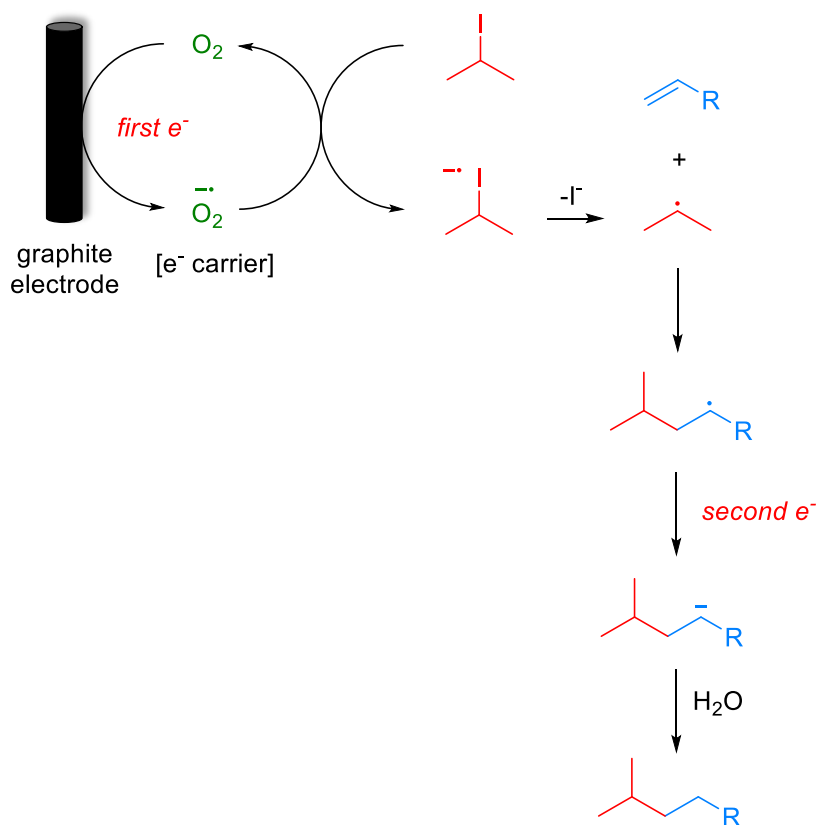


Figure 19 Charge transferred over the course of the reaction.

Given that we know that a small quantity of oxygen is required for a successful reaction, the first and simplest pathway we envisaged to explain the observed reactivity is outlined in **Scheme 37**.

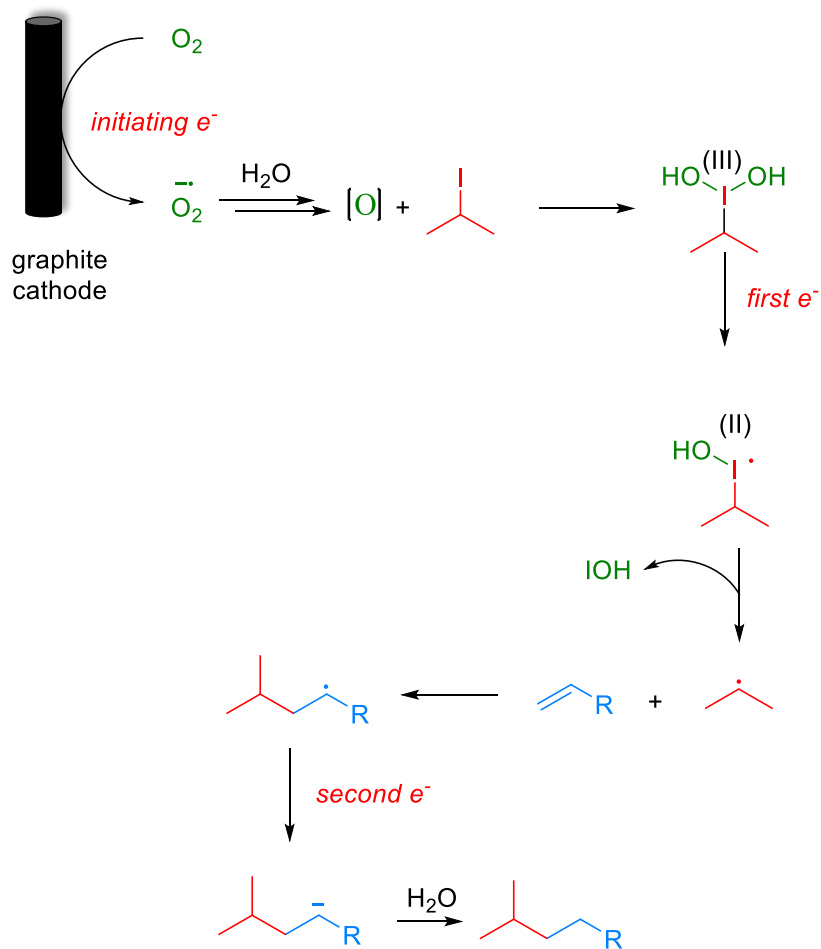


Scheme 37 Electron transfer pathway

Pathway 1 involves initial reduction of O_2 to generate superoxide which then acts as an

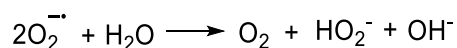
electron carrier, transferring the electron to σ^* of the C–I bond and liberating O_2 which is therefore, formally catalytic. This leads to collapse of the subsequent radical anion and the release of the required carbon-centred radical. Although this pathway is superficially attractive in its simplicity, we concluded that this pathway was unlikely to be in operation. Two experimental observations led us to this conclusion: firstly, as mentioned above, cyclic voltammetry of isopropyl iodide demonstrated that the alkyl halide is not reduced within the redox window of the solvent so it is unlikely that superoxide (which is relatively easily generated and with low reactivity in water as introduced before in the introduction part) will be a sufficiently powerful reducing agent to deliver an electron to σ^* of the C–I bond to effect homolysis. Secondly, entry 3 in Table 3 shows that water is an essential component for successful reaction, again suggesting that more reactive oxygen species are formed.

Based on this reasoning we proposed pathway 2 (**Scheme 38**), which is *via* a more powerful oxidative agent produced from oxygen and water under the electrochemical conditions. Although not identified at this stage, it is known that other powerful reactive oxygen species (ROS) are generated from $O_2^{\cdot-}$ under aqueous conditions. We therefore sought to proceed on this reasonable assumption.



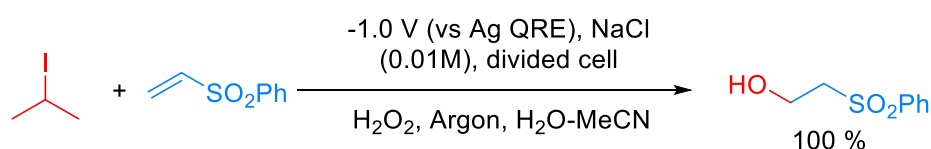
Scheme 38 Pathway 2 via hypervalent iodide

A previous study reported that in the absence of a proton source, $O_2^{\cdot-}$ is stable and reversible voltammetry for O_2 reduction was observed in several aprotic media.^{66,94} By contrast, when it applies to protic solvents, $O_2^{\cdot-}$ is highly reactive and spontaneously disproportionate in H_2O , forming O_2 and hydroperoxide anion (HO_2^-) (**Scheme 39**).^{66,94} The hydroperoxide anion would then easily react with another molecule of water or H^+ to form hydrogen peroxide.⁶⁶



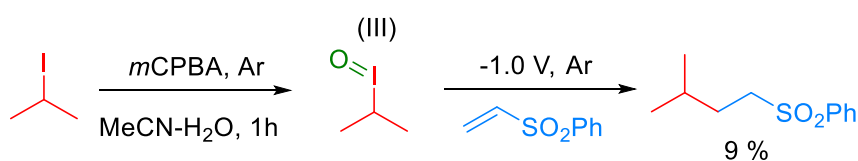
Scheme 39 $O_2^{\cdot-}$ disproportionation to oxygen and HO_2^- .^{66,94}

Now we begin to consider the possibility that under the acidic conditions employed, the reduction of molecular oxygen to give hydrogen peroxide could also be occurring and therefore this reactive oxygen species could be implicated in the process. To ascertain if this was the case, we also performed the reaction in the absence of oxygen but with hydrogen peroxide added dropwise. Under these conditions however, only the OH addition product was isolated rather than the radical addition product. (**Scheme 40**)



Scheme 40 H_2O_2 control experiment.

Despite this, we could not be sure that low concentrations of H_2O_2 were being generated in quantities that would not affect the alkene. Since direct addition of H_2O_2 yields only side product, we then switched our strategy to use *m*CPBA (meta-Chloroperoxybenzoic acid) as a replacement of H_2O_2 . *m*CPBA is stronger oxidant than H_2O_2 and is already known to be capable of forming hypervalent iodide and its excess can be easily removed after oxidation. Based on that, we have treated isopropyl iodide with 2 eq of *m*CPBA for 1 hour under argon in a 1:2 MeCN- H_2O mixture, followed by processing oxidised isopropyl iodide with our electrochemical conditions under argon (**Scheme 41**).



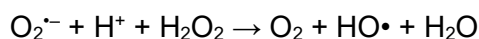
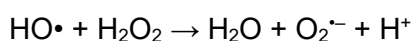
Scheme 41 *m*CPBA control experiment.

The isolated yield of radical addition product was only 9 % and consequently we concluded that hydrogen peroxide was unlikely to be a major player in the main reaction process, although it is possible that traces of H_2O_2 generated *via* initial reduction of aerial O_2 are responsible for initiation of the process.

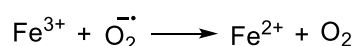
3.9 Introduction of Haber-Weiss cycle and Hydroxyl radical

Since hydrogen peroxide is not believed to be the key oxidant, we then considered other oxygen species that might originate from hydrogen peroxide. Among these ROS, the most powerful one should be hydroxyl radical, which is ordinarily produced *via* Haber-Weiss reaction. We believed that hydroxyl radical might be the ROS that responsible for the initial oxidation of the alkyl halide and trace metals (possibly the iron from clay of graphite rod) in the reaction could be responsible for the generation of hydroxyl radical and the observed reactivity and as such, we chose to examine the literature precedent in the area.

In 1932, Haber and Willstätter first reported the following chain reactions⁹⁵:

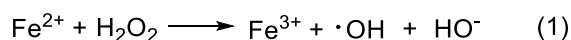


The two reactions were then commonly known as the Haber-Weiss cycle.^{95,96} The second reaction is a net reaction, which is kinetically slow but could be catalysed by dissolved iron ions.^{95,96} The first step of the catalytic cycle involves the reduction of the ferric (Fe^{3+}) ion into the ferrous (Fe^{2+}) ion^{95,96}:



The second step is known as Fenton reaction. In 1876, Fenton's pioneering work pointed out the possibility of destroying tartaric acid by using a mixture of H_2O_2 and Fe^{2+} .^{96,97} However, the most recognised starting point of Fenton's chemistry was not until 1894 when a deeper study on the strong promotion of the oxidation of this acid with such a reagent was published by Fenton.⁹⁸ From 1901 to 1928, the stoichiometry of the reaction between H_2O_2 and Fe^{2+} has been studied by Manchot and coworkers^{96,99}. Especially after the Haber Weiss cycle had been reported, the Fenton reaction became extraordinary useful for the oxidation of organic compounds. Mechanistic studies and valuable discussions about Fenton's reaction have been extensively reported by Merz,¹⁰⁰ Barb et al.,^{101,102} Walling,¹⁰³ and Prousek,¹⁰⁴ after that, in the mid-1960s widespread interest in Fenton's reagent as an application to oxidize toxic organics has been widely applied.¹⁰⁵

The generally accepted mechanism of the Fenton process is initiated by the formation of hydroxyl radical in accordance with the classical reaction, (1):^{95,96,106-110}



When takes place in acidic medium, such reaction can alternatively be written as:⁹⁶



The generation of hydroxyl radical in this process has been very well defended by Walling^{96,111} and confirmed using chemical probes or spectroscopic techniques (eg. spin trapping).^{96,112}

Alternatively, trace amounts of iodide present in the alkyl halide starting materials could also be responsible since H_2O_2 and iodide under acidic conditions has been suggested as a source of hydroxyl radicals in iodine-based chemical oscillators.^{96,113} During this procedure, $\text{HO}_2\cdot$ will also be produced, however, such ROS exhibit such a low oxidization power and is quite inert to organic matter compared with hydroxyl radical.^{96,114}

After getting the literature precedent of the Fenton reaction, we then examined the addition of iron(II) sulfate to the reaction medium in order to catalyse the formation of hydroxyl radicals from any putative hydrogen peroxide in the solution,¹¹⁵ in the hope that this might accelerate the rate of these reactions. However, no effect was observed on the reaction and now we can exclude the hypothesis in the first paragraph of this part that the hydroxyl radical is unlikely to be produced *via* trace metal catalysis.

3.10 Detecting hydroxyl radical by Photoluminescence spectroscopy

Ordinary methods are normally not available to detect reactive oxygen species.¹¹⁶ These obstacles are caused by some characteristics presented by these ROS such as very short lifetime and the capable of being captured by variety antioxidants in *vivo*.¹¹⁶ The fluorescence methodology, associated with the use of suitable probes, is an excellent approach to measure ROS due to their high sensitivity, simplicity in data collection, and high spatial resolution in microscopic imaging techniques.¹¹⁶ In this part, we have introduced the photoluminescence spectroscopy mainly for demonstrates that hydroxyl radical is in abundance in our system and as such Sodium terephthalate was selected as our fluorescence probe. Sodium terephthalate is a non-fluorescent compound that reacts with hydroxyl radical and forms an aromatic hydroxylated product, sodium 2-hydroxyterephthalate, which has strong fluorescence ($\lambda_{\text{excitation}} \approx 310 \text{ nm}$, $\lambda_{\text{emission}} \approx 430 \text{ nm}$) (Figure 20)¹¹⁸

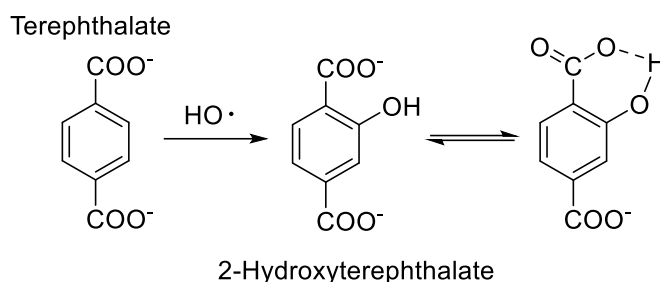


Figure 20. Reaction of terephthalate with hydroxyl radical to produce 2-hydroxyterephthalate.¹¹⁷

Accordingly, there are already some examples of using sodium terephthalate to trap the hydroxyl radical and form the fluorescence product. Tang et al have developed a method of using a flow injection spectro-fluorimeter to measure the fluorescence product.^{116,117} This method is using H₂O₂ and Co²⁺ to produce hydroxyl radical and the optimum pH range for the aromatic hydroxylation was 6.80–7.90.^{116,117}

Before probing our reaction system with sodium terephthalate, a classic Fenton reaction was firstly carried out in the presence of this molecular probe to validate this approach.¹¹⁸ An aliquot of the reaction mixture was extracted, and the fluorescence emission was recorded. By comparing that emission spectrum (**Figure 21**, blue curve) with the emission spectrum of unreacted sodium terephthalate (**Figure 21**, black curve), hydroxyl radicals were detected, giving rise to the intense fluorescence emission at 430 nm. By applying this technique to the cathodic chamber of the reaction vessel where radical cyclisation of *N*-allyl-*N*-(2-iodoethyl)-4-methylbenzenesulfonamide (**Scheme 35**) occurred, the same emission was observed (**Figure 21**, red curve), confirming the presence of hydroxyl radicals in the reaction mixture.

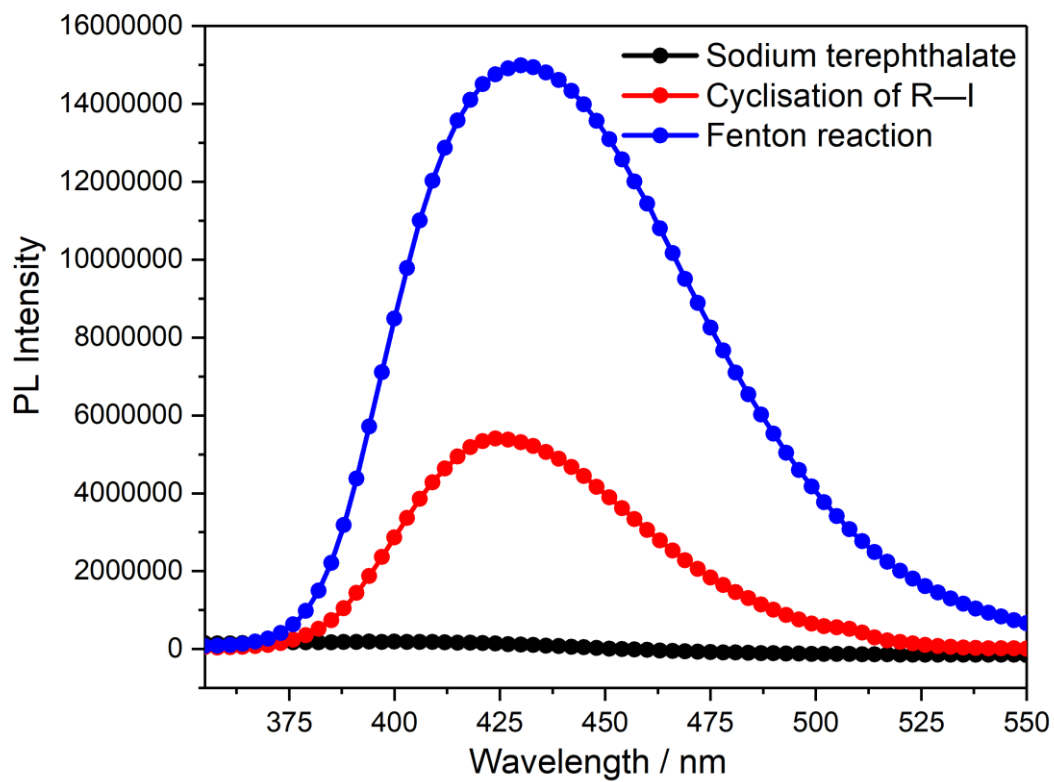


Figure 21 Sodium terephthalate in Fenton conditions, itself and cyclisation of R-I condition.

With this encouraging result in hand, the focus was switched to examine the origin of hydroxyl radicals in the reaction vessel (Figure 22).

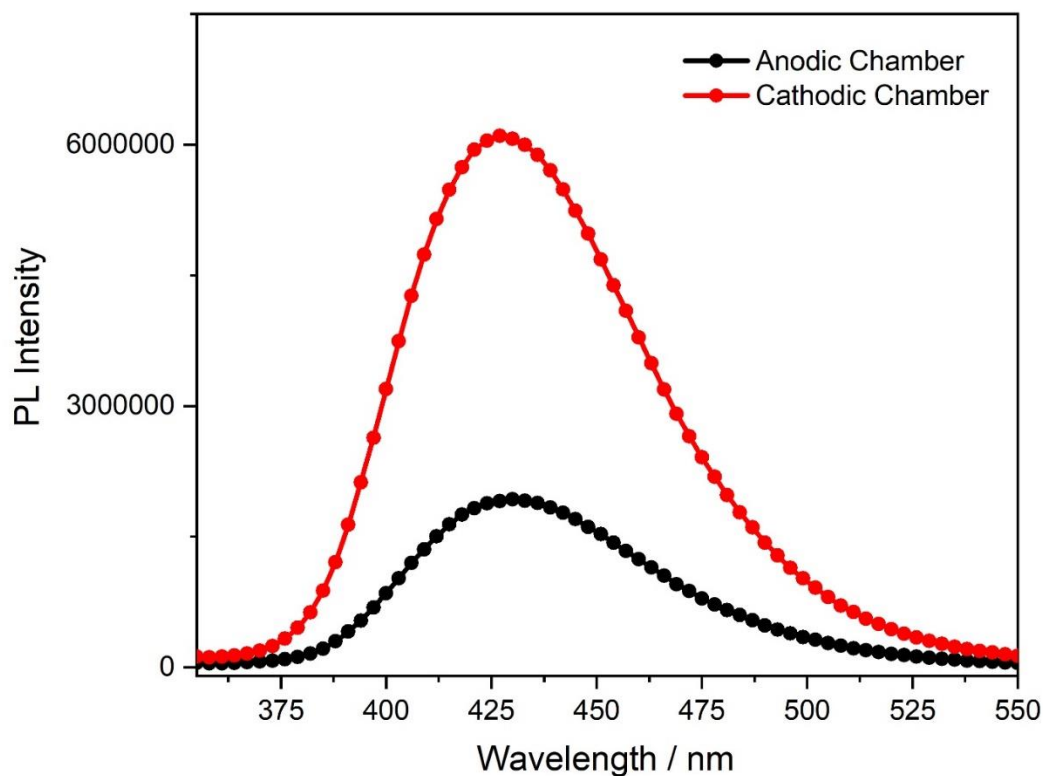
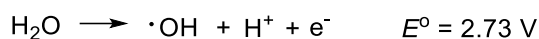
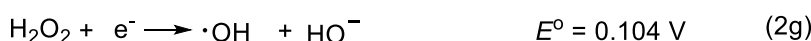
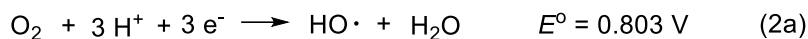


Figure 22 Sodium terephthalate in anodic and cathodic chamber.

Sodium terephthalate was added to a solution of acetonitrile-water (pH 3.6) with sodium chloride as the electrolyte and exposed to a mild reducing potential (constant potential, -1.0 V vs. Ag wire quasi-reference electrode, graphite rod working electrode, divided cell). It is observed that hydroxyl radicals are present at both the anodic and cathodic chambers, but they are relatively more concentrated at the cathodic chambers. This observation is somewhat counterintuitive because compared with the anodic chamber, the hydroxyl radical should be relatively less stable in cathodic chamber where they could be reduced to hydroxide ions. We have attributed the relative low concentration of hydroxyl radicals in the anodic chamber to the formation of ozone, *via* a relatively well-understood process, allow it in the gaseous state.¹¹⁹ In addition to the commonly seen anodic production of hydroxyl radicals from water (Scheme 42), the formation of hydroxyl radicals at the cathodic chamber is possible *via* various one-electron redox reactions (Scheme 43, equations 2a – 2g) under the operating potential.¹²⁰⁻¹²²



Scheme 42 Oxidative formation of hydroxyl radical.¹²⁰⁻¹²²



Scheme 43 Formation of reactive oxygen species equations 2a – 2g.¹²⁰⁻¹²²

The operative reactions generate oxygenic radicals which would lead to the formation of hydrogen peroxide and homolysed to form hydroxyl radicals. This would also indicate that a buffered acidic solvent system would be essential for the steady formation of hydroxyl radicals at the cathodic chamber to facilitate the radical reactions of alkyl iodides. Moreover, the auto-decomposition of hydrogen peroxide which could homolyse into hydroxyl radicals would be inhibited at a low pH environment. At higher pH, the decomposition of hydrogen peroxide into molecular oxygen and water would be dominated, limiting the supply of hydroxyl radicals and, therefore, lead to no reactivity.¹²³

Lastly, the effect of alkyl iodide on the consumption of hydroxyl radicals was examined. Control experiments have shown that the relative concentration of hydroxyl radicals decreases when *N*-allyl-*N*-(2-iodoethyl)-4-methylbenzenesulfonamide is present (**Figure 23**) and indicated that hydroxyl radicals are involved directly in facilitating the radical cyclisation of *N*-allyl-*N*-(2-iodoethyl)-4-methylbenzenesulfonamide.

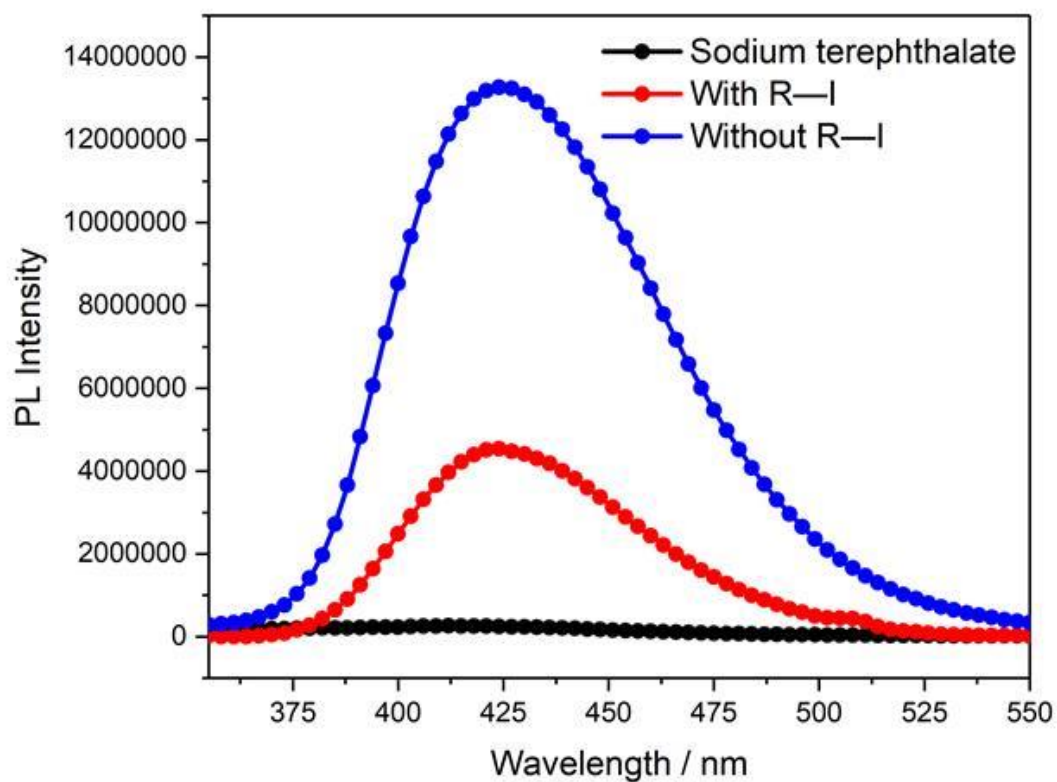
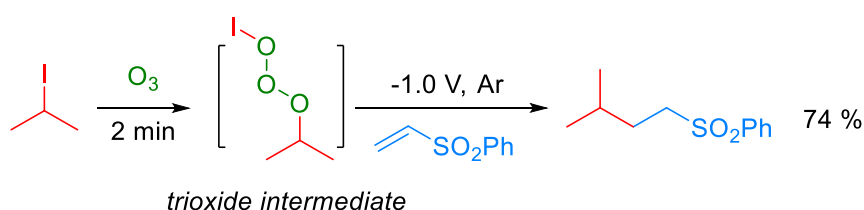


Figure 23 Hydroxyl radical consumption examination.

As such we believe that the presence of hydroxyl radical as a key player in this reaction has been confirmed.

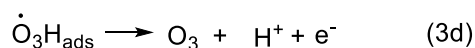
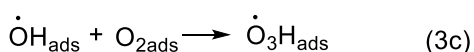
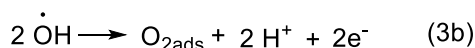
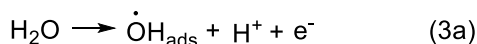
3.11 Electrochemical generation of ozone

As 3.10 part has suggested the relative low concentration of hydroxyl radicals in the anodic chamber might be caused by the formation of ozone which might be another key reactive oxygen species, then exposure of the alkyl iodide to ozone for several minutes follow by cathodic reduction at the potential that applied for our former reaction should give us the terminal product. Such control experiment has successfully yielded the desired terminal radical addition product in high yield. (**Scheme 44**)



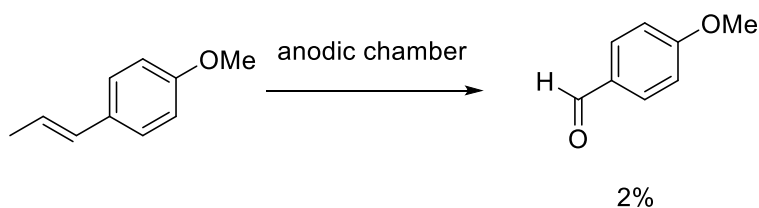
Scheme 44 Ozonolysis control experiment.

It is postulated that ozonation of isopropyl iodide produced an unstable trioxide intermediate, which decomposes into the corresponding alkyl radical, IO· radical and molecular oxygen to initiate the radical reaction.^{124,125} The proposed trioxide intermediate is analogous to the reaction between aqueous ozone with halide anions as well as alkanes.¹²⁴⁻¹²⁷ The necessity of molecular oxygen and water in the reaction vessel could be explained by the requirement of ozone production electro-catalytically. Since the formation of ozone involves the hydroxyl radical and the adding of hydroxyl scavenger inhibited the reaction, the ozone formation process is suggested relying on the reaction between adsorbed hydroxyl free radicals and molecular oxygen at the anode (equations 3a – 3d, **Scheme 45**).¹¹⁹



Scheme 45 Electro-catalytic ozone production.¹¹⁹

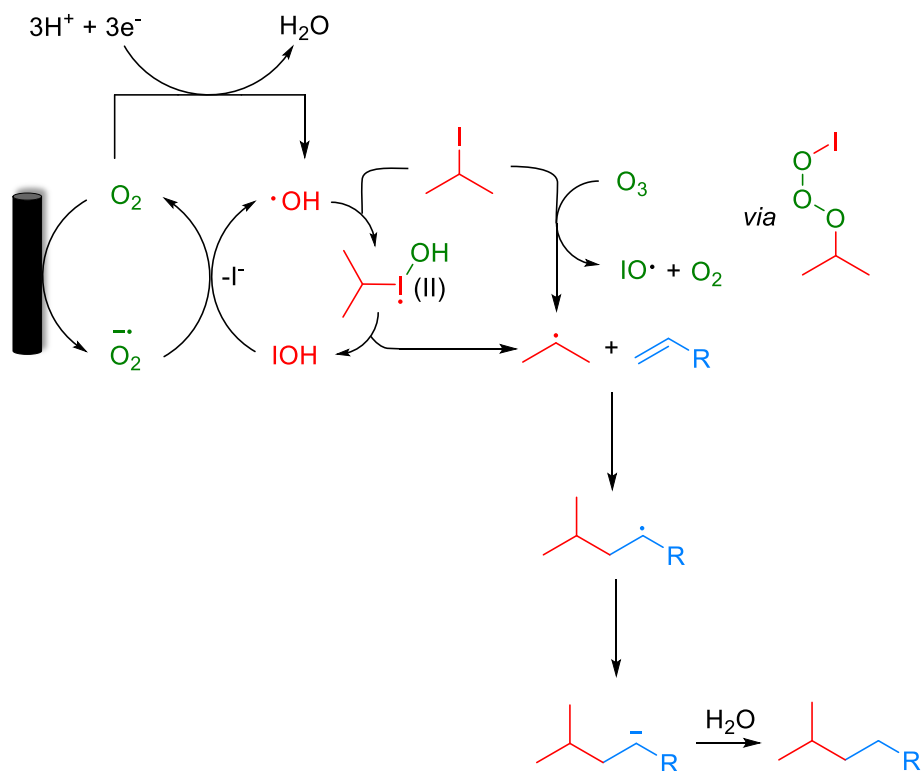
Although the operating potential (-1.0 V), which is actually the potential difference between the working and reference electrodes, is much lower than for the literature value of direct oxidation of water to ozone ($E^\circ = 1.51$ V), direct oxidative production from water to ozone is still likely to occur.¹²⁰ This has been demonstrated by our measurement of the real potential value between working electrode and counter electrode (3.5 V). To further validate this hypothesis, Dr Tsz Kan Ma, the postdoc of my group has added excess ethyl vinyl ether to the anodic chamber to quench the ozone generated from the anode where another sample of isopropyl iodide and phenyl vinyl sulfone were subjected to the standard conditions in the cathodic chamber. Indeed, addition of ethyl vinyl ether completely terminated the reaction and the substrates are fully recovered. However, due to the high volatility of the aldehyde products, he only got a crude NMR for the reaction mixture. In order to get a more convincing result, anethole was then subjected to the reaction condition at the anodic chamber which resulted in the formation of the corresponding 4-methoxybenzaldehyde (2%) (**Scheme 46**). The ^1H NMR spectrum of the aldehyde is showing in the appendix. Now, it could be concluded safely that ozone as the key factor in our reactive pathway is rapidly consumed by those alkenes in a standard ozonolysis process and a key link is removed from the pathway.



Scheme 46 Evidence for ozone existence in anodic chamber.

Following with the results of these experiments, we propose the following mechanism for the generation of alkyl radicals (**Scheme 47**). Two productive reaction pathways are responsible for the oxidation of the alkyl iodide. The reaction is initiated by the generation of ozone at the anode *via* an electro-catalytic process and the resulting ozone is reacted with the alkyl iodide in the cathodic chamber, by slow diffusion in the closed divided cell. Reaction between ozone and alkyl iodide generated an unstable trioxide intermediate that is subsequently fragment into the corresponding alkyl radical, IO· radical and molecular oxygen. The generated IO· radicals lead to the accumulation of hypoiodous acid that is known to react with superoxide radicals to yield highly reactive hydroxyl radicals to oxidise more alkyl iodides into the corresponding unstable I(II) species that fragment to yield hypoiodous acid and alkyl radicals.¹²⁸ As a result, alkyl iodides could be activated by both productive pathways. Furthermore, additional redox reactions of molecular oxygen and hydrogen peroxide would also supply more hydroxyl

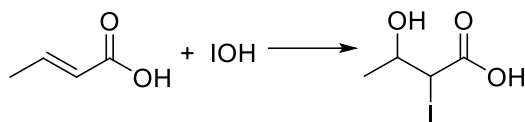
radicals to facilitate the radical reaction of alkyl iodides.



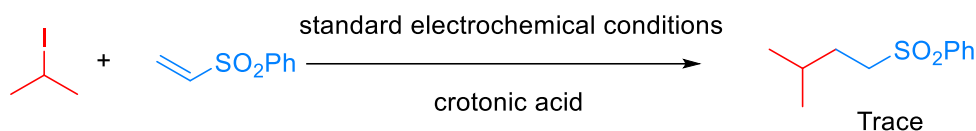
Scheme 47 Plausible mechanism for the generation of alkyl radicals.

3.12 Evidence for IOH in the reaction

As shown in **Scheme 47**, IOH was proposed to be another important ROS in the reaction. Thus, we need to prove the existence of IOH as well as its involvement in the reaction process. However, since it is not possible to isolate IOH, the strategy of adding an IOH scavenger could be viable evidence to prove its existence. Crotonic acid, with the ability of forming iodohydrin with IOH, has been reported as an effective IOH scavenger (**Scheme 48**),¹²⁹ was added to our reaction mixture. As expected, the addition of crotonic acid stopped the reaction. (**Scheme 49**)



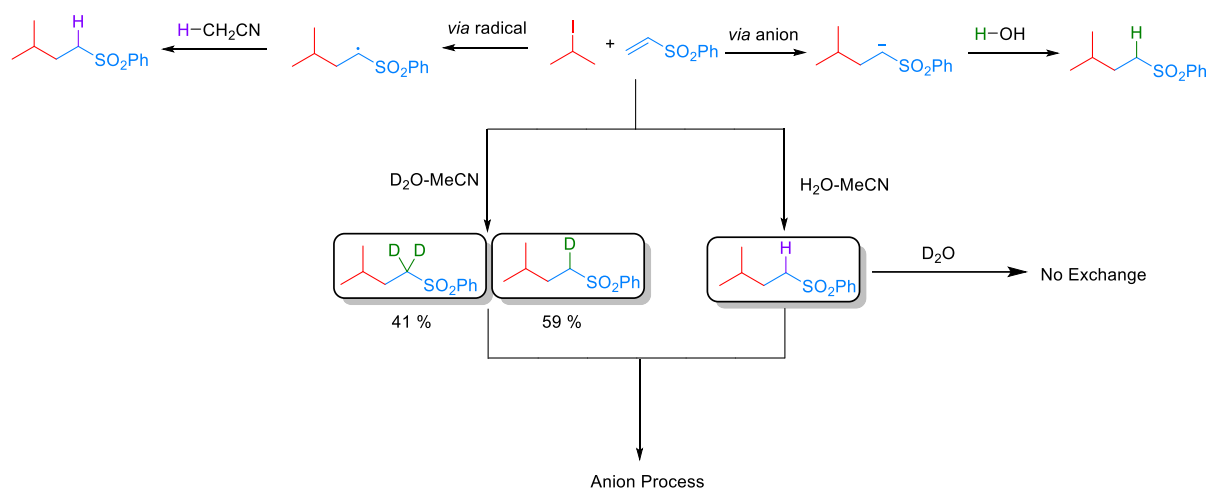
Scheme 48 Iodohydrin formation between crotonic acid and IOH.¹²⁹



Scheme 49 Crotonic acid attenuates the radical addition reaction.

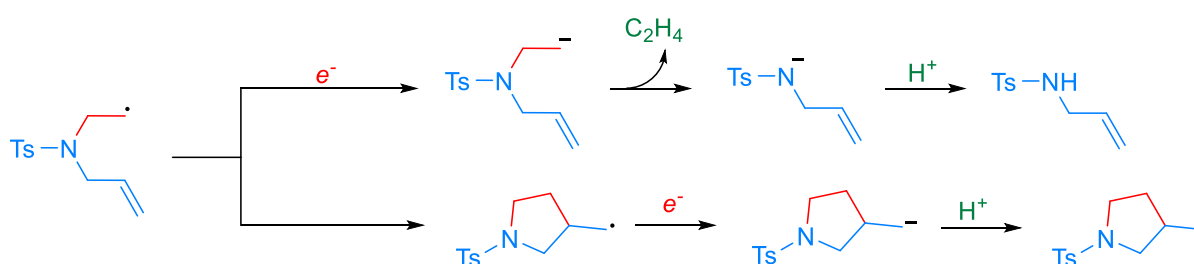
3.13 Other mechanistic aspects

We also wished to demonstrate that the intermediate radical after addition is reduced by an electron transfer step resulting in an anion which is then quenched by a proton from the aqueous reaction medium rather than a radical hydrogen atom transfer step (most likely from acetonitrile). This was easily achieved by performing the reaction in a D₂O–MeCN mixture as shown in **Scheme 50**. Performing the reaction in this way led to deuterium incorporation adjacent to the sulfonyl group. To check that the alkyl sulfone was not simply undergoing exchange after the reaction had occurred, we also subjected the undeuterated alkyl sulfone to the reaction conditions for 72 h. No deuterium incorporation was observed.



Scheme 50 D₂O–MeCN control experiment.

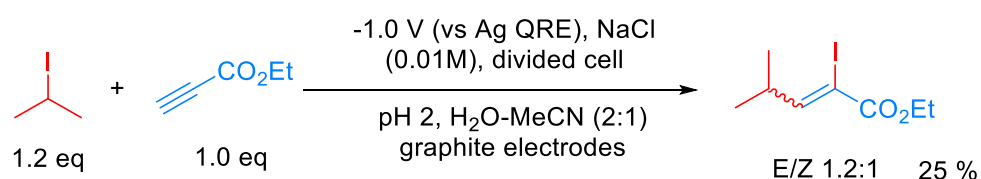
Now, with all these results in hand, the reactivity of *N*-allyl-*N*-(2-iodoethyl)-4-methylbenzenesulfonamide first discussed in section 3.5 could also be rationalised as follows (**Scheme 51**): Once the primary radical is formed, there are two competing reaction pathways lead to the formation of pyrrolidine and *N*-allyltosylamide. When the primary alkyl radical is reduced by the electrode, the resulting anion would then undergo rapid elimination to produce ethene and an anionic intermediate, which could be protonated to give *N*-allyltosylamide. Another pathway involves the reaction of the primary radical with the allyl group *via* an intramolecular pathway to give a cyclised primary radical intermediate, which can then be reduced by the electrode to the corresponding anion to be protonated and form the pyrrolidine.



Scheme 51 Reductive cyclisation of *N*-allyl-*N*-(2-iodoethyl)-4-methylbenzenesulfonamide.

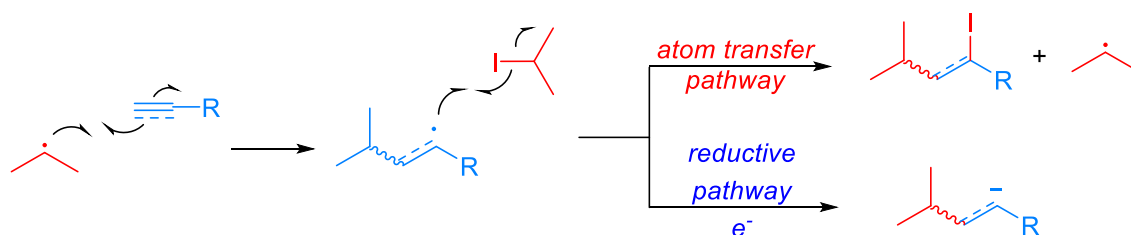
3.14 Extending the methodology to alkynes

With some understanding of the reaction mechanism and some excellent results employing alkenes, we were keen to test our methodology with alkynes to discover if they would be suitable partners for intermolecular radical reactions. Consequently, we employed our optimised conditions from **Table 3**, replacing the alkene acceptor with ethyl propiolate (**Scheme 52**). To our surprise, we isolated not the expected reduced addition product, but the addition product as the α -iodo alkene as a 1.2:1 mixture of *E* and *Z* isomers. The electrochemical conditions appear to have promoted the atom transfer radical addition (ATRA) reaction in this case.



Scheme 52 Radical addition reaction of ethyl propiolate.

The results are consistent with the experiments of Curran, who achieved the same transformation employing heat and dibutyl tin.¹³⁰ Presumably the mechanism outlined in **Scheme 53** is in operation.



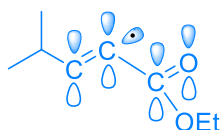
Scheme 53 proposed two competitive pathways.

We have attributed this observation to the stability of the intermediate radical B.



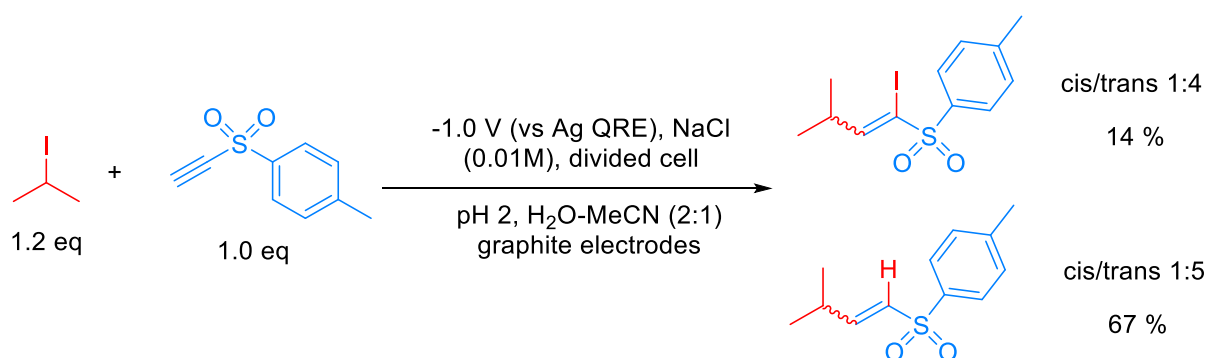
Radical B

In our previous reactions with alkenes the intermediate radical is directly resonance stabilised by the adjacent electron withdrawing group. In the example outlined in [Scheme 52](#) however, the intermediate will be a highly reactive vinyl radical not directly stabilised by the adjacent ester ([Scheme 54](#)).



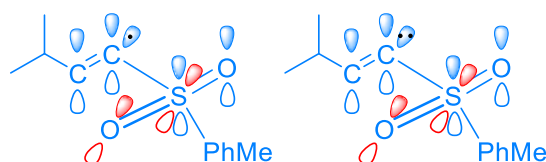
Scheme 54 Radical not stabilised by the adjacent ester

As such, presumably the rate of iodine atom abstraction is significantly faster than reduction to give a similarly unstabilised vinyl anion. Support for this hypothesis is observed when 4-methylphenyl ethynyl sulfone is employed as the reacting partner ([Scheme 55](#)). The product of this reaction is a mixture of the atom transfer reaction and reduction.



Scheme 55 Radical addition reaction of 4-methylphenyl ethynyl sulfone.

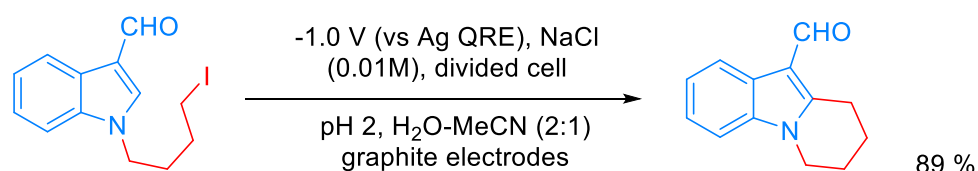
This is explained by the fact that although still highly reactive, both the vinyl radical and anion obtain some degree of stabilisation *via* $n-\sigma^*$ interactions between the radical or anion and the C–S σ^* orbital (**Scheme 56**).^{131,132} As such in this case, both pathways are competitive in terms of rate.



Scheme 56 Radical and anion partially stabilised

3.15 Extending the methodology to redox-neutral intramolecular cyclisation

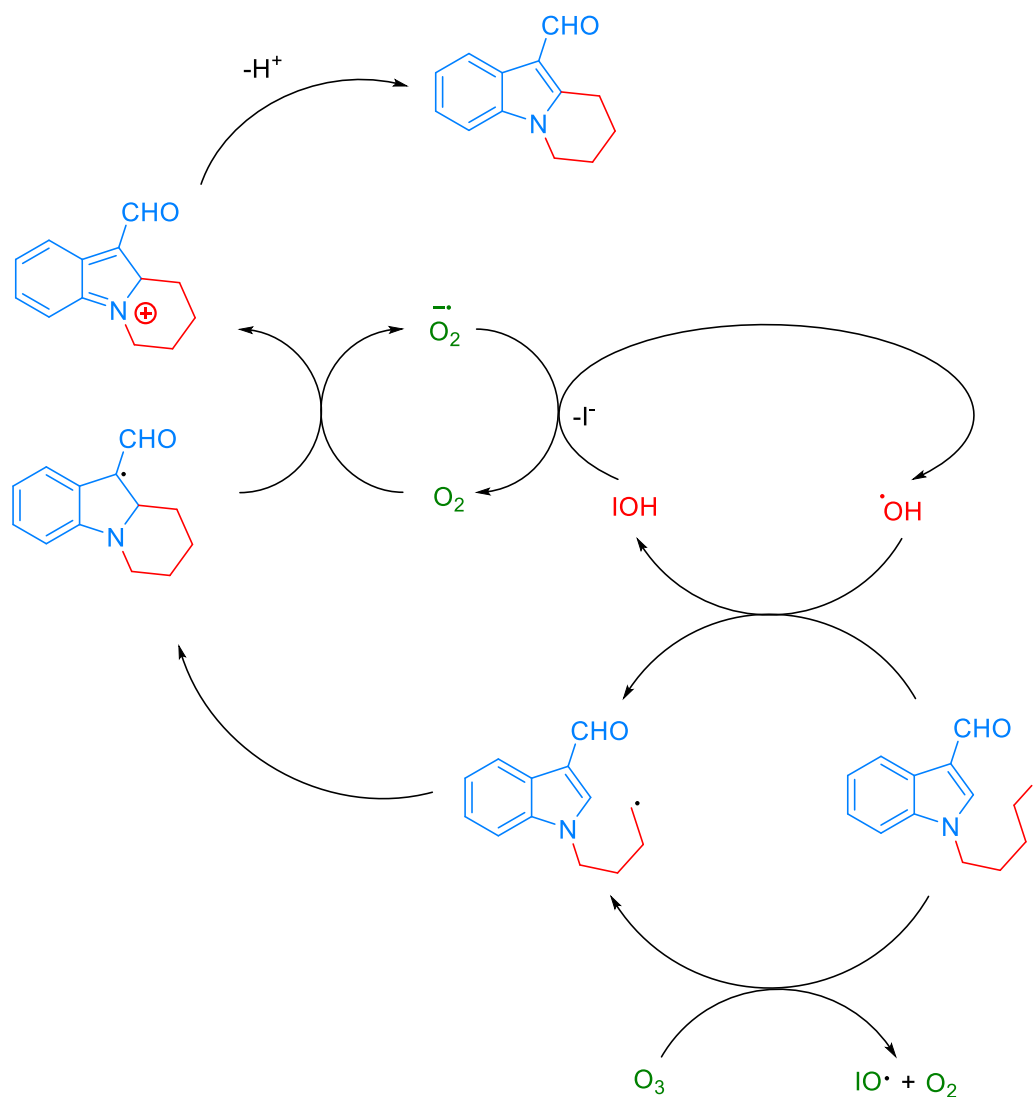
Finally, with such encouraging intermolecular radical processes and normal reductive intramolecular cyclisation in hand we also wanted to examine if our conditions could be applied to redox-neutral intramolecular cyclisation to aromatic systems. Accordingly, we prepared 1-(4-iodobutyl)-1Hindole-3-carbaldehyde. Pleasingly, exposure of this molecule to our conditions led to the cyclised, oxidised system in excellent yield (**Scheme 57**).



Scheme 57 Redox-neutral intramolecular cyclisation.

Although it is tempting to assume that the oxidative cyclisation would require an excess of molecular oxygen to deliver the observed product, we did not perform this reaction under such conditions but rather using the optimised procedure outlined in **Table 3**. The rate and efficiency also seemed to be comparable (or better) than the other examples in **Table 4** suggesting that adventitious aerial oxygen was not responsible for this observation. In 1991 Bowman suggested a pseudo $S_{RN}1$ process to explain this phenomenon for tin mediated cyclisations to aryl systems in the absence of any other oxidising agent, where the radical resulting from

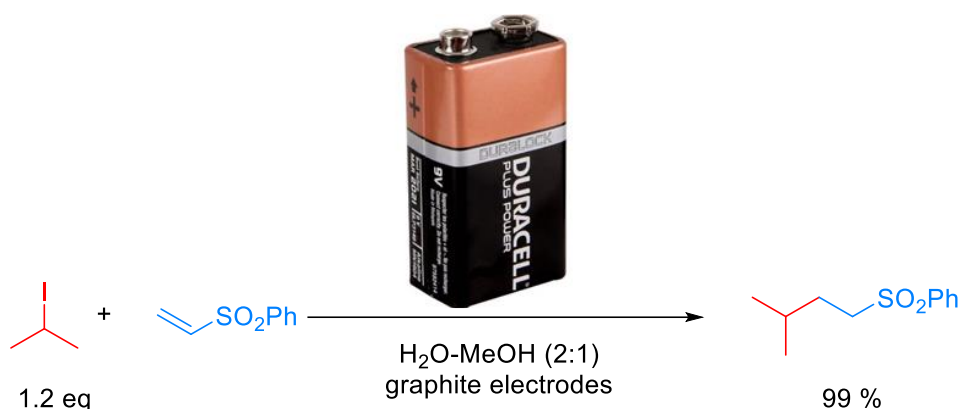
cyclisation is a powerful single electron donor capable of activating another molecule of iodide.¹³³ This explanation was also favoured by Moody for the Bu_3SnH mediated cyclisation of the same frameworks as those outlined in **Scheme 57**.¹³⁴ For our system following electrochemical initiation, this would lead to a self-perpetuating combination of three different cycles leading to the oxidised product as illustrated in **Scheme 58**.



Scheme 58 Likely pathway for redox-neutral cyclisation.

3.16 Trials with battery and Photo-electrochemistry

As illustrated at the history part before, one factor that restricts the development of electro organic chemistry is the expensive electrochemical equipment which is off-putting for non-experts. With an aim of make electro-organic chemistry set-up as easy and accessible as possible, we have also aimed to use a cheap supermarket purchased battery as a substitution for the more expensive dedicated potential stat in our laboratory. This is based on measuring the potential difference between the two electrodes at the two electrodes system with working and counter electrodes only. By doing this, we established that a common 9-volt battery might be suitable to be applied to our apparatus in place of the potentialstat. To our delight, substituting the potentialstat for the battery led to the desired radical reaction and the product being isolated in excellent yield. ([Scheme 59](#))

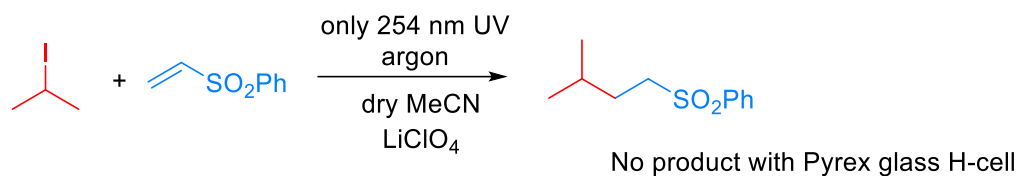


Scheme 59 Battery promoted radical addition reaction.

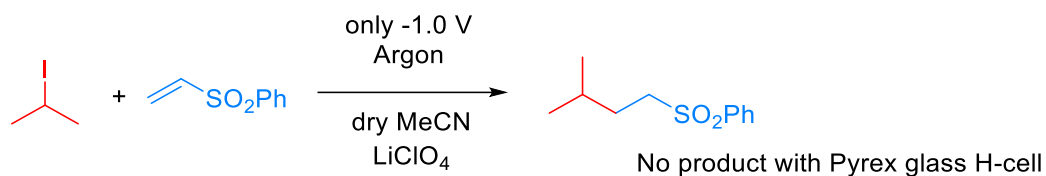
Inspired by the two-step oxidation-reduction process of the mechanism, we have targeted the second extension of our newly developed electrochemical methodology for carbon centred radical combing with photochemistry. As photochemistry is already a developed method for organic synthesis which could provide novel approaches, while electrochemical method is highly selective and could directly add or remove electrons from substrates without using expensive photocatalyst, combination of the two, might allow the development of powerful new methods which exploits their respective strengths. We wondered if the application of UV light could lead to the oxidation of the alkyl halide which could then be reduced by the cathode. This would obviate the requirement for O_2 to be present and the subsequent generation of ozone. Ultimately this would allow the reaction to occur under even milder conditions.

Accordingly, we performed the following control experiments ([Scheme 60](#), [61](#), [62](#)). As the reaction was performed with a simple UV torch, a professional UV box might be helpful to

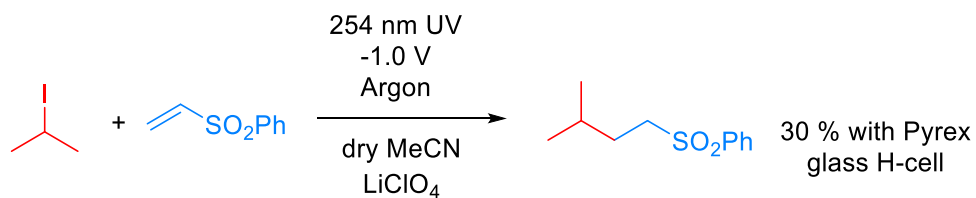
increase the yield. Besides, this approach has allowed to be applied at a pure organic solvent, which is promising for further cross-over reaction.



Scheme 60 Pure photoredox reaction under argon condition



Scheme 61 Pure electrochemical reduction under argon condition

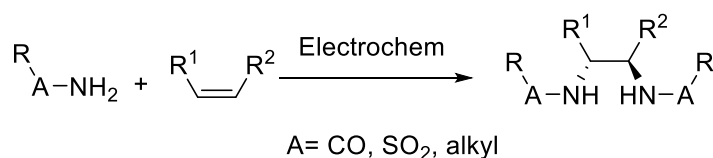


Scheme 62 Photoelectrochemical reaction under argon condition

Chapter 4 Conclusions and future work

In conclusion, some major progress has been made in several iodide-based reactions using electrochemistry.

We have firstly established an electrochemical method of generating both I₂ and Zn(II) Lewis acid *in situ* from stable and non-toxic starting materials which can then be employed to effect efficient iodocyclisation. This green and sustainable protocol is competitive with the traditional method of employing bulk reagents. Furthermore, mechanistic investigations reveal that the reaction pathway involves a transient iodoxyphenolic intermediate which is the active oxidant. We have also shown that excessive iodination of the activated phenolic rings is avoided *via* a reversible deiodination process and that the cyclised dihydrobenzofuran is less activated towards iodination which leads to extremely good yields of the desired products. Early-stage extension of this approach to aniline has successfully revealed a novel one step diamination of alkene. Future work on this part will be focused on utilizing different amines and amides to do the diamination reaction ([Scheme 63](#)).



Scheme 63 Diamination reaction to alkene.

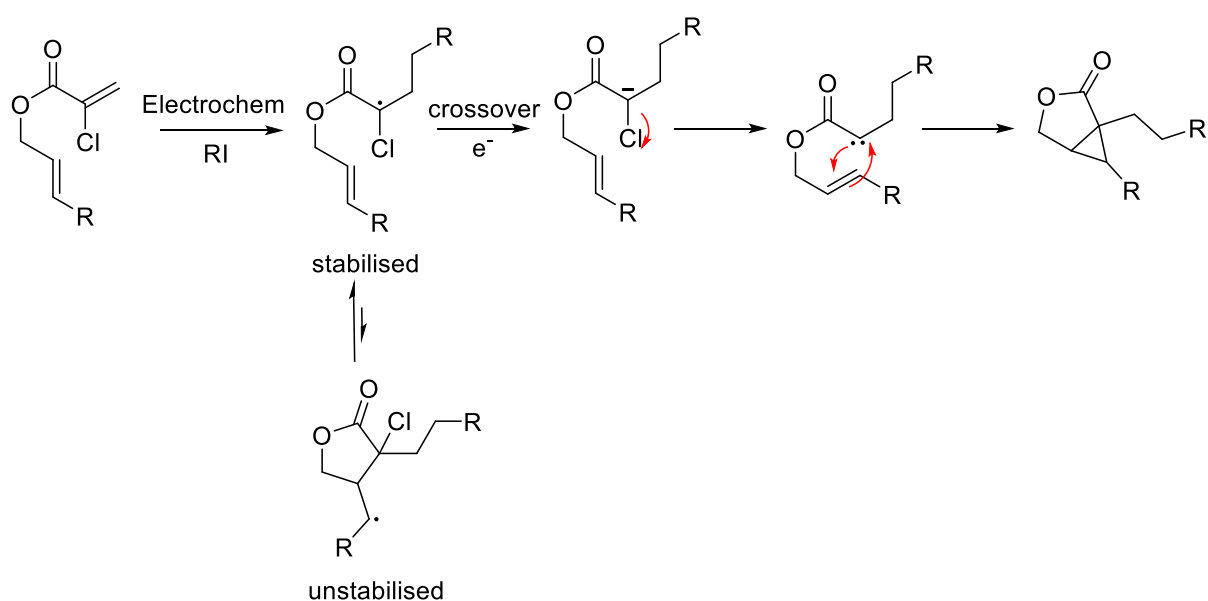
We then described a new electrochemical approach to performing intermolecular radical addition reaction as well as intramolecular radical cyclisation reactions between different alkyl iodides and a variety of alkene and alkyne acceptors. The conditions employed are environmentally benign and compatible to water and air conditions as well as various functional groups. The yield and efficiency of the reaction often exceeds the classical method employing tin reagents. We have described the reaction mechanism as initiated by electrochemically generated ozone, where alkyl iodides are first ozonolysed to yield an unstable intermediate that fragments into the corresponding alkyl and IO radicals as well as molecular oxygen. This activates a superoxide radical and hypoiodous acid mediated 'redox relay' reaction sequence to oxidise more alkyl iodides into the corresponding unstable I(II) species to produce more alkyl radicals. The use of sodium terephthalate as a fluorescence

molecular probe provided insight to the role of hydroxyl radicals in this reaction sequence. We have also successfully undertaken the reaction with a cheap supermarket purchased battery as replacement of expensive electrochemical equipment. This allows an easy and cheap access to this area for those inexperienced in electrochemical synthesis. In addition, an early stage photoelectrochemical approach has also been built which extended the reaction applied range in aprotic and degassed environment.

Further studies on other radical reactions with this electrochemical approach are ongoing in our laboratory, ideas can be mainly concluded into three parts:

1, Crossover reaction:

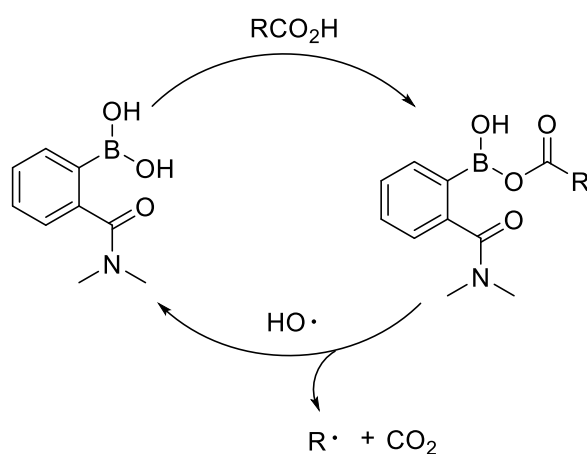
Cyclopropane group is very useful in organic synthesis while its formation would normally recourse to hazardous diazo compounds. Here, this disadvantage might be circumvented *via* crossover reaction. It should be possible to affect a radical addition to an electron deficient alkene bearing a leaving group, which upon crossover, then yields a carbene which could be trapped by an internal π -bond to yield cyclopropanes. Such highly functionalised and chemically malleable frameworks are highly sought after in the early stages of synthetic routes. With the particular example in [Scheme 64](#), the intramolecular radical ring closure could occur prior to crossover. However, this step would be expected to be reversible due to the stability of the two alternative radicals. Even if the radical cyclisation is faster than carbene formation however, rapid reduction of the less stable radical would lead to an anion which would displace the adjacent chloride to yield the same product as would be expected from a carbene pathway.



Scheme 64 An example of crossover reaction.

2. Extension with hydroxyl radical (**Scheme 65**):

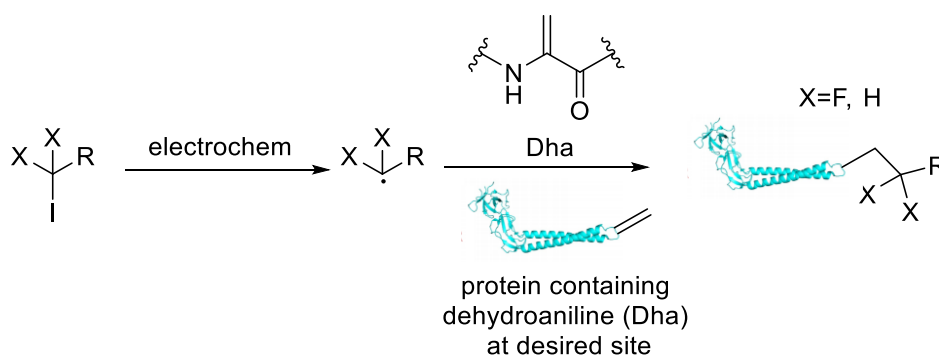
Employ an aryl boronic acid might be an interesting alternative to a halide atom in the mediator. Boron compounds are known to react with radical oxygen species to eject various radical species as well as reacting reversibly with carboxylic acids to give the boronate ester anhydrides. Such approach will allow the radical to be generated in a controlled manner and the presence of the mediator will prevent the rapid dimerization that has often dogged oxidative electrochemical attempts to generate C-centred radicals *via* decarboxylation (normally promoted with silver and copper). In addition, no metal catalyst is required fits with my ambition to undertake green and sustainable transformations.



Scheme 65 An example of ROS extension.

3. Use for protein post-translational modifications (**Scheme 66**):

Post-translational modifications greatly expand the structures and functions of proteins in nature, but these modifications are normally processed using photocatalysis. Here I might could further apply the developed electrochemical method to do such modification without using photocatalysts.



Scheme 66 An example of protein post-translational modification.

Chapter 5 Experimental

5.1 General Information (Chapter 2)

All solvents and reagents were purchased from suppliers and used directly without any further purification. Biotage automatic column (IS11579109) was used for column chromatography. All reactions were monitored by TLC except where specifically mentioned. TLC plates pre-coated with silica gel 60 F254 on aluminium (Merck KGaA) were used, detection by UV (254 nm) and chemical stain (potassium permanganate). Mass spectra were measured on Thermo Finnigan MAT900 XE and Waters LCT Premier XE machines operating in EI, and ESI modes. ^1H NMR and ^{13}C NMR spectra were recorded at 400 and 600 MHz and 100 and 150 MHz respectively on Bruker Avance spectrometers at ambient temperature. All chemical shifts were referenced to the residual proton impurity of the deuterated solvent. In ^1H NMR the multiplicity of the signal is indicated as s (singlet), d (doublet), t (triplet), dd (doublet of doublets), dt (doublet of triplets), dq (doublet of quartets), ddt (doublet of doublet of triplets), and m (multiplet), defined as all multiplex signals where overlap or complex coupling of signals makes definitive descriptions of peaks difficult. Coupling constants are defined as J and quoted in Hz to one decimal place. Infrared spectra were obtained on a Bruker Alpha FTIR Spectrometer operating in ATR mode. Melting points were measured with a Gallenkamp apparatus and are uncorrected. For NMR experiments, CDCl_3 denotes deuterated (d_1) chloroform. Electrochemical reactions were carried out using an Ivium Technologies Vertex model potentiostat operating in chronoamperometry mode. CV plots were measured using the same machine with a glassy carbon working electrode, silver wire reference electrode and Pt wire counter electrode.

5.2 Details of Electrochemical Methods (Chapter 2)

The general experimental setup we used for electrochemical reactions was designed to be as simple and accessible as possible. In doing so we hope to minimise the disparity and lack of reproducibility of results inherent in electro-organic synthesis due to there being a lack of standardised experimental setups. For all reactions we used a divided 'H' cell as our reaction vessel (dimensions shown in **Figure S1**) with each chamber having a size B19 ground-glass neck and a total volume of 20 mL. A semi-porous sintered glass divider sits between each

chamber. All reactions were however carried out using 10 mL of electrolyte solution in each chamber as this was sufficient to sit above the line of the sintered glass divider and thus allow sufficient ion transfer. Zinc electrodes were made by cutting strips from a roll of metallic zinc sheet metal (around 0.5 mm thickness) to create plates with dimensions of 10 mm x 100 mm. When used, these were placed into solution to a depth of 25 mm, meaning the area of electrode exposed to solution was approximately 530 mm². A silver wire, which was 1 mm thick, was used as a quasi-reference electrode and was likewise placed into solution to a depth of 25 mm giving an effective area of 79 mm². Both the zinc plate and the silver wire were placed into the same chamber to minimise the potential drop deriving from resistance and kept 10 mm apart. A platinum wire of 1 mm thickness was used as the counter-electrode and placed in the other chamber of the H cell, this time at a depth of 40 mm giving an effective area of 126 mm². Where graphite electrodes were used for the working-electrode and/or counter electrode, rods of 5 mm diameter were used at a depth of 25 mm giving an effective area of 412 mm². Reactions were run using an Ivium Technologies Vertex model potentiostat operating in chronoamperometry mode. This model allowed for real-time charge over time and current over time graphs to be generated which we found exceedingly useful for this work, especially for measuring charge passed over the course of reactions.

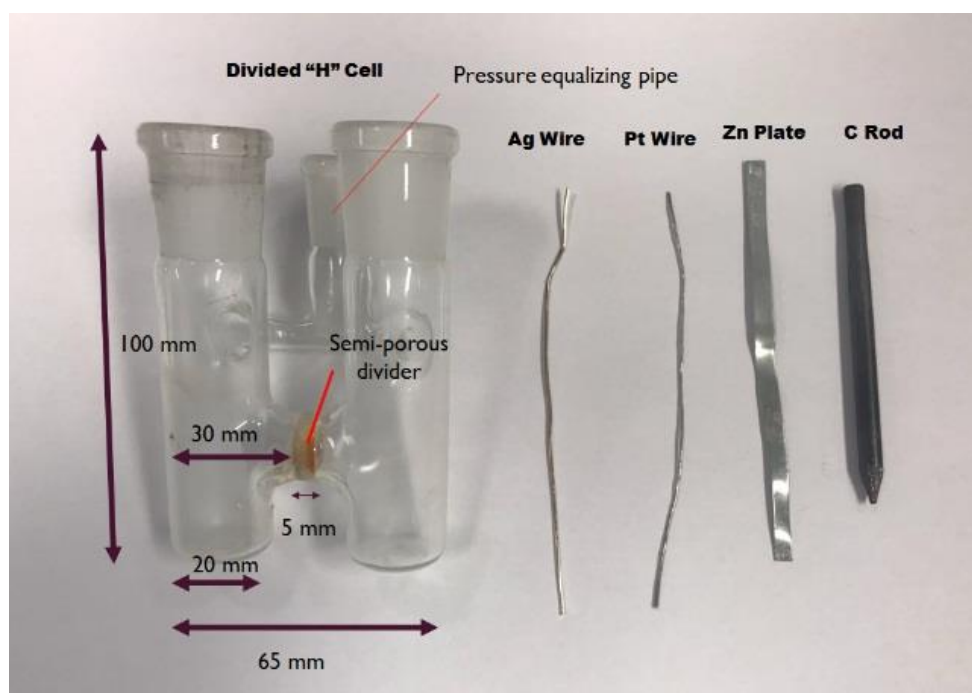


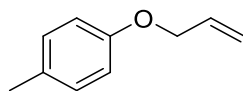
Figure S1. Image of H Cell and electrodes used with dimensions

5.3 Experimental Procedures (Chapter 2)

General Procedure of O-allylphenol:

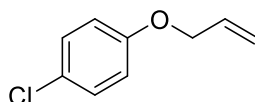
To a flame-dried flask with a mixture of phenol (1.0 eq) and potassium carbonate (1.5 eq) in anhydrous MeCN (20 mL), allyl bromide (1.5 eq) was added dropwise. The reaction mixture was then allowed to heat to 60 °C and stirred for 16 h before being cooled to room temperature. The MeCN was then removed under vacuum and the crude product was washed with water and brine and extracted with CH₂Cl₂ (3 × 20 mL). The organic layer was dried over magnesium sulfate and concentrated under vacuum to give the O-allylphenol product.

4-Methylphenyl allyl ether



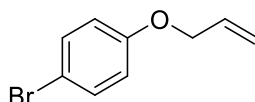
4-Methylphenol (0.50 g, 4.6 mmol) used to yield a dark yellow oil (0.67 g, 98%); $R_f = 0.4$ (10% EtOAc/pet. ether.); $^1\text{H NMR}$ (400 MHz, CDCl₃) $\delta = 7.08$ (*d*, $J = 8.4$ Hz, 2H, ArH), 6.83 (*d*, $J = 8.4$ Hz, 2H, ArH), 6.06 (*ddt*, $J = 17.3, 10.5, 5.3$ Hz, 1H, CH=CH₂), 5.41 (*dq*, $J = 17.3, 1.7$ Hz, 1H, CH=CH _{α} H _{β}), 5.28 (*dq*, $J = 10.5, 1.5$ Hz, 1H, CH=CH _{α} H _{β}), 4.52 (*d*, $J = 5.3$ Hz, 2H, CH₂), 2.29 (*s*, 3H, CH₃) ppm; Data in agreement with literature.¹³⁵

4-(Allyloxy)-chlorobenzene



4-Chlorophenol (1.00 g, 7.8 mmol) used to yield a yellow oil (1.18 g, 90%); $R_f = 0.4$ (10% EtOAc/pet. ether.); $^1\text{H NMR}$ (400 MHz, CDCl₃) $\delta = 7.23$ (*d*, $J = 9.0$ Hz, 2H, ArH), 6.84 (*d*, $J = 9.0$ Hz, 2H, ArH), 6.03 (*ddt*, $J = 17.3, 10.5, 5.3$ Hz, 1H, CH=CH₂), 5.40 (*dq*, $J = 17.2, 1.6$ Hz, 1H, CH=CH _{α} H _{β}), 5.33-5.26 (*dq*, $J = 10.5, 1.4$ Hz, 1H, CH=CH _{α} H _{β}), 4.51 (*dt*, $J = 5.3, 1.5$ Hz, 2H, CH₂) ppm; Data in agreement with literature.¹³⁶

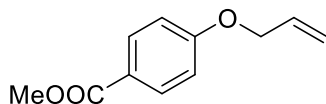
4-(Allyloxy)-bromobenzene



4-Bromophenol (2.00 g, 11.6 mmol) used to yield a yellow oil (2.32 g, 94%); $R_f = 0.4$ (10% EtOAc/pet. ether.); $^1\text{H NMR}$ (400 MHz, CDCl₃) $\delta = 7.37$ (*d*, $J = 9.0$ Hz, 2H, ArH), 6.80 (*d*, $J = 9.0$ Hz, 2H, ArH), 6.03 (*ddt*, $J = 17.2, 10.5, 5.3$ Hz, 1H, CH=CH₂), 5.40 (*dq*, $J = 17.3, 1.6$ Hz,

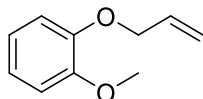
1H, CH=CH α H β), 5.30 (*dq*, *J* = 10.5, 1.4 Hz, 1H, CH=CH α H β), 4.51 (*dt*, *J* = 5.3, 1.5 Hz, 2H, CH₂) ppm; Data in agreement with literature.¹³⁷

Methyl 4-allyloxybenzoate



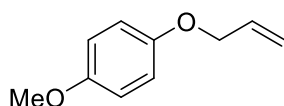
Methyl-4-hydroxylbenzoate (5.00 g, 32.9 mmol) used to yield a colourless oil (6.06 g, 96%); *R_f* = 0.4 (10% EtOAc/pet. ether.); **¹H NMR** (400 MHz, CDCl₃) δ = 7.98 (*d*, *J* = 9.1 Hz, 2H, *ArH*), 6.93 (*d*, *J* = 9.1 Hz, 2H, *ArH*), 6.05 (*ddt*, *J* = 17.2, 10.5, 5.3 Hz, 1H, CH=CH₂), 5.42 (*dq*, *J* = 17.2, 1.6 Hz, 1H, CH=CH α H β), 5.31 (*dq*, *J* = 10.5, 1.4 Hz, 1H, CH=CH α H β), 4.59 (*dt*, *J* = 5.3, 1.6 Hz, 2H, CH₂), 3.88 (*s*, 3H, CH₃) ppm; Data in agreement with literature.¹³⁸

O-Allyl-guaiacol



2-Methoxy-phenol (3.60 mL, 32.9 mmol) used to yield a yellow oil (4.96 g, 92%); *R_f* = 0.4 (10% EtOAc/pet. ether.); **¹H NMR** (400 MHz, CDCl₃) δ = 6.96-6.85 (*m*, 4H, *ArH*), 6.10 (*ddt*, *J* = 17.2, 10.7, 5.4 Hz, 1H, CH=CH₂), 5.41 (*dq*, *J* = 17.3, 1.6 Hz, 1H, CH=CH α H β), 5.28 (*dq*, *J* = 10.5, 1.4 Hz, 1H, CH=CH α H β), 4.63-4.59 (*m*, 2H, CH₂), 3.87 (*s*, 3H, CH₃) ppm; Data in agreement with literature.¹³⁹

1-Allyloxy-4-methoxybenzene

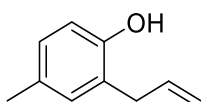


2-Methoxy-phenol (1.75 g, 14.1 mmol) used to yield a colourless oil (2.22 g, 96%); *R_f* = 0.4 (10% EtOAc/pet. ether.); **¹H NMR** (400 MHz, CDCl₃) δ = 6.89-6.81 (*m*, 4H, *ArH*), 6.05 (*ddt*, *J* = 17.3, 10.6, 5.3 Hz, 1H, CH=CH₂), 5.40 (*dq*, *J* = 17.3, 1.6 Hz, 1H, CH=CH α H β), 5.27 (*dq*, *J* = 10.5, 1.4 Hz, 1H, CH=CH α H β), 4.49 (*dt*, *J* = 5.3, 1.6 Hz, 2H, CH₂), 3.77 (*s*, 3H, CH₃) ppm; Data in agreement with literature.¹⁴⁰

General Procedure of 2-allylphenol:

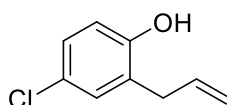
To a flask containing O-allyl ether (1.0 eq), ethylene glycol (2 mol% weighing by volume) was added. The reactants were then allowed to heat to 200 °C under argon and refluxed for 16 h, followed by direct purification by column chromatography to give the 2-allylphenol.

2-Allyl-4-methylphenol



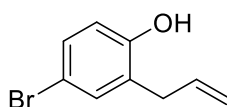
4-Methylphenyl allyl ether (0.60 g, 4.1 mmol) used to yield a yellow oil (0.48 g, 80%); $R_f = 0.3$ (10% EtOAc/pet. ether.); $^1\text{H NMR}$ (400 MHz, CDCl_3) $\delta = 6.96\text{-}6.90$ (*m*, 2H, ArH), 6.72 (*d*, $J = 8.1$ Hz, 1H, ArH), 6.08-5.96 (*m*, 1H, CH=), 5.18 (*dq*, $J = 7.5, 1.7$ Hz, 1H, =CH $_{\alpha}$ H $_{\beta}$), 5.14 (*t*, $J = 1.6$ Hz, 1H, =CH $_{\alpha}$ H $_{\beta}$) 4.82 (*broad s*, 1H, OH), 3.39 (*dt*, $J = 6.3, 1.6$ Hz, 2H, CH $_2$), 2.27 (*s*, 3H, CH $_3$) ppm; Data in agreement with literature.¹⁴¹

2-Allyl-4-chlorophenol



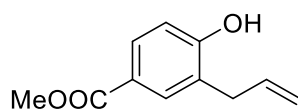
4-(Allyloxy)-chlorobenzene (1.18 g, 7.0 mmol) used to yield a yellow oil (0.89 g, 76%); $R_f = 0.3$ (10% EtOAc/pet. ether.); $^1\text{H NMR}$ (400 MHz, CDCl_3) $\delta = 7.11\text{-}7.06$ (*m*, 2H, ArH), 6.74 (*d*, $J = 8.9$ Hz, 1H, ArH), 5.98 (*ddt*, $J = 16.8, 10.3, 6.4$ Hz, 1H, CH=), 5.19 (*dq*, $J = 4.3, 1.6$ Hz, 1H, =CH $_{\alpha}$ H $_{\beta}$), 5.16 (*dq*, $J = 11.0, 1.6$ Hz, 1H, =CH $_{\alpha}$ H $_{\beta}$), 5.00 (*broad s*, 1H, OH), 3.37 (*dt*, $J = 6.3, 1.6$ Hz, 2H, CH $_2$) ppm; Data in agreement with literature.¹³⁶

2-Allyl-4-bromophenol



4-(Allyloxy) bromobenzene (2.00 g, 9.4 mmol) used to yield a yellow solid (1.44 g, 72%); $R_f = 0.3$ (10% EtOAc/pet. ether.); **m.p.** 54-56 °C (lit.¹⁴⁵: 58-59 °C); $^1\text{H NMR}$ (400 MHz, CDCl_3) $\delta = 7.25\text{-}7.20$ (*m*, 2H, ArH), 6.70 (*d*, $J = 8.9$ Hz, 1H, ArH), 5.98 (*ddt*, $J = 16.7, 10.3, 6.4$ Hz, 1H, CH=), 5.19 (*dt*, $J = 4.2, 1.6$ Hz, 1H, =CH $_{\alpha}$ H $_{\beta}$), 5.16 (*dq*, $J = 10.8, 1.6$ Hz, 1H, =CH $_{\alpha}$ H $_{\beta}$), 4.96 (*broad s*, 1H, OH), 3.37 (*dt*, $J = 6.4, 1.6$ Hz, 2H, CH $_2$) ppm; Data in agreement with literature.¹⁴²

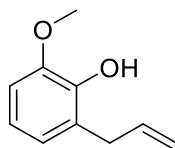
Methyl 3-allyl-4-hydroxybenzoate



Methyl 4-allyloxybenzoate (6.00 g, 31.2 mmol) used to yield a white solid (4.50 g, 75%); $R_f = 0.3$ (25% EtOAc/pet. ether.); **m.p.** 93-95 °C (lit.¹⁴⁵: 89-90 °C); $^1\text{H NMR}$ (400 MHz, CDCl_3) $\delta = 7.87\text{-}7.82$ (*m*, 2H, ArH), 6.83 (*d*, $J = 9.1$ Hz, 1H, ArH), 6.07-5.95 (*m*, 1H, CH=), 5.49 (*broad s*, 1H, OH), 5.20 (*t*, $J = 1.6$ Hz, 1H, =CH $_{\alpha}$ H $_{\beta}$) 5.17 (*dq*, $J = 7.8, 1.6$ Hz, 1H, =CH $_{\alpha}$ H $_{\beta}$), 3.88 (*s*, 3H,

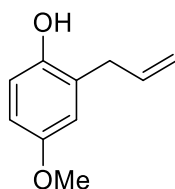
CH₃), 3.44 (dt, *J* = 6.3, 1.7 Hz, 2H, CH₂) ppm; Data in agreement with literature.¹⁴³

2-Allyl-6-methoxyphenol



O-Allyl-guaiacol (4.00 g, 24.4 mmol) used to yield a yellow oil (2.28 g, 57%); *R_f* = 0.4 (10% EtOAc/pet. ether.); ¹H NMR (400 MHz, CDCl₃) δ = 6.83-6.72 (*m*, 3H, ArH), 6.01 (*ddt*, *J* = 16.8, 10.0, 6.5 Hz, 1H, CH=), 5.70 (*broad s*, 1H, OH), 5.12-5.02 (*m*, 2H, =CH₂), 3.88 (*s*, 3H, CH₃), 3.42 (*dt*, *J* = 6.5, 1.5 Hz, 2H, CH₂) ppm; Data in agreement with literature.¹⁴⁴

2-Allyl-4-methoxyphenol



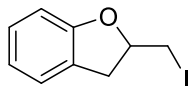
1-Allyloxy-4-methoxybenzene (2.22 g, 13.5 mmol) used to yield a yellow oil (1.20 g, 54%). *R_f* = 0.4 (10% EtOAc/pet. ether.); ¹H NMR (600 MHz, CDCl₃) δ = 6.74 (*d*, *J* = 7.8 Hz, 1H, ArH), 6.70-6.66 (*m*, 2H, ArH), 6.00 (*ddt*, *J* = 17.5, 9.6, 6.4 Hz, 1H, CH=), 5.18-5.13 (*m*, 2H, =CH₂), 4.70 (*broad s*, 1H, OH), 3.76 (*s*, 3H, CH₃), 3.38 (*dt*, *J* = 6.4, 1.6 Hz, 2H, CH₂) ppm; Data in agreement with literature.¹⁴⁸

General Electrochemical Procedure of Iodocyclization:

A graphite rod working-electrode (4.12 cm² area) was first coated with a layer Zn by placing it into an undivided cell containing a 0.1 M ZnCl_{2(aq.)} solution with K₂CO₃ (0.04 g). A silver wire quasi reference-electrode (0.79 cm² area) and a Zn plate counter-electrode (2.00 cm² area) were added and all electrodes were then connected to a potentiostat. The voltage was set to -1.2 V for 800 s (34 C passed, 352.99 μmol e⁻, 11.54 mg Zn deposited. According to the amount of 2-allylphenol used, the time could be switched to satisfy 40 mol% Zn). These electrodes were then carefully cleaned with water and acetone and placed into a flame-dried divided 'H' cell (Zn-coated graphite and Ag wire in one chamber, Pt wire in the other chamber). Each side was charged with 10 mL anhydrous MeCN and LiClO₄ (0.32 g) to make a 0.3 M solution. 2-Allylphenol (1.0 eq) and sodium iodide (4.0 eq) were added to the anode side. The reaction mixture was then allowed to heat and stir vigorously at 60 °C under argon with a +1.2 V constant potential to the anode for 16 h before being cooled to room temperature. The

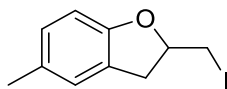
reaction mixture was then treated with saturated sodium thiosulfate solution and extracted with CH_2Cl_2 (3×20 mL). The organic layer was dried over magnesium sulfate and concentrated under vacuum followed then purified by column chromatography to give the final iodo-cyclized product.

2-(Iodomethyl)-2,3-dihydro-benzofuran



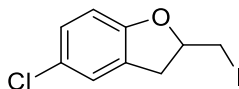
2-Allylphenol (0.10 mL, 0.8 mmol) and sodium iodide (0.48 g, 3.2 mmol) used to yield a yellow oil (0.19 g, 99%); $R_f = 0.5$ (10% EtOAc/pet. ether.); $^1\text{H NMR}$ (600 MHz, CDCl_3) $\delta = 7.17$ (*dq*, $J = 7.4, 1.4$ Hz, 1H, ArH), 7.14 (*ddd*, $J = 8.2, 7.5, 1.6, 0.9$ Hz, 1H, ArH), 6.88 (*td*, $J = 7.4, 1.0$ Hz, 1H, ArH), 6.80 (*d*, $J = 8.0$ Hz, 1H, ArH), 4.89 (*dddd*, $J = 9.1, 7.6, 6.6, 4.9$ Hz, 1H, OCH), 3.45 (*dd*, $J = 10.1, 4.9$ Hz, 1H, $\text{ICH}_\alpha\text{H}_\beta$), 3.40 (*dd*, $J = 15.9, 9.1$ Hz, 1H, $\text{CH}_\alpha\text{H}_\beta$), 3.35 (*dd*, $J = 10.1, 7.6$ Hz, 1H, $\text{ICH}_\alpha\text{H}_\beta$), 3.05 (*dd*, $J = 15.9, 6.5$ Hz, 1H, $\text{CH}_\alpha\text{H}_\beta$) ppm; Data in agreement with literature.¹³⁶

2-(Iodomethyl)-5-methyl-2,3-dihydro-benzofuran



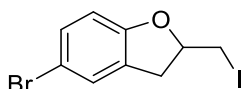
2-Allyl-4-methylphenol (0.15 g, 1.0 mmol) and sodium iodide (0.61 g, 4.0 mmol) used to yield a yellow oil (0.26 g, 93% yield). $R_f = 0.5$ (10% EtOAc/pet. ether.); $^1\text{H NMR}$ (400 MHz, CDCl_3) $\delta = 6.99$ -6.96 (*m*, 1H, ArH) 6.93 (*d*, $J = 8.1$ Hz, 1H, ArH) 6.68 (*d*, $J = 8.1$ Hz, 1H, ArH), 4.86 (*dddd*, $J = 9.1, 7.6, 6.5, 4.9$ Hz, 1H, OCH), 3.46-3.30 (*m*, 3H, $\text{CH}_\alpha\text{H}_\beta$, ICH_2), 3.01 (*dd*, $J = 15.9, 6.5$ Hz, 1H, $\text{CH}_\alpha\text{H}_\beta$), 2.28 (*s*, 3H, CH_3) ppm. Data in agreement with literature.¹⁴⁷

2-(Iodomethyl)-5-chloro-2,3-dihydro-benzofuran



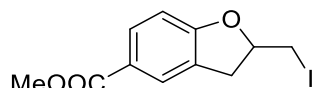
2-Allyl-4-chlorophenol (0.20 g, 1.2 mmol) and sodium iodide (0.71 g, 4.8 mmol) used to yield a yellow oil (0.28 g, 81% yield). $R_f = 0.5$ (10% EtOAc/pet. ether.); $^1\text{H NMR}$ (400 MHz, CDCl_3) $\delta = 7.14$ -7.05 (*m*, 2H, ArH), 6.69 (*d*, $J = 8.4$ Hz, 1H, ArH), 4.89 (*dddd*, $J = 9.1, 7.4, 6.6, 4.7$ Hz, 1H, OCH), 3.46-3.30 (*m*, 3H, ICH_2 , $\text{CH}_\alpha\text{H}_\beta$), 3.03 (*dd*, $J = 16.2, 6.7$ Hz, 1H, $\text{CH}_\alpha\text{H}_\beta$) ppm. Data in agreement with literature.¹³⁶

2-(Iodomethyl)-5-bromo-2,3-dihydro-benzofuran



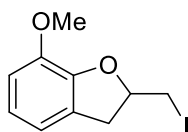
2-Allyl-4-bromophenol (0.20 g, 0.9 mmol) and sodium iodide (0.54 g, 3.6 mmol) used to yield a colourless oil (0.26 g, 83% yield). $R_f = 0.5$ (10% EtOAc/pet. ether.); $^1\text{H NMR}$ (400 MHz, CDCl_3) $\delta = 7.28\text{--}7.26$ (*m*, 1H, ArH), 7.24–7.20 (*m*, 1H, ArH), 6.66 (*d*, $J = 8.5$ Hz, 1H, ArH), 4.89 (*dddd*, $J = 9.1, 7.4, 6.6, 4.7$ Hz, 1H, OCH), 3.45–3.30 (*m*, 3H, ICH₂, CH _{α} H _{β}), 3.04 (*dd*, $J = 16.2, 6.7$ Hz, 1H, CH _{α} H _{β}) ppm; $^{13}\text{C NMR}$ (100 MHz, CDCl_3) $\delta = 158.4$ (ArC), 131.1 (ArC), 128.3 (ArC), 128.0 (ArC), 112.7 (ArC), 111.2 (ArC), 82.2 (CH), 36.0 (CH₂), 8.6 (CH₂I) ppm; **HRMS (ESI)** calc'd for [C₉H₈IO⁷⁹Br+H]⁺ 338.8876, found 338.8876; **IR v_{max} (film)** 2952, 1229, 621, 540 cm⁻¹.

Methyl 2-(iodomethyl)-2,3-dihydro-1-benzofuran-5-carboxylate



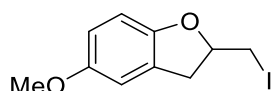
3-Allyl-4-hydroxybenzoate (0.20 g, 1.0 mmol) and sodium iodide (0.60 g, 4.0 mmol) used to yield a white solid (0.22 g, 67% yield). $R_f = 0.3$ (10% EtOAc/pet. ether.); **m.p.** 75–77 °C; $^1\text{H NMR}$ (400 MHz, CDCl_3) $\delta = 7.90\text{--}7.85$ (*m*, 2H, ArH), 6.79 (*d*, $J = 8.3$ Hz, 1H, ArH), 4.96 (*dddd*, $J = 9.2, 7.3, 6.6, 4.7$ Hz, 1H, OCH), 3.87 (*s*, 3H, COOCH₃), 3.48–3.34 (*m*, 3H, CH _{α} H _{β} , ICH₂), 3.06 (*dd*, $J = 16.1, 6.6$ Hz, 1H, CH _{α} H _{β}) ppm; $^{13}\text{C NMR}$ (100 MHz, CDCl_3) $\delta = 166.9$ (C=O), 163.2 (ArC), 131.4 (ArC), 126.9 (ArC), 126.3 (ArC), 123.3 (ArC), 109.3 (ArC), 82.7 (CH), 52.0 (CH₃), 36.0 (CH₂), 8.4 (CH₂I) ppm; **HRMS (ESI)** calc'd for [C₁₁H₁₁IO₃+H]⁺ 318.9826, found 318.9827. **IR v_{max} (film)** 2952, 1716, 1240, 569 cm⁻¹.

2-(Iodomethyl)-7-methoxy-2,3-dihydro-benzofuran



2-Allyl-6-methoxyphenol (0.20 g, 1.2 mmol) and sodium iodide (0.72 g, 4.8 mmol) used to yield a brown solid (0.23 g, 64% yield). $R_f = 0.3$ (10% EtOAc/pet. ether.); **m.p.** 61–63 °C; $^1\text{H NMR}$ (400 MHz, CDCl_3) $\delta = 6.89\text{--}6.72$ (*m*, 3H, ArH), 4.99–4.88 (*m*, 1H, OCH), 3.87 (*s*, 3H, OCH₃), 3.55–3.31 (*m*, 3H, CH _{α} H _{β} , ICH₂), 3.10 (*dd*, $J = 15.8, 6.9$ Hz, 1H, CH _{α} H _{β}) ppm; $^{13}\text{C NMR}$ (150 MHz, CDCl_3) $\delta = 147.7$ (ArC), 144.6 (ArC), 127.0 (ArC), 121.6 (ArC), 117.3 (ArC), 111.4 (ArC), 82.3 (CH), 56.1 (CH₃), 36.7 (CH₂), 9.0 (CH₂I) ppm; **HRMS (ESI)** calc'd for [C₁₀H₁₁IO₂+H]⁺ 290.9876, found 290.9874. **IR v_{max} (film)** 2935, 1197, 1078, 611 cm⁻¹

2-(Iodomethyl)-5-methoxy-2,3-dihydro-benzofuran



2-Allyl-4-methoxyphenol (0.20 g, 1.2 mmol) and sodium iodide (0.72 g, 4.8 mmol) used to yield a yellow solid (0.28 g, 79% yield). $R_f = 0.3$ (10% EtOAc/pet. ether.); **m.p.** 61-63 °C (lit.¹⁴⁹: 62-63.3 °C); **¹H NMR** (400 MHz, CDCl₃) $\delta = 6.76-6.73$ (*m*, 1H, ArH), 6.71-6.64 (*m*, 2H, ArH), 4.84 (*dddd*, $J = 9.0, 7.5, 6.6, 4.9$ Hz, 1H, OCH), 3.75 (*s*, 3H, OCH₃), 3.45-3.29 (*m*, 3H, CH _{α} H _{β} , ICH₂), 3.01 (*dd*, $J = 16.1, 6.6$ Hz, 1H, CH _{α} H _{β}) ppm. Data in agreement with literature.¹³⁶

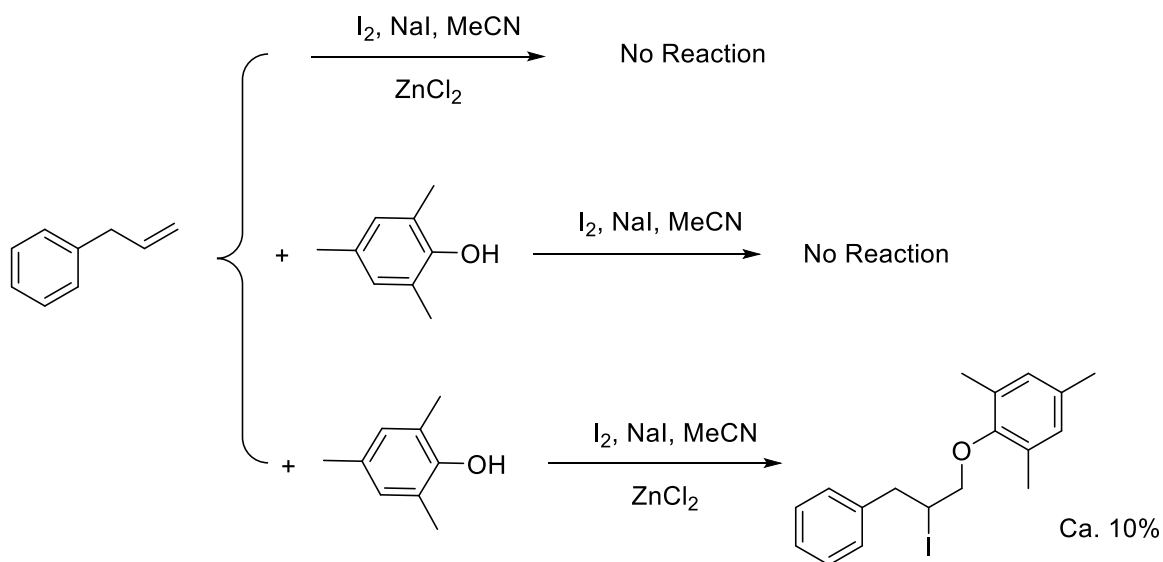
Control Experiment Using Purchased 4-Iodophenol and 4-Iodoanisole:

The set-ups and operations were the same as the general electrochemical process illustrated above, except an additional 2 equivalents of MeSO₃H was added to the working chamber.

Control Experiment Without Electricity and Electrodes:

For cyclisation experiment: Same amount of 2-allylphenol used in electrochemically promoted cyclisation, 2.0 eq of iodine, 2.0 eq of sodium iodide, 0.5 eq of ZnCl₂ and 20 mL of anhydrous MeCN were added to a pre-flame-dried flask, the reaction was then allowed to stir at 60 °C under argon for 16 h.

For scheme 13:



Top reaction: To a flame-dried flask, 1.0 eq of allylbenzene, 2.0 eq of iodine, 2.0 eq of sodium iodide, 0.5 eq of ZnCl₂ and 20 mL of anhydrous MeCN were added, the reaction was then allowed to stir at 60 °C under argon for 16 h.

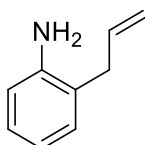
Middle reaction: To a flame-dried flask, 1.0 eq of allylbenzene, 1.0 eq of 2,4,6-trimethylphenol, 2.0 eq of iodine, 2.0 eq of sodium iodide and 20 mL of anhydrous MeCN were added, the

reaction was then allowed to stir at 60 °C under argon for 16 h.

Bottom reaction: Same procedure as middle, except another 0.5 eq of ZnCl₂ was added to the flask.

Aniline Claisen rearrangement

2-Allylaniline



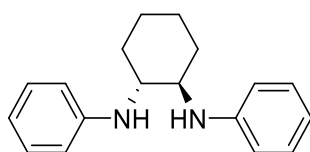
To a flame-dried flask with *N*-allylaniline (2.66 g, 20.0 mmol, 1.0 eq) in *m*-xylene (40 mL), boron trifluoride etherate (3.0 mL, 24.0 mmol, 1.2 eq) was added dropwisely at -78 °C under argon. After 15 min, the reaction mixture was then allowed to warm to r.t, heat to 180 °C and stirred for 17 h before being cooled to room temperature and quenched with 2M NaOH solution (30 mL) at 0 °C. The organic layer was separated and the aqueous layer was extracted with diethyl ether (30 mL × 2). The combined organic layers were dried over magnesium sulfate and concentrated under vacuum before purified by column chromatography to yield a yellow oil (1.49 g, 56% yield). $R_f = 0.4$ (Petroleum ether : Ethyl acetate = 5:1); **¹H NMR** (400 MHz, CDCl₃) $\delta = 7.12-7.02$ (*m*, 2H, *ArH*), 6.76 (*t*, $J = 7.4$ Hz, 1H, *ArH*), 6.69 (*d*, $J = 7.8$ Hz, 1H, *ArH*), 6.04-5.89 (*m*, 1H, =*CH*), 5.17-5.06 (*m*, 2H, =*CH*₂), 3.67 (*bs*, 2H, *NH*₂) 3.32 (*d*, $J = 6.2$ Hz, 2H, *CH*₂); **¹³C NMR** (150 MHz, CDCl₃) $\delta = 144.9$ (*ArC*), 136.0 (*CH*=), 130.2 (*ArC*), 127.6 (*ArC*), 124.1 (*ArC*), 119.0 (*ArC*), 116.2 (*ArC*), 115.9 (=CH₂), 36.6 (CH₂) ppm; Data in agreement with literature.¹⁵⁰

Aniline iodocyclisation

The procedure is completely the same as doing phenol iodocyclisation except the temperature has been increased to 65 °C.

Diamination

Trans-*N,N'*-Diphenyl-1,2-cyclohexanediamine



To a flame-dried H-Cell, a zinc coated carbon anode and Pt cathode were equipped. Each

side was charged with 10 mL dry MeCN and LiClO₄ (0.32 g) to make a 0.3 M solution. Aniline (0.20 mL, 2.15 mmol, 1.0 eq), cyclohexene (0.87 g, 8.6 mmol, 4.0 eq) and sodium iodide (1.29 g, 8.6 mmol, 4.0 eq) were added to the anode side. The reaction mixture was then allowed to heat and stir violently at 65 °C under argon with a +1.2 V constant potential to the anode for 16 h before being cooled to room temperature. The reaction mixture was then treated with saturated sodium thiosulfate solution and extracted with CH₂Cl₂ (3 × 20 mL). The organic layer was dried over magnesium sulfate and concentrated under vacuum followed then purified by column chromatography to give a light yellow oil (0.20 g, 70% yield). *R*_f = 0.4 (Petroleum ether : Ethyl acetate = 9:1); **¹H NMR** (400 MHz, CDCl₃) δ = 7.20-7.16 (*m*, 4H, *ArH*), 6.74-6.70 (*m*, 2H, *ArH*), 6.64-6.61 (*m*, 4H, *ArH*), 3.82 (*bs*, 2H, *NH*), 3.24-3.18 (*m*, 2H, *CH*), 2.39-2.33 (*m*, 2H, *CH*₂), 1.83-1.74 (*m*, 2H, *CH*₂), 1.45-1.40 (*m*, 2H, *CH*₂), 1.29-1.18 (*m*, 2H, *CH*₂) ppm; **¹³C NMR** (100 MHz, CDCl₃) δ = 147.9 (*ArC*), 129.5 (*ArC*), 117.7 (*ArC*), 113.6 (*ArC*), 57.4 (*CHNH*), 32.7 (*CH*₂), 24.8 (*CH*₂) ppm; **HRMS (ESI)** calc'd for [C₁₈H₂₂N₂+H]⁺ 267.1856, found 267.1858. Data in agreement with literature.¹⁵¹

5.4 General Information (Chapter 3)

All reagents and solvents were used directly without further purification unless otherwise stated. Reaction progress was monitored by analytical thin layer chromatography (TLC) on silica gel coated aluminum oxide F254 plates (Merck KGaA). Developed TLC were visualized under UV light (254 nm). Flash column chromatography was performed using Biotage automatic column system (IS11579109). Reactions are terminated when the developed TLC plates showed complete consumption of reaction substrate. Mass spectra were measured on Thermo Finnigan MAT900 XE and Waters LCT Premier XE machines operating in ESI modes with the use of TOF analyzer. All ¹H and ¹³C NMR spectra were recorded at 400 MHz and 100 MHz respectively on Bruker Avance spectrometers at ambient temperature in CDCl₃ unless otherwise noted. NMR spectra were referenced to residual solvent peaks (CDCl₃: δ = 7.26 for ¹H NMR and δ = 77.0 for ¹³C NMR) and chemical shifts were reported in ppm. In ¹H NMR, the multiplicity of the signal is indicated as *s* (singlet), *d* (doublet), *t* (triplet) and *m* (multiplet), defined as all multiplex signals where overlap or complex coupling of signals makes definitive descriptions of peaks difficult. Coupling constants are defined as *J* and quoted in Hz to one decimal place. IR spectra were obtained on a Bruker Alpha FTIR Spectrometer operating in ATR mode. Melting points were measured with a Gallenkamp apparatus and are uncorrected. Electrochemical reactions were carried out using an Ivium Technologies Vertex model potentiostat operating in chronoamperometry mode. CV plots were measured using the same machine with a glassy carbon working electrode, silver wire reference electrode and Pt wire

counter electrode.

5.5 Details of Electrochemical Methods (Chapter 3)

For all reactions we used a divided 'H' cell as our reaction vessel (dimensions shown in **Figure S2**) with each chamber having a size B19 ground-glass neck and a total volume of 30 mL. A semiporous sintered glass divider sits between each chamber. All reactions were carried out using 15 mL of electrolyte solution in each. Where graphite electrodes were used for the working-electrode and counter electrode, rods of 5 mm diameter were used at a depth of 25 mm giving an effective area of 412 mm². A silver wire, which was 1 mm thick, was used as a quasi-reference electrode and was likewise placed into solution to a depth of 25 mm giving an effective area of 79 mm². One graphite and the silver wire were placed into the same chamber to minimise the potential drop deriving from resistance and kept 10 mm apart. Another graphite was used as the counter-electrode and placed in the other chamber of the H cell. Reactions were run using an Ivium Technologies Vertex model potentiostat operating in chronoamperometry mode. This mode provides real-time charge over time and current over time graphs for measuring the total charges passed over the course of reaction.

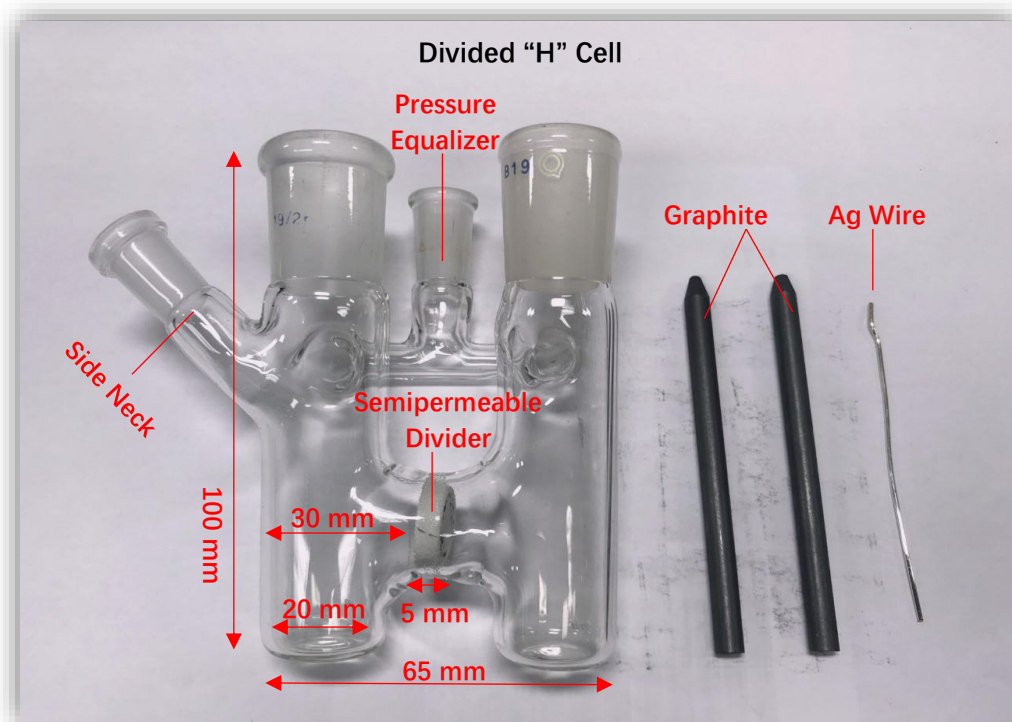
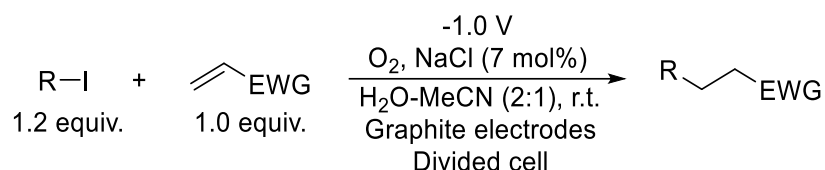


Figure S2. Image of divided H-cell and electrodes used with dimensions.

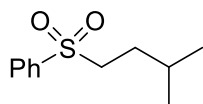
5.6 Experimental Procedures (Chapter 3)

General Procedure for the Electrochemical Radical Alkene Addition Reactions



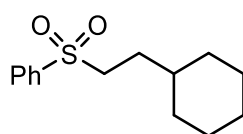
Two graphite electrodes (4.12 cm² area each) were placed into each chamber of the divided H cell and HCl_(aq) (pH = 2, 10 mL), MeCN (5 mL) and NaCl (7 mol%) were added to each chamber. Alkene and alkyl halide were added to the cathodic chamber and the reaction mixture was stirred at room temperature under a constant reductive potential (-1.0 V) applied to the cathode for 20 to 45 h. The reaction mixture was then diluted with water (10 mL) and phases were separated. The aqueous layer was extracted with CH₂Cl₂ (3 × 20 mL). The combined organic layer was dried (MgSO₄), filtered, concentrated under reduced pressure and purified by column chromatography (cyclohexane : EtOAc 100 : 0 to 9 : 1) to yield the addition product.

3-Methylbutyl phenyl sulfone



3-Methylbutyl phenyl sulfone (250 mg, 1.18 mmol, 99%), prepared from phenyl vinyl sulfone (200 mg, 1.19 mmol, 1.0 equiv.) and 2-iodopropane (0.142 mL, 1.43 mmol, 1.2 equiv.), was obtained as a colourless oil in 20 h: *R_f* 0.30 (petroleum ether : EtOAc 9 : 1). ¹H NMR (400 MHz, CDCl₃) δ 7.94 – 7.86 (m, 2H), 7.70 – 7.63 (m, 1H), 7.60 – 7.54 (m, 2H), 3.11 – 3.05 (m, 2H), 1.66 – 1.54 (m, 3H), 0.86 (d, *J* = 6.3 Hz, 6H). ¹³C NMR (100 MHz, CDCl₃) δ 139.3 (ArC), 133.7 (ArC), 129.3 (ArC), 128.1 (ArC), 54.8 (CH₂SO₂), 31.1 (CH₂), 27.3 (CH), 22.1 (CH₃). HRMS (ESI) *m/z* [M + H]⁺ calcd for C₁₁H₁₇O₂S 213.0949; found 213.0949. The analytical data were in excellent agreement with those reported in the literature.¹⁵²

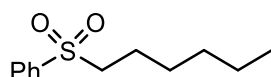
2-(Cyclohexyl)ethyl phenyl sulfone



2-(Cyclohexyl)ethyl phenyl sulfone (300 mg, 1.19 mmol, 100%), prepared from phenyl vinyl

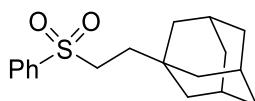
sulfone (200 mg, 1.19 mmol, 1.0 equiv.) and iodocyclohexane (0.185 mL, 1.43 mmol, 1.2 equiv.), was obtained as a colourless oil in 20 h: R_f 0.30 (petroleum ether : EtOAc 9 : 1). $^1\text{H NMR}$ (400 MHz, CDCl_3) δ 7.89 – 7.84 (m, 2H), 7.65 – 7.57 (m, 1H), 7.55 – 7.49 (m, 2H), 3.13 – 2.97 (m, 2H), 1.67 – 1.52 (m, 7H), 1.32 – 0.96 (m, 4H), 0.90 – 0.74 (m, 2H). $^{13}\text{C NMR}$ (100 MHz, CDCl_3) δ 139.3 (ArC), 133.7 (ArC), 129.3 (ArC), 128.1 (ArC), 54.4 (CH_2SO_2), 36.7 (CH), 32.8 (CH_2), 29.7 (CH_2), 26.3 (CH_2), 26.0 (CH_2). **HRMS (ESI)** m/z $[\text{M} + \text{H}]^+$ calcd for $\text{C}_{14}\text{H}_{21}\text{O}_2\text{S}$ 253.1257; found 253.1257. The analytical data were in excellent agreement with those reported in the literature.¹⁵³

(Hexylsulfonyl)benzene



(Hexylsulfonyl)benzene (220 mg, 0.98 mmol, 82%), prepared from phenyl vinyl sulfone (200 mg, 1.19 mmol, 1.0 equiv.) and 1-iodobutane (0.163 mL, 1.43 mmol, 1.2 equiv.), was obtained as a colourless oil in 20 h: R_f 0.30 (petroleum ether : EtOAc 9 : 1). $^1\text{H NMR}$ (400 MHz, CDCl_3) δ 7.93 – 7.86 (m, 2H), 7.68 – 7.61 (m, 1H), 7.60 – 7.52 (m, 2H), 3.13 – 3.01 (m, 2H), 1.77 – 1.60 (m, 2H), 1.38 – 1.29 (m, 2H), 1.29 – 1.18 (m, 4H), 0.84 (t, $J = 6.9$ Hz, 3H). $^{13}\text{C NMR}$ (100 MHz, CDCl_3) δ 139.3(ArC), 133.7(ArC), 129.3 (ArC), 128.1 (ArC), 56.4 (CH_2SO_2), 31.2 (CH_2), 28.0 (CH_2), 22.7 (CH_2), 22.3 (CH_2), 14.0 (CH_3). **HRMS (ESI)** m/z $[\text{M} + \text{H}]^+$ calcd for $\text{C}_{12}\text{H}_{19}\text{O}_2\text{S}$ 227.1106; found 227.1111. The analytical data were in excellent agreement with those reported in the literature.¹⁵²

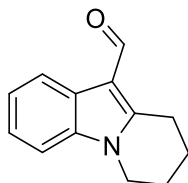
(3r,5r,7r)-1-[2-(Phenylsulfonyl)ethyl]adamantane



(3r,5r,7r)-1-[2-(Phenylsulfonyl)ethyl]adamantane (217 mg, 0.71 mmol, 60%), prepared from phenyl vinyl sulfone (200 mg, 1.19 mmol, 1.0 equiv.) and 1-iodoadamantane (0.44 mL, 1.43 mmol, 1.2 equiv.), was obtained as a white solid in 45 h: R_f 0.40 (petroleum ether : EtOAc 9 : 1). $^1\text{H NMR}$ (400 MHz, CDCl_3) δ 7.90 – 7.86 (m, 2H), 7.67 – 7.60 (m, 1H), 7.58 – 7.52 (m, 2H), 3.07 – 3.00 (m, 2H), 1.95 – 1.85 (m, 3H), 1.69 – 1.61 (m, 3H), 1.58 – 1.50 (m, 3H), 1.48 – 1.41 (m, 2H), 1.37 (d, $J = 2.9$ Hz, 6H). $^{13}\text{C NMR}$ (100 MHz, CDCl_3) δ 139.2 (ArC), 133.5 (ArC), 129.2 (ArC), 127.9 (ArC), 51.2 (CH_2SO_2), 41.8 (CH_2), 36.7 (CH_2), 35.8 (CH_2), 31.8 (CH_2), 28.3

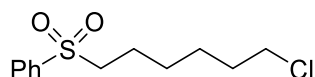
(CH). **HRMS (ESI)** m/z $[M + H]^+$ calcd for $C_{18}H_{25}O_2S$ 305.1570; found 305.1570. The analytical data were in excellent agreement with those reported in the literature.¹⁵⁴

6,7,8,9-Tetrahydropyrido[1,2-a]indole-10-carbaldehyde



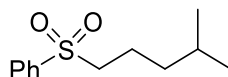
6,7,8,9-Tetrahydropyrido[1,2-a]indole-10-carbaldehyde (206 mg, 1.03 mmol, 89%), prepared from 1-(4-iodobutyl)-1H-indole-3-carbaldehyde (0.380 g, 1.16 mmol), was obtained as a white solid in 66 h: R_f 0.50 (petroleum ether : EtOAc 9 : 1). **m.p.** 121 – 123 °C (lit.¹⁵⁶ 124 °C). **¹H NMR** (400 MHz, $CDCl_3$) δ 10.16 (s, 1H), 8.20 (dd, $J = 8.2, 1.6$ Hz, 1H), 7.37 – 7.18 (m, 3H), 4.10 (t, $J = 6.2$ Hz, 2H), 3.32 (t, $J = 6.4$ Hz, 2H), 2.22 – 2.09 (m, 2H), 2.05 – 1.91 (m, 2H). **¹³C NMR** (100 MHz, $CDCl_3$) δ 183.6 (C=O), 148.2 (N-C=), 136.5 (ArC), 126.0 (ArC), 123.2 (ArC), 122.8 (ArC), 120.6 (ArC), 113.0 (C-C=O), 109.2 (ArC), 42.5 (N-CH₂), 22.8 (CH₂), 22.5 (CH₂), 19.7 (CH₂). **HRMS (ESI)** m/z $[M + H]^+$ calcd for $C_{13}H_{14}NO$ 200.1070; found 200.1070. The analytical data were in excellent agreement with those reported in the literature.¹⁵⁵

((6-Chlorohexyl)sulfonyl)benzene



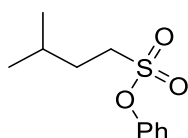
((6-Chlorohexyl)sulfonyl)benzene (295 mg, 1.13 mmol, 95%), prepared from phenyl vinyl sulfone (200 mg, 1.19 mmol, 1.0 equiv.) and 1-chloro-4-iodobutane (0.44 mL, 3.57 mmol, 3.0 equiv.), was obtained as a yellow oil in 32 h: R_f 0.30 (petroleum ether : EtOAc 4 : 1). **¹H NMR** (400 MHz, $CDCl_3$) δ 7.93 – 7.88 (m, 2H), 7.69 – 7.63 (m, 1H), 7.61 – 7.54 (m, 2H), 3.49 (t, $J = 6.6$ Hz, 2H), 3.14 – 3.03 (m, 2H), 1.81 – 1.65 (m, 4H), 1.49 – 1.34 (m, 4H). **¹³C NMR** (100 MHz, $CDCl_3$) δ 139.1 (ArC), 133.7 (ArC), 129.3 (ArC), 128.0 (ArC), 56.1 (CH₂SO₂), 44.7 (CH₂Cl), 32.1 (CH₂), 27.5 (CH₂), 26.2 (CH₂), 22.5 (CH₂). **HRMS (ESI)** m/z $[M + H]^+$ calcd for $C_{12}H_{18}ClO_2S$ 261.0711; found 261.0712. The analytical data were in excellent agreement with those reported in the literature.¹⁵⁶

4-Methylpentyl phenyl sulfone



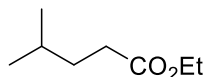
4-Methylpentyl phenyl sulfone (263 mg, 1.17 mmol, 98%), prepared from phenyl vinyl sulfone (200 mg, 1.19 mmol, 1.0 equiv.) and 1-iodo-2-methylpropane (0.16 mL, 3.57 mmol, 3.0 equiv.), was obtained as a colourless oil in 40 h: R_f 0.30 (petroleum ether : EtOAc 9 : 1). $^1\text{H NMR}$ (400 MHz, CDCl_3) δ 7.94 – 7.88 (m, 2H), 7.68 – 7.62 (m, 1H), 7.60 – 7.53 (m, 2H), 3.11 – 2.98 (m, 2H), 1.78 – 1.65 (m, 2H), 1.49 (dh, $J = 13.3, 6.7$ Hz, 1H), 1.30 – 1.15 (m, 2H), 0.84 (d, $J = 6.6$ Hz, 5H). $^{13}\text{C NMR}$ (100 MHz, CDCl_3) δ 139.3 (ArC), 133.7 (ArC), 129.3 (ArC), 128.1 (ArC), 56.6 (CH_2SO_2), 37.4 (CH_2), 27.7 (CH), 22.3 (CH_3), 20.6 (CH_2). **HRMS (ESI)** m/z [$\text{M} + \text{H}$] $^+$ calcd for $\text{C}_{12}\text{H}_{19}\text{O}_2\text{S}$ 227.1100; found 227.1100. The analytical data were in excellent agreement with those reported in the literature.¹⁵⁷

Phenyl 3-Methylbutane-1-sulfonate



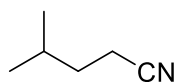
Phenyl 3-Methylbutane-1-sulfonate (245 mg, 1.08 mmol, 99%), prepared from phenyl vinyl sulfone (200 mg, 1.19 mmol, 1.0 equiv.) and 2-iodopropane (0.13 mL, 1.30 mmol, 1.2 equiv.), was obtained as a yellow oil in 40 h: R_f 0.40 (petroleum ether : EtOAc 1 : 1). $^1\text{H NMR}$ (400 MHz, CDCl_3) δ 7.45 – 7.37 (m, 2H), 7.35 – 7.30 (m, 1H), 7.30 – 7.25 (m, 2H), 3.28 – 3.20 (m, 2H), 1.92 – 1.83 (m, 2H), 1.75 (dp, $J = 13.4, 6.6$ Hz, 1H), 0.97 (d, $J = 6.6$ Hz, 6H). $^{13}\text{C NMR}$ (100 MHz, CDCl_3) δ 149.2 (ArC), 130.0 (ArC), 127.3 (ArC), 122.1 (ArC), 48.9 (CH_2), 32.0 (CH_2), 27.3 (CH), 22.1 (CH_3). **HRMS (ESI)** m/z [$\text{M} + \text{H}$] $^+$ calcd for $\text{C}_{11}\text{H}_{17}\text{O}_3\text{S}$ 229.0893; found 229.0892.

Ethyl 4-methylpentanoate



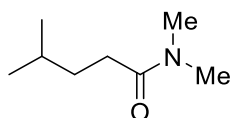
Ethyl 4-methylpentanoate (256 mg, 1.78 mmol, 89%), prepared from ethyl acrylate (0.22 mL, 1.99 mmol, 1.0 equiv.) and 2-iodopropane (0.239 mL, 2.39 mmol, 1.2 equiv.), was obtained as a red oil in 20 h without further purification: $^1\text{H NMR}$ (400 MHz, CDCl_3) δ 4.12 (q, $J = 7.1$ Hz, 2H), 2.34 – 2.26 (m, 2H), 1.66 – 1.45 (m, 3H), 1.25 (t, $J = 7.1$ Hz, 3H), 0.89 (d, $J = 6.3$ Hz, 6H). $^{13}\text{C NMR}$ (100 MHz, CDCl_3) δ 174.1 (C=O), 60.2 (OCH_2), 33.8 ($\text{CH}_2\text{C}=\text{O}$), 32.5 (CH_2), 27.7 (CH), 22.2 (CH_3), 14.2 (CH_3). **HRMS (ESI)** m/z [$\text{M} + \text{H}$] $^+$ calcd for $\text{C}_8\text{O}_2\text{H}_{17}$ 145.1223; found 145.1223.

4-Methylpentanenitrile



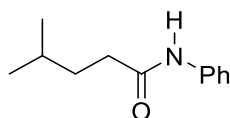
4-Methylpentanenitrile (359 mg, 3.69 mmol, 98%), prepared from acrylonitrile (0.25 mL, 3.77 mmol, 1.0 equiv.) and 2-iodopropane (0.45 mL, 4.52 mmol, 1.2 equiv.), was obtained as a yellow oil in 30 h without further purification: **¹H NMR** (400 MHz, CDCl₃) δ 2.33 (t, *J* = 7.4 Hz, 2H), 1.73 (dp, *J* = 13.3, 6.7 Hz, 1H), 1.55 (q, *J* = 7.4 Hz, 2H), 0.93 (d, *J* = 6.6 Hz, 6H). **¹³C NMR** (100 MHz, CDCl₃) δ 120.0 (CN), 34.0 (CH₂), 27.3 (CH), 21.9 (CH₃), 15.2 (CH₂CN). **HRMS (ESI)** *m/z* [M + H]⁺ calcd for C₆H₁₂N 227.1100; found 227.1100.

N,N,4-Trimethylpentanamide



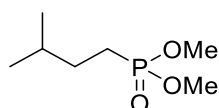
N,N,4-Trimethylpentanamide (277 mg, 1.94 mmol, 96%), prepared from *N,N*-dimethylacrylamide (0.21 mL, 2.02 mmol, 1.0 equiv.) and 2-iodopropane (0.24 mL, 2.42 mmol, 1.2 equiv.), was obtained as an orange oil in 32 h: **R_f** 0.3 (petroleum ether : EtOAc 1 : 1). **¹H NMR** (400 MHz, CDCl₃) δ 3.00 (s, 3H), 2.93 (s, 3H), 2.35 – 2.26 (m, 2H), 1.65 – 1.47 (m, 3H), 0.90 (d, *J* = 6.4 Hz, 6H). **¹³C NMR** (100 MHz, CDCl₃) δ 173.5 (C=O), 37.3 (CH₃), 35.4 (CH₂), 34.1 (CH₂), 31.5 (CH₂), 27.9 (CH), 22.4 (CH₃). **HRMS (ESI)** *m/z* [M + H]⁺ calcd for C₈H₁₈NO 144.1383; found 144.1384.

4-Methyl-*N*-phenylpentanamide



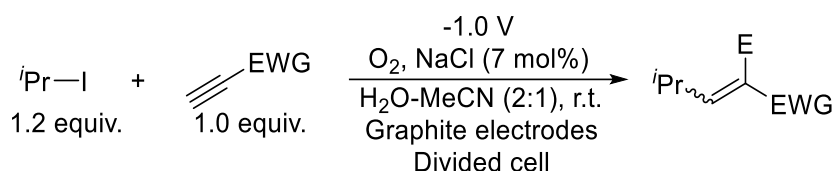
4-Methyl-*N*-phenylpentanamide (255 mg, 1.33 mmol, 98%), prepared from *N*-methyl-*N*-phenylacrylamide (200 mg, 1.36 mmol, 1.0 equiv.) and 2-iodopropane (0.16 mL, 1.63 mmol, 1.2 equiv.), was obtained as a white foam in 32 h: **R_f** 0.4 (petroleum ether : EtOAc 4 : 1). **¹H NMR** (400 MHz, CDCl₃) δ 7.51 (d, *J* = 8.0 Hz, 2H), 7.31 (dd, *J* = 8.5, 7.4 Hz, 2H), 7.10 (t, *J* = 7.5 Hz, 1H), 2.44 – 2.31 (m, 2H), 1.63 (dd, *J* = 7.0, 4.6 Hz, 3H), 0.94 (d, *J* = 6.0 Hz, 6H). **¹³C NMR** (100 MHz, CDCl₃) δ 171.5 (C=O), 137.9 (ArC), 129.0 (ArC), 124.2 (ArC), 119.7 (ArC), 35.9 (CH₂), 34.4 (CH₂), 27.8 (CH), 22.3 (CH₃). **HRMS (ESI)** *m/z* [M + H]⁺ calcd for C₁₂H₁₈NO 192.1383; found 192.1383. The analytical data were in excellent agreement with those reported in the literature.¹⁵⁸

Dimethyl isopentylphosphonate



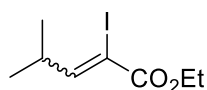
Dimethyl isopentylphosphonate (252 mg, 1.40 mmol, 95%), prepared from dimethyl vinylphosphonate (200 mg, 1.47 mmol, 1.0 equiv.) and 2-iodopropane (0.22 mL, 2.21 mmol, 1.5 equiv.), was obtained as a yellow oil in 32 h: **¹H NMR** (400 MHz, CDCl₃) δ 3.74 (s, 3H), 3.71 (s, 3H), 1.78 – 1.66 (m, 2H), 1.64 – 1.52 (m, 1H), 1.52 – 1.42 (m, 2H), 0.89 (d, *J* = 6.5 Hz, 6H). **¹³C NMR** (100 MHz, CDCl₃) δ 52.3 (CH₃), 30.9 (CH₂), 28.8 (CH₂), 28.6 (CH), 23.2 (CH₃), 21.9 (CH₃). **HRMS (ESI)** *m/z* [M + H]⁺ calcd for C₇H₁₈O₃P 181.0988; found 181.0988.

General Procedure for the Electrochemical Radical Alkyne Addition Reactions



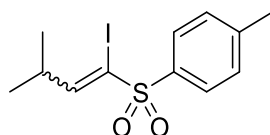
Two graphite electrodes (4.12 cm² area each) were placed into each chamber of the divided H cell and HCl_(aq) (pH = 2, 10 mL), MeCN (5 mL) and NaCl (7 mol%) were added to each chamber. Alkyne and alkyl halide were added to the cathodic chamber and the reaction mixture was stirred at room temperature under a constant reductive potential (-1.0 V) applied to the cathode for 20 h. The reaction mixture was then diluted with water (10 mL) and phases were separated. The aqueous layer was extracted with CH₂Cl₂ (3 × 20 mL). The combined organic layer was dried (MgSO₄), filtered, concentrated under reduced pressure and purified by column chromatography (cyclohexane : EtOAc 100 : 0 to 9 : 1) to yield the addition product.

Ethyl 2-iodo-4-methylpent-2-enoate



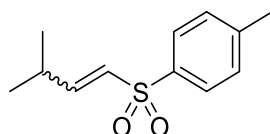
Ethyl 2-iodo-4-methylpent-2-enoate (140 mg, 0.552 mmol, 25%), prepared from ethyl propiolate (0.21 mL, 2.07 mmol, 1.0 equiv.) and 2-iodopropane (0.25 mL, 2.49 mmol, 1.2 equiv.), was obtained as a colourless oil in 20 h: **¹H NMR** (400 MHz, CDCl₃) δ 6.96 (d, *J* = 9.1 Hz, 1H), 4.25 (q, *J* = 7.1 Hz, 2H), 2.71 (dp, *J* = 9.1, 6.7 Hz, 1H), 1.32 (t, *J* = 7.1 Hz, 3H), 1.08 (d, *J* = 6.6 Hz, 6H). **¹³C NMR** (100 MHz, CDCl₃) δ 163.1 (C=O), 158.6 (CH=), 92.5 (C-I), 62.6 (OCH₂), 36.5 (CH), 20.7 (CH₃), 14.2 (CH₃). **HRMS (ESI)** *m/z* [M + H]⁺ calcd for C₈H₁₄I₂O₂ 269.0033; found 269.0033.

1-((1-Iodo-3-methylbut-1-en-1-yl)sulfonyl)-4-methylbenzene



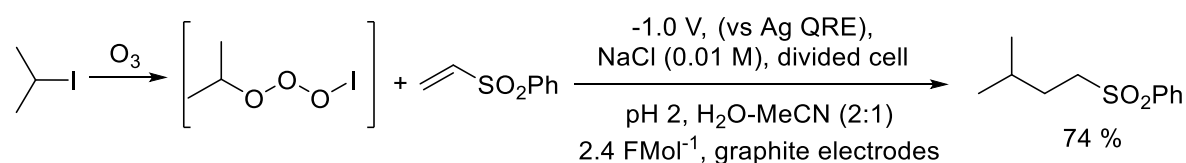
1-((1-Iodo-3-methylbut-1-en-1-yl)sulfonyl)-4-methylbenzene (54 mg, 0.155 mmol, 14%, cis : trans 1 : 4), prepared from 1-(ethynylsulfonyl)-4-methylbenzene (0.200 g, 1.11 mmol, 1.0 equiv.) and 2-iodopropane (0.11 mL, 1.33 mmol, 1.2 equiv.), was obtained as a white foam in 24 h: Major isomer: **¹H NMR** (400 MHz, CDCl₃) δ 7.79 (d, *J* = 8.3 Hz, 2H), 7.33 (d, *J* = 7.9 Hz, 2H), 7.10 (d, *J* = 9.1 Hz, 1H), 2.56 (hept, *J* = 9.2, 6.7 Hz, 1H), 2.44 (s, 3H), 1.09 (d, *J* = 6.7 Hz, 6H). **¹³C NMR** (100 MHz, CDCl₃) δ 156.5 (CH=), 144.9 (ArC), 134.5 (ArC), 129.8 (ArC), 129.3 (ArC), 99.9 (C-I), 35.8 (CH), 21.8 (CH₃), 20.7 (CH₃). Minor isomer: **¹H NMR** (400 MHz, CDCl₃) δ 7.79 (d, *J* = 8.3 Hz, 2H), 7.73 (d, *J* = 8.4 Hz, 1H), 7.33 (d, *J* = 7.9 Hz, 2H), 3.03 (hept, *J* = 7.4 Hz, 1H), 2.44 (s, 3H), 1.14 (d, *J* = 7.2 Hz, 6H). **HRMS (ESI)** *m/z* [M + H]⁺ calcd for C₁₂H₁₆I₂O₂S₁ 350.9910; found 350.9910.

1-Methyl-4-((3-methylbut-1-en-1-yl)sulfonyl)benzene



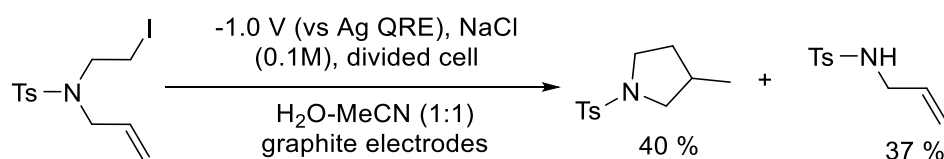
1-Methyl-4-((3-methylbut-1-en-1-yl)sulfonyl)benzen (167 mg, 0.744 mmol, 67%, cis : trans 1 : 5), prepared from 1-(ethynylsulfonyl)-4-methylbenzene (0.200 g, 1.11 mmol, 1.0 equiv.) and 2-iodopropane (0.11 mL, 1.33 mmol, 1.2 equiv.), was obtained as a colourless oil in 24 h: *trans*-Isomer **¹H NMR** (400 MHz, CDCl₃) δ 7.75 (d, *J* = 8.4 Hz, 2H), 7.32 (d, *J* = 7.9 Hz, 2H), 6.94 (dd, *J* = 15.1, 6.3 Hz, 1H), 6.23 (dd, *J* = 15.2, 1.5 Hz, 1H), 2.57 – 2.45 (m, 1H), 2.43 (s, 3H), 1.05 (d, *J* = 6.8 Hz, 6H). *cis*-Isomer **¹H NMR** (400 MHz, CDCl₃) δ 7.79 (d, *J* = 8.3 Hz, 2H), 7.32 (d, *J* = 7.9 Hz, 2H), 6.16 (dd, *J* = 11.0, 0.8 Hz, 1H), 5.99 (d, *J* = 10.9 Hz, 1H), 2.57 – 2.45 (m, 1H), 2.43 (s, 3H), 0.98 (d, *J* = 6.6 Hz, 6H). **¹³C NMR** (100 MHz, CDCl₃) δ 152.4 (SO₂CH=), 144.2 (CH=), 137.9 (ArC), 137.5 (ArC), 129.9 (ArC), 127.7 (ArC), 30.6 (CH), 21.7 (CH₃), 20.9 (CH₃). **HRMS (ESI)** *m/z* [M + H]⁺ calcd for C₁₂H₁₇SO₂ 225.0944; found 225.0943.

Electrochemical Radical Alkene Addition Reaction



Ozone was bubbled to a *i*-PrI (2 mL, 20.0 mmol) for 2 min and then purged with Ar for 5 min. The sample was stored under Ar for the following experiment. Two graphite electrodes (4.12 cm² area each) were placed into each chamber of the divided H cell and HCl(aq) (pH = 2, 10 mL), MeCN (5 mL) and NaCl (7 mol%) were added to each chamber and degassed with argon. Phenyl vinyl sulfone (200 mg, 1.19 mmol, 1.0 equiv.) and ozonized 2-iodopropane (0.142 mL, 1.43 mmol, 1.2 equiv.) were added to the cathodic chamber. The reaction mixture was stirred at room temperature under argon and a constant reductive potential (-1.0 V) applied to the cathode for 20 h. The reaction mixture was then diluted with water (10 mL) and phases were separated. The aqueous layer was extracted with CH₂Cl₂ (3 × 20 mL). The combined organic layer was dried (MgSO₄), filtered, concentrated under reduced pressure and purified by column chromatography (cyclohexane : EtOAc 100 : 0 to 9 : 1) to yield 3-methylbutyl phenyl sulfone (187 mg, 0.88 mmol, 74 %) as colourless oil: **Rf** 0.30 (petroleum ether : EtOAc 9 : 1). **¹H NMR** (400 MHz, CDCl₃) δ 7.94 – 7.86 (m, 2H), 7.70 – 7.63 (m, 1H), 7.60 – 7.54 (m, 2H), 3.11 – 3.05 (m, 2H), 1.66 – 1.54 (m, 3H), 0.86 (d, *J* = 6.3 Hz, 6H). Data in agreement with literature.¹⁵⁹

Electrochemical Radical Reductive Cyclisation Reaction



Two graphite electrodes (4.12 cm² area each) were placed into each chamber of the divided H cell and sodium acetate buffer (pH = 3.6, 7.5 mL), MeCN (7.5 mL) and NaCl (88 mg, 1.51 mmol) were added to each chamber. N-Allyl-N-(2-iodoethyl)-4-methylbenzenesulfonamide (182 mg, 0.5 mmol) was added to the cathodic chamber and the reaction mixture was stirred at room temperature under a constant reductive potential (-1.0 V) applied to the cathode for 6 h. The reaction mixture was then diluted with aqueous Na₂S₂O₃ (1 M; 10 mL) and phases were separated. The aqueous layer was extracted with CH₂Cl₂ (3 × 20 mL). The combined organic layer was dried (MgSO₄), filtered, concentrated under reduced pressure and purified by column chromatography (cyclohexane : EtOAc 100 : 0 to 4 : 1) to yield the corresponding pyrrolidine (40%) and N-allyltosylamide (37%).

3-Methyl-1-tosylpyrrolidine: **Rf** 0.33 (petroleum ether : EtOAc 4 : 1). **¹H NMR** (400 MHz, CDCl₃) δ 7.71 (d, *J* = 8.3 Hz, 2H), 7.32 (d, *J* = 8.0 Hz, 2H), 3.42 (dd, *J* = 9.7, 7.2 Hz, 1H), 3.34 (ddd, *J* = 9.9, 8.2, 4.2 Hz, 1H), 3.22 (ddd, *J* = 9.8, 8.3, 7.3 Hz, 1H), 2.75 (dd, *J* = 9.7, 7.8 Hz, 1H), 2.43 (s, 3H), 2.12 (dq, *J* = 14.6, 7.1 Hz, 1H), 1.90 (dtd, *J* = 14.1, 6.9, 4.1 Hz, 1H), 1.35 (dd, *J*

= 12.4, 8.4 Hz, 1H), 0.91 (d, J = 6.7 Hz, 3H). Data in agreement with literature.¹⁶⁰

N-Allyl-4-methylbenzenesulfonamide: **Rf** 0.20 (petroleum ether : EtOAc 4 : 1). **¹H NMR** (400 MHz, CDCl₃) δ 7.75 (d, J = 8.3 Hz, 2H), 7.31 (d, J = 7.9 Hz, 2H), 5.72 (ddt, J = 17.1, 10.2, 5.8 Hz, 1H), 5.25 – 5.00 (m, 2H), 4.58 (s, 1H), 3.60 – 3.55 (m, 2H), 2.43 (s, 3H). Data in agreement with literature.¹⁶¹

Photoluminescence Spectroscopy

Fenton Reaction

FeSO₄·7H₂O (28 mg, 0.101 mmol), H₂O₂ (10 μ L) and disodium terephthalate (21 mg, 0.100 mmol) were added to a mixture of sodium acetate buffer (pH = 3.6, 1 mL) and H₂O (6 mL) and the resulting mixture was stirred at room temperature for 30 min. An analytical sample of the reaction mixture (1 mL) was basified with aqueous NaOH (1 M, 0.1 mL). The fluorescence intensity was then measured at 431 nm with excitation at 310 nm.

Reductive Cyclisation Reaction with Fluorescence Probe

Two graphite electrodes (4.12 cm² area each) were placed into each chamber of the divided H cell and sodium acetate buffer (pH = 3.6, 7.5 mL), MeCN (7.5 mL) and NaCl (88 mg, 1.51 mmol) were added to each chamber. *N*-Allyl-*N*-(2-iodoethyl)-4-methylbenzenesulfonamide (182 mg, 0.5 mmol) and disodium terephthalate (21 mg, 0.100 mmol) were added to the cathodic chamber and the reaction mixture was stirred at room temperature under a constant reductive potential (-1.0 V) applied to the cathode for 20 h. An analytical sample of the reaction mixture (1 mL) was basified with aqueous NaOH (2 M, 0.05 mL). The fluorescence intensity was then measured at 431 nm with excitation at 310 nm. A control experiment was performed with the sample procedure without the addition of *N*-allyl-*N*-(2-iodoethyl)-4-methylbenzenesulfonamide.

Detection of Hydroxyl Radicals in Anodic and Cathodic Chambers with Fluorescence Probe

Two graphite electrodes (4.12 cm² area each) were placed into each chamber of the divided H cell and disodium terephthalate (21 mg, 0.100 mmol), sodium acetate buffer (pH = 3.6, 7.5 mL), MeCN (7.5 mL) and NaCl (88 mg, 1.51 mmol) were added to each chamber. The reaction mixture was stirred at room temperature under a constant reductive potential (-1.0 V) applied to the cathode for 20 h. An analytical sample of the reaction mixture (1 mL) from each chamber was basified with aqueous NaOH (2 M, 0.05 mL). The fluorescence intensity was then

measured at 431 nm with excitation at 310 nm.

Battery method

Same as the standard procedure except the potentiostat was replaced by using battery (DURACELL PLUS POWER, 9 V) to connect with the anode and cathode without reference electrode.

Photoelectrochemical method

Two graphite electrodes (4.12 cm² area each) were placed into each chamber of the divided H cell and each side was charged with 10 mL anhydrous MeCN and LiClO₄ (0.32 g) to make a 0.3 M solution. Phenyl vinyl sulfone (200 mg, 1.19 mmol, 1.0 equiv.) and 2-iodopropane (0.142 mL, 1.43 mmol, 1.2 equiv.) were added to the cathodic chamber and the reaction mixture was stirred at room temperature under argon, a constant reductive potential (-1.0 V) applied to the cathode and a 254 nm constant UV light for 24 h. The reaction mixture was then diluted with aqueous Na₂S₂O₃ (1 M; 10 mL) and phases were separated. The aqueous layer was extracted with CH₂Cl₂ (3 × 20 mL). The combined organic layer was dried (MgSO₄), filtered, concentrated under reduced pressure and purified by column chromatography (cyclohexane : EtOAc 100 : 0 to 9 : 1) to yield the 3-Methylbutyl phenyl sulfone (75.8 mg, 0.36 mmol, 30%).

Chapter 6 References

1. D. Pollok and S. R. Waldvogel, *Chem. Sci.*, 2020, **11**, 12386–12400.
2. M. Yan, Y. Kawamata and P. S. Baran, *Chem. Rev.*, 2017, **117**, 13230–13319.
3. M. Yan, Y. Kawamata and P. S. Baran, *Angew. Chem. Int. Ed.*, 2018, **57**, 4149–4155.
4. A. Volta, *Philos. Trans. R. Soc.*, 1800, **90**, 403–431.
5. E. Steckhan, *Angew. Chem. Int. Ed.*, 1986, **25**, 683–701.
6. R. D. Little, D. P. Fox, L. Van Hijfte, R. Dannecker, G. Sowell, R. L. Wolin, L. Moens and M. M. Baizer, *J. Org. Chem.*, 1988, **53**, 2287–2294.
7. K. D. Moeller, *Tetrahedron*, 2000, **56**, 9527–9554.
8. J. I. Yoshida, T. Murata and S. Isoe, *Tetrahedron Lett.*, 1986, **27**, 3373–3376.
9. B. R. Rosen, E. W. Werner, A. G. O'Brien and P. S. Baran, *J. Am. Chem. Soc.*, 2014, **136**, 5571–5574.
10. B. Elsler, D. Schollmeyer, K. M. Dyballa, R. Franke and S. R. Waldvogel, *Angew. Chem. Int. Ed.*, 2014, **53**, 5210–5213.
11. M. Faraday, *Philos. Trans. R. Soc.*, 1834, **124**, 77–122.
12. H. Kolbe, *J. Prakt. Chem.*, 1847, **41**, 137–139.
13. M. Paidar, V. Fateev and K. Bouzek, *Electrochim. Acta*, 2016, **209**, 737–756.
14. A. Hickling, *Trans. Faraday Soc.*, 1942, **38**, 27–33.
15. J. E. B. Randles, *Trans. Faraday Soc.*, 1948, **44**, 327–338.
16. P. E. Iversen and H. Lund, *Tetrahedron Lett.*, 1969, **40**, 3523–3524.
17. T. Shono, H. Hamaguchi and Y. Matsumura, *J. Am. Chem. Soc.*, 1975, **97**, 4264–4268.
18. P. W. Seavill, K. B. Holt and J. D. Wilden, *Green Chem.*, 2018, **20**, 5474–5478.
19. Lebreux, F. D. R., Buzzo, F., Marko, I. N., *Synlett.*, 2008, **18**, 2815–2820.
20. N. Elgrishi, K. J. Rountree, B. D. McCarthy, E. S. Rountree, T. T. Eisenhart and J. L. Dempsey, *J. Chem. Educ.*, 2018, **95**, 197–206.
21. Vishal A. Mahajan, Popat D. Shinde, Anil S. Gajare, M. Karthikeyan and Radhika D. Wakharkar, *Green Chem.*, 2002, **4**, 325–327.
22. P. T. Kissinger, in *Laboratory Techniques in Electroanalytical Chemistry*, eds. P. T. Kissinger and W. R. Heineman, Marcel Dekker, New York, 2nd edn re., 1996, ch. 1, pp. 1–9.
23. G. Hilt, *ChemElectroChem*, 2020, **7**, 395–405.
24. S. Torii, K. Uneyama, T. Nakai and T. Yasuda, *Tetrahedron Lett.*, 1981, **22**, 2291–2294.
25. K. Mitsudo, T. Shiraga, J.-I. Mizukawa, S. Suga and H. Tanaka, *Chem. Commun.*, 2010, **46**, 9256–9258.
26. H. Maeda and H. Ohmori, *Acc. Chem. Rev.*, 1999, **32**, 72–80.

27. A. G. O'Brien, A. Maruyama, Y. Inokuma, M. Fujita, P. S. Baran and D. G. Blackmond, *Angew. Chem. Int. Ed.*, 2014, **53**, 11868–11871.
28. E. J. Horn, B. R. Rosen and P. S. Baran, *ACS Cent. Sci.*, 2016, **2**, 302–308.
29. A. Sagadevan, A. Ragupathi and K. C. Hwang, *Angew. Chem. Int. Ed.*, 2015, **54**, 13896–13901.
30. E. Barrado, R. A. S. Couto, M. B. Quinaz, J. L. F. C. Lima and Y. Castrillejo, *J. Electroanal. Chem.*, 2014, **720–721**, 139–146.
31. N. G. Tsierkezos and U. Ritter, *J. Appl. Electrochem.*, 2010, **40**, 409–417.
32. Z. Chen, M. Pitchakuntla and Y. Jia, *Nat. Prod. Rep.*, 2019, **36**, 666-690.
33. F. Yang, T. Jin, M. Bao, Y. Yamamoto, *Chem. Commun.*, 2011, **47**, 4541- 4543.
34. F. Yang, T. Jin, M. Bao, Y. Yamamoto, *Tetrahedron*, 2011, **67**, 10147- 10155.
35. T. Okitsu, K. Nakata, K. Nishigaki, N. Michioka, M. Karatani, A. Wada, *J. Org. Chem.*, 2014, **79**, 5914-5920.
36. T. Okitsu, R. T. Nakazawa, A. Wada, *Org. Lett.*, 2008, **10**, 4967-4970.
37. Y. Li, J. Li, S. Yu, J. Wang, Y. Yu, J. Deng, *Tetrahedron*, 2015, **71**, 8271-8277.
38. K. Orito, T. Hatakeyama, M. Takeo, H. Suginome, M. Tokuda, *Synthesis*, 1997, 23–25.
39. V. A. Mahajan, P. D. Shinde, A. S. Gajare, M. Karthikeyan, R. D. Wakharkar, *Green Chem.*, 2002, **4**, 325–327.
40. V. R. Annamalai, E. C. Linton and M. C. Kozlowski, *Org. Lett.*, 2009, **11**, 621–624.
41. A. S. H. Makhlouf and R. Rodriguez, *Advances in Smart Coatings and Thin Films for Future Industrial and Biomedical Engineering Applications*, 2020, ch. 15, pp. 407-427.
42. N. Kanani, *Electroplating: Basic Principles, Processes and Practice; Elsevier Advanced Technology*: Oxford, U.K., 2004.
43. R. L. Geerts, J. C. Huffman, K. G. Caulton, *Inorg. Chem.*, 1986, **25**, 1803-1805.
44. T. Kometani, D. S. Watt, T. Ji, *Tetrahedron Lett.*, 1985, **26**, 2043–2046.
45. T. Kometani, D. S. Watt, T. Ji, T. Fitz, *J. Org. Chem.*, 1985, **50**, 5384–5387.
46. C. Hansch, A. Leo, R. W. Taft, *Chem. Rev.*, 1991, 165–195.
47. G. J. Rowlands, *Annu. Rep. Prog. Chem., Sect. B: Org. Chem.*, 2011, **107**, 19–33.
48. P. Renaud and M. P. Sibi, *Radicals in Organic Synthesis*, Wiley-VCH, Weinheim, Germany, 2001, vol. 1 and 2.
49. P. A. Baguley and J. C. Walton, *Angew. Chem., Int. Ed.*, 1998, **37**, 3072–3082.
50. B. Giese, J. A. Gonzalez-Gomez, T. Witzel, *Angew. Chem. Int. Ed.*, 1984, **23**, 69-70.
51. B. Giese, *Angew. Chem. Int. Ed. Engl.*, 1983, **22**, 753-764.
52. C. P. O. Jasperese, D. P. Curran, T. L. Fevig, *Chem. Rev.*, 1991, **91**, 1237-1286.
53. G. J. Rowland, *Tetrahedron*, 2009, **65**, 8603-8655.
54. D. Kamimura, D. Urabe, M. Nagatomo, M. Inoue, *Org. Lett.*, 2013, **15**, 5122-5125.
55. G. L. Lackner, K. W. Quasdorf, L. E. Overman, *J. Am. Chem. Soc.*, 2013, **135**, 15342-

15345.

56. K. Miura, M. Tojino, N. Fujisawa, A. Hosomi, I. Ryu, *Angew. Chem. Int. Ed.*, 2004, **43**, 2423-2425.

57. J. D. Nguyen, E. M. D'Amato, J. M. R. Narayanam and C. R. J. Stephenson, *Nat. Chem.*, 2012, **4**, 854–859.

58. B. Schweitzer-Chaput, M. A. Horwitz, E. de Pedro Beato and P. Melchiorre, *Nat. Chem.*, 2019, **11**, 129–135.

59. J. A. Cleary, M. S. Mubarak, K. L. Vieira, M. R. Anderson and D. G. Peters, *J. Electroanal. Chem. Interfacial Electrochem.*, 1986, **198**, 107–124.

60. J.H. Wagenknecht, *J. Electroanal. Chem.*, 1974, **52**, 489.

61. A. J. Bard and A. Merz, *J. Am. Chem. Soc.*, 1979, **101**, 2959-2965.

62. C. A. Paddon, F. L. Bhatti, T. J. Donohoe and R. G. Compton, *J. Phys. Org. Chem.*, 2007, **20**, 115–121.

63. D. Vasudivan, *Russ. J. Electrochem.*, 2005, **41**, 310–314.

64. H. Miyabe, M. Ueda, A. Nishimura and T. Naito, *Org. Lett.*, 2002, **4**, 131–134.

65. A. Hosomi, M. Hojo, J. Yoshizawa, Y. Funahashi, R. Okada, S. Nakamura and J. Tateiwa, *Heterocycles*, 1998, **49**, 85-88.

66. M. Hayyan, M. A. Hashim and I. M. AlNashef, *Chem. Rev.*, 2016, **116**, 3029–3085

67. B. Halliwell, *Plant Physiology.*, 2006, **141**, 312-322.

68. M. Mohammad, A. Y. Khan, M. S. Subhani, N. Bibi, S. Ahmad, S. Saleemi, *Res. Chem. Intermed.*, 2001, **27**, 259–267.

69. A. Naqui, B. Chance, E. Cadenas, *Annu. Rev. Biochem.*, 1986, **55**, 137–166.

70. I. Gülçin, Z. Huyut, M. Elmastas, H. Y. Aboul-Enein, *Arabian J. Chem.*, 2010, **3**, 43–53.

71. J. Nordberg, E. S. J. Arnér, *Free Radical Biol. Med.* 2001, **31**, 1287–1312.

72. P. D. C. Dietzel, R. K. Kremer, M. Jansen, *J. Am. Chem. Soc.*, 2004, **126**, 4689–4696.

73. Z. Wu, M. Li, J. Howe, H. M. Meyer, S. H. Overbury, *Langmuir*, 2010, **26**, 16595–16606.

74. D. T. Sawyer, J. S. Valentine, *Acc. Chem. Res.*, 1981, **14**, 393–400.

75. H. Xiao, H. Hu, W. H. E. Schwarz, J. Li, *J. Phys. Chem. A*, 2010, **114**, 8837–8844.

76. M. Hayyan, F. S. Mjalli, I. M. AlNashef, M. A. Hashim, *Int. J. Electrochem. Sci.*, 2012, **7**, 8116–8127.

77. A. A. Frimer, *Organic Reactions Involving the Superoxide Anion. In The Chemistry of Functional Groups, Peroxides*, John Wiley & Sons: New York, 1983, pp 429–461.

78. D. T. Sawyer, *Oxygen Chemistry*, Oxford University Press: New York, 1991.

79. F. Haber, J. Weiss, *Proc. R. Soc. London, Ser. A* 1934, **147**, 332–351.

80. I. M. AlNashef, M. L. Leonard, M. C. Kittle, M. A. Matthews, J. M. Weidner, *Electrochem. Solid-State Lett.* 2001, **4**, D16–D18.

81. I. M. AlNashef, *Destruction of Chlorinated Hydrocarbons Using Potassium Superoxide*, King Saud University: Riyadh, Saudi Arabia, November 2006.
82. M. Hayyan, F. S. Mjalli, I. M. AlNashef, M. A. Hashim, *J. Fluorine Chem.*, 2012, **142**, 83–89.
83. J. Divisek, B. Kastening, *J. Electroanal. Chem.*, 1975, **65**, 603–621.
84. M. V. Merritt, D. T. Sawyer, *J. Org. Chem.*, 1970, **35**, 2157–2159.
85. R. A. Johnson, E. G. Nidy, M. V. Merritt, *J. Am. Chem. Soc.*, 1978, **100**, 7960–7966.
86. M. J. Gibian, T. Ungermann, *J. Org. Chem.*, 1976, **41**, 2500–2502.
87. A. A. Frimer, I. Rosenthal, *Photochem. Photobiol.*, 1978, **28**, 711–717.
88. C. P. Andrieux, P. Hapiot, J. M. Saveant, *J. Am. Chem. Soc.*, 1987, **109**, 3768–3775.
89. M. E. Ortiz, L. J. Núñez-Vergara, C. Camargo, J. A. Squella, *Pharm. Res.*, 2004, **21**, 428–435.
90. A. Miyata, M. Murakami, R. Irie, T. Katsuki, *Tetrahedron Lett.*, 2001, **42**, 7067–7070.
91. M. A. Casadei, S. Cesa, F. M. Moracci, A. Inesi, M. Feroci, *J. Org. Chem.*, 1996, **61**, 380–383.
92. M. A. Casadei, F. M. Moracci, G. Zappia, A. Inesi, L. Rossi, *J. Org. Chem.*, 1997, **62**, 6754–6759.
93. D. R. Weinberg, C. J. Gagliardi, J. F. Hull, C. F. Murphy, C. A. Kent, B. C. Westlake, A. Paul, D. H. Ess, D. G. McCafferty, T. J. Meyer, *Chem. Rev.*, 2012, **112**, 4016–4093.
94. X. J. Huang, E. I. Rogers, C. Hardacre, R. G. Compton, *J. Phys. Chem. B*, 2009, **113**, 8953–8959.
95. F. Haber, J. Weiss, *Naturwissenschaften*, 1932, **51**, 948-950.
96. E. Brillas, I. Sire's and M. A. Oturan, *Chem. Rev.*, 2009, **109**, 6570–6631.
97. H. J. H. Fenton, *Chem. News*, 1876, **33**, 190.
98. H. J. H. Fenton, *J. Chem. Soc.*, 1894, **65**, 899-910.
99. W. Manchot, *Liebigs Ann. Chem.*, 1901, **314**, 177-199.
100. J. H. W. Merz, A. Waters, *Discuss. Faraday Soc.*, 1947, **2**, 179-188.
101. W. G. Barb, J. H. Baxendale, P. George, K. R. Hargrave, *Trans. Faraday Soc.*, 1951, **47**, 462-500.
102. W. G. Barb, J. H. Baxendale, P. George, K. R. Hargrave, *Trans. Faraday Soc.*, 1951, **47**, 591-616.
103. C. Walling, *Acc. Chem. Res.* 1975, **8**, 125-131.
104. J. Prousek, *Chem. Listy*, 1995, **89**, 11-21.
105. R. F. Brown, S. E. Jamison, K. Pandit, J. Pinkus, G. R. White, H. P. Braendlin, *J. Org. Chem.*, 1964, **29**, 146-153.
106. F. Haber, J. Weiss, *Proc. R. Soc. London A*, 1934, **147**, 332-351.
107. D. I. Metelitsa, *Russ. Chem. Rev.*, 1971, **40**, 563-580.
108. Y. Sun, J. J. Pignatello, *Environ. Sci. Technol.*, 1993, **27**, 304-310.

109. Y. Sun, J. J. Pignatello, *J. Agric. Food Chem.*, 1993, **41**, 308-312.
110. H. Gallard, J. D. Laat, B. Legube, *New J. Chem.*, 1998, **22**, 263-268.
111. C. Walling, *Acc. Chem. Res.*, 1998, **31**, 155-157.
112. M. E. Lindsey, M. A. Tarr, *Chemosphere*, 2000, **41**, 409-417.
113. D. R. Stanisavljev, M. C. Milenković, M. D. Mojović and A. D. Popovic-Bijelic, *J. Phys. Chem. A*, 2011, **115**, 2247–2249.
114. B. H. J. Bielski, D. E. Cabelli, R. L. Arudi, A. B. Ross, *J. Phys. Chem. Ref. Data*, 1985, **14**, 1041-1100.
115. W. H. Koppenol, *Free Radical Biol. Med.*, 1993, **15**, 645–651.
116. A. Gomes, E. F. Jose, L.F.C. Lima, *J. Biochem. Biophys. Methods*, 2005, **65**, 45–80.
117. B. Tang, L. Zhang and Y. Geng, *Talanta*, 2005, **65**, 769–775.
118. H. J. H. Fenton, *J. Chem. Soc., Trans.*, 1894, **65**, 899–910.
119. Y. Wang and Q. Chen, *Int. J. Electrochem.*, 2013, **2013**, 1–7.
120. J. M. Noël, A. Latus, C. Lagrost, E. Volanschi and P. Hapiot, *J. Am. Chem. Soc.*, 2012, **134**, 2835–2841.
121. M. H. Shao, P. Liu and R. R. Adzic, *J. Am. Chem. Soc.*, 2006, **128**, 7408–7409.
122. S. C. Perry, D. Pangotra, L. Vieira, L. I. Csepei, V. Sieber, L. Wang, C. Ponce de León and F. C. Walsh, *Nat. Rev. Chem.*, 2019, **3**, 442–458.
123. L. Szpyrkowicz, C. Juzzolino and S. N. Kaul, *Water Res.*, 2001, **35**, 2129–2136.
124. Y. Sakamoto, A. Yabushita, M. Kawasaki and S. Enami, *J. Phys. Chem. A*, 2009, **113**, 7707–7713.
125. T. M. Hellman and G. A. Hamilton, *J. Am. Chem. Soc.*, 1974, **96**, 1530–1535.
126. S. W. Hunt, M. Roeselová, W. Wang, L. M. Wingen, E. M. Knipping, D. J. Tobias, D. Dabdub and B. J. Finlayson-Pitts, *J. Phys. Chem. A*, 2004, **108**, 11559–11572.
127. Q. Liu, L. M. Schurter, C. E. Muller, S. Aloisio, J. S. Francisco and D. W. Margerum, *Inorg. Chem.*, 2001, **40**, 4436–4442.
128. L. P. Candeias, K. B. Patel, M. R. L. Stratford and P. Wardman, *FEBS Lett.*, 1993, **333**, 151–153.
129. G. Schmitz, S.D. Furrow, *Int. J. Chem. Kinet.*, 2013, **45**, 525–530.
130. D. P. Curran and D. Kim, *Tetrahedron*, 1991, **47**, 6171–6188.
131. S. Wolfe, A. Stolow and L. A. LaJohn, *Tetrahedron Lett.*, 1983, **24**, 4071–4074.
132. D. A. Bors and A. J. Streitwieser, *J. Am. Chem. Soc.*, 1986, **108**, 1397–1404.
133. W. R. Bowman, H. Heaney and B. M. Jordan, *Tetrahedron*, 1991, **47**, 10119–10128.
134. C. J. Moody and C. L. Norton, *Tetrahedron Lett.*, 1995, **36**, 9051–9052.
135. A. Saha, J. Leazer and R. S. Varma, *Green Chem.*, 2012, **14**, 67-71.
136. W. Chen, X. Yang, Y. Li, J. Li, X. Wang, G. Zhang and H. Zhang, *Org. Biomol. Chem.*, 2011, **9**, 4250-4255.

137. C. Chardin, J. Rouden, S. Livi and J. Baudoux, *Green Chem.*, 2017, **19**, 5054-5059.
138. M. Chouhan, K. Kumar, R. Sharma, V. Grover and V. A. Nair, *Tetrahedron Lett.*, 2013, **54**, 4540-4543.
139. A. Llevot, B. Monney, A. Sehlinger, S. Behrens and M. A. R. Meier, *Chem. Commun.*, 2017, **53**, 5175-5178.
140. R. Trivedi, J. A. Tunge, *Org. Lett.*, 2009, **11**, 5650.
141. M. Rehan, R. Nallagonda, B. Das, T. Meena and P. Ghorai, *J. Org. Chem.*, 2017, **82**, 3411-3424.
142. R. Bujok, M. Bieniek, M. Masnyk, A. Michrowska, A. Sarosiek, H. Stepowska, D. Arlt and K. Grela, *J. Org. Chem.*, 2004, **69**, 6894-6896.
143. J. A. Burlison, L. Neckers, A. B. Smith, A. Maxwell and B. S. J. Blagg, *J. Am. Chem. Soc.*, 2006, **128**, 15529-15536.
144. M. Yoshida, M. Higuchi and K. Shishido, *Org. Lett.*, 2009, **11**, 4752-4755.
145. J. Gomez, *Pharmacie et de Chimie*, 1934, **8**, 337-340.
146. W. N. White, D. Gwynn, R. Schlitt, C. Girard and W. Fife, *J. Am. Chem. Soc.*, 1958, **80**, 3271-3272.
147. M. Fousteris, C. Chevrin, J. L. Bras and J. Muzart, *Green Chem.*, 2006, **8**, 522-523.
148. M. Yoshida, M. Higuchi, K. Shishido, *Org. Lett.*, 2009, **11**, 4752-4755.
149. S. E. Yagunov, S. V. Kholshin, N. V. Kandalintseva, and A. E. Prosenko, *Russ. Chem. Bull. Int. Ed.*, **66**, 1024-1029.
150. K. Yip, M. Yang, K. Law, N. Zhu and D. Yang, *J. Am. Chem. Soc.*, 2006, **128**, 3130-3131.
151. G. Sekar and V. K. Singh, *J. Org. Chem.*, 1999, **64**, 2537-2539.
152. F. Xue, F. Wang, J. Liu, J. Di, Q. Liao, H. Lu, M. Zhu, L. He, H. He, D. Zhang, H. Song, X. Liu and Y. Qin. *Angew. Chem. Int. Ed.*, 2018, **57**, 6667-6671.
153. A. C. Bonaparte, M. P. Betush, B. M. Panseri, D. J. Mastarone, R. K. Murphy, S. S. Murphree. *Org. Lett.*, 2011, **13**, 1447-1449.
154. N. P. Ramirez, J. C. Gonzalez-Gomez. *Eur. J. Org. Chem.*, 2017, 2154-2163.
155. C. J. Moody and C. L. Norton, *J. Chem. Soc., Perkin Trans. 1*, 1997, 2639-2644.
156. A. Horn and P. H. Dussault. *J. Org. Chem.*, 2019, **84**, 14611-14626.
157. A. C. Bonaparte, M. P. Betush, B. M. Panseri, D. J. Mastarone, R. K. Murphy, S. S. Murphree. *Org. Lett.*, 2011, **13**, 1447-1449.
158. H. Dao, C. Li, Q. Michaudel, B. D. Maxwell, P. S. Baran, *J. Am. Chem. Soc.*, 2015, **137**, 8046-8049.
159. F. Xue, F. Wang, J. Liu, J. Di, Q. Liao, H. Lu, M. Zhu, L. He, H. He, D. Zhang, H. Song, X. Liu and Y. Qin. *Angew. Chem. Int. Ed.*, 2018, **57**, 6667-6671.
160. J. Y. Hwang, J. H. Baek, T. Il Shin, J. H. Shin, J. W. Oh, K. P. Kim, Y. You and E. J. Kang, *Org. Lett.*, 2016, **18**, 4900-4903.

161. N. Cabrera-Lobera, M. T. Quirós, W. W. Brennessel, M. L. Neidig, E. Buñuel and D. J. Cárdenas, *Org. Lett.*, 2019, **21**, 6552–6556.

162. D. Pletcher and F. Walsh, *Industrial Electrochemistry*, Blackie Academic & Professional, London, New York, 2nd edn, 1993.

Cite this: *Chem. Sci.*, 2020, **11**, 5333

All publication charges for this article have been paid for by the Royal Society of Chemistry

Received 24th March 2020

Accepted 7th May 2020

DOI: 10.1039/d0sc01694b

rsc.li/chemical-science

Electrochemical radical reactions of alkyl iodides: a highly efficient, clean, green alternative to tin reagents†

Diyuan Li,¹ Tsz-Kan Ma, Reuben J. Scott and Jonathan D. Wilden¹*

An electrochemical 'redox-relay' system has been developed which allows the generation of C-centered radicals. Intermolecular 'tin-like' radical reactions can subsequently be conducted under the most benign of conditions. The yields and efficiency of the processes are competitive and even superior in most cases to comparable conditions with tributyltin hydride. The use of air and electricity as the promotor (instead of a tin or other reagent) combined with the aqueous reaction media make this a clean and 'green' alternative to these classic C–C bond forming processes.

Introduction

The use of radical reactions for the construction of complex organic molecules are now almost ubiquitous in synthetic chemistry.¹ Historically however, organic chemistry has relied on tributyltin hydride (and similar reagents) to mediate such processes.² Organotin reagents have proved remarkably efficient for the generation and mediation of carbon-centered radicals. Their drawbacks however are significant; the reagents are extremely toxic, expensive and the side-products are often difficult to remove from the reaction medium post reaction. As such, recent years have seen intense interest in alternatives to these extremely useful reagents.³ Almost without exception however, none have matched the efficiency, generality and functional group tolerance of tin-based reagents. The result of this is that many chemists, particularly those in industry have shunned tin reagents, however, in doing so they necessarily preclude the advantages that this class of radical reactions can offer in terms of the construction of complex organic architectures. Two methods that are becoming more popular for the generation of radical species are electrochemistry and photoredox catalysis.^{4,5} Photoredox catalysis has already, in a short amount of time, proved to be a powerful tool for the activation of organic molecules.⁶ Similarly, synthetic organic electrochemistry is becoming an increasingly popular alternative way to activate organic molecules *via* direct addition or removal of electrons to generate reactive radical species.⁷ Unfortunately, the direct electrochemical reduction of alkyl halides requires highly reducing potentials and as such has not found general

application because of the incompatibility of these extreme potentials with various functional groups.^{8,9} Herein, we outline an operationally simple, mild and molecular oxygen mediated indirect electrochemical approach to the formation of carbon centered radicals from alkyl iodides using the 'standard' feedstocks used in tributyltin hydride mediated reactions, namely an alkyl halide and an alkene acceptor (*i.e.* the classic Giese reaction).¹⁰ We also demonstrate its synthetic utility in intermolecular C–C bond formation with a range of alkene and alkyne acceptors.

We here demonstrate that 'tin-like' radical reactions can be achieved using only mildly reductive electrochemical conditions combined with aerial oxygen in semi-aqueous conditions. The mildly reducing conditions (–1.0 V vs. Ag QRE) are selective for the activation of molecular oxygen and the desired radical reaction only and does not interfere with other functional groups in the molecule. Similarly, although aqueous conditions are employed, the applied potential is not sufficient to effect the reduction of water (*ca.* –1.5 V vs. Ag QRE under our conditions). Furthermore, no tin, silicon, phosphorous or any other mediator apart from air is required, and the construction of the electrochemical cell employs only environmentally benign and cheap materials. In particular, inexpensive graphite electrodes

Department of Chemistry, University College London, 20 Gordon Street, London WC1H 0AJ, UK. E-mail: j.wilden@ucl.ac.uk

† Electronic supplementary information (ESI) available: Experimental procedures and details of the electrochemical apparatus employed. See DOI: 10.1039/d0sc01694b

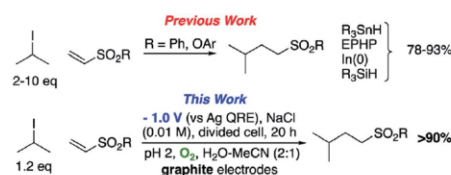


Fig. 1 Comparison of classic intermolecular Giese reactions with the electrochemical method.



are employed. Fig. 1 compares the previous conditions with the work described here.^{11–14}

Results & discussion

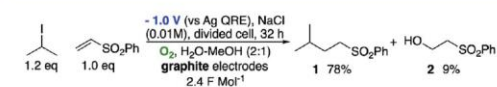
We first made the observation that a methanol–water solution of phenyl vinyl sulfone and 2-iodopropane when exposed to a mild reducing potential (constant potential, 1.0 V vs. Ag wire quasi-reference electrode, graphite rod working electrode, divided cell) undergo efficient C–C bond formation to yield the sulfone **1** in good yield as well as some β -hydration product **2** (Scheme 1). The reactants were contained in the cathodic chamber and no mixing of organic species were observed with the anodic compartment. Furthermore, only the electrochemical oxidation of a small amount of water was observed in the anodic chamber, meaning no toxic or hazardous materials are required to be removed from the apparatus after the reaction.

Intrigued by this reaction and suspecting that exposure to air was a critical facet, we set about exploring the optimal conditions for this process as shown in Table 1. It seems likely that the hydroxy product results from a simple base-mediated addition reaction of water to the electron deficient alkene. As such, this undesired product was relatively easily eliminated by lowering the pH and employing acetonitrile as the organic co-solvent.

Table 1 shows the optimisation for the reaction outlined in Scheme 1. A number of observations are noteworthy. Firstly, water is essential for the success of the reaction. Secondly, it was noted that the pH of the solution slowly rises as the reaction proceeds, and as such, the formation of the undesired hydroxy addition product accelerates. Lowering the pH from the outset, therefore, minimises this undesired side-reaction. Finally, as demonstrated in entry 7, oxygen is required for the reaction to proceed however entry 8 demonstrates that there is no advantage to performing the reaction in an oxygen atmosphere. In fact, such an approach is actually detrimental and almost completely attenuates the reaction with only traces of products detected and the almost quantitative recovery of starting material. This gave us the first inclination that oxygen may be required only in sub-stoichiometric quantities for the putative radical reaction that ensues.

Having established a robust set of conditions that resulted in high yields of the desired product **1**, we were then keen to establish the scope of the reaction with a more diverse set of alkyl halides and acceptors. The results are outlined in Table 2.

It is noteworthy that, in terms of the amount of the alkyl iodide employed, the efficiency of the reactions outlined in Table 2 is generally higher than with other radical chain carriers such as tributyltin hydride where, in order to circumvent



Scheme 1 Initial observations.

Table 1 Optimisation experiments

Entry	Solvent	Atmos.	Time, h	pH	1 ^a , %	2 ^a , %
1	MeOH	Air	32	7	0	70
2	H ₂ O-MeOH (2 : 1)	Air	32	7	78	9
3	MeCN	Air	32	7	Trace	0
4	H ₂ O-MeCN (1 : 3)	Air	32	7	Trace	Trace
5	H ₂ O-MeCN (1 : 1)	Air	32	7	68	Trace
6	H ₂ O-MeCN (2 : 1)	Air	32	7	90	Trace
7	H ₂ O-MeCN (2 : 1)	Ar degassed	32	7	0	0
8	H ₂ O-MeCN (2 : 1)	Stream of O ₂	32	7	Trace	Trace
9	H ₂ O-MeCN (2 : 1)	Air	20	9 ^b	47	53
10	H ₂ O-DMF (2 : 1)	Air	20	2 ^c	74	0
11	H ₂ O-MeCN (2 : 1)	Air	20	7.4 ^d	86	14
12	H ₂ O-MeCN (2 : 1)	Air	20	5 ^c	82	18
13	H ₂ O-MeCN (2 : 1)	Air	20	2 ^c	100	0

^a Isolated yield. ^b pH adjusted with NaOH. ^c pH adjusted with HCl. ^d PBS 7.4 buffer.

competing reduction by Bu₃SnH, multiple equivalents of the alkyl halide are typically employed. Tertiary iodides are also applicable (*e.g.* entry 3) however the high reactivity and poor solubility of accessible tertiary-iodides prevented a more diverse screen at this point. Surprisingly, even some alkyl bromides proved reasonably effective (entry 6) although admittedly, this is far from optimised. Table 2 demonstrates that a wide range of alkyl iodides could be coupled with various electron-deficient acceptors in generally excellent yields. We were also encouraged by entry 10 where an amide with a free N–H can be employed in excellent yields. The conditions employed are more amenable to our future ambitions to manipulate biological molecules than classical tin-mediated radical methods and illustrate a further advantage of the mild electrochemical technique.

With these results in hand, we were keen to undertake some preliminary mechanistic investigations into this reaction. We first turned to cyclic voltammetry (plots available in the ESI†) of the various reactants present in the solution. We discovered that the only species that was redox active at the potentials employed was molecular oxygen which was reduced between –0.7 and –0.8 V (vs. QRE in our system). We then examined the total amount of charge passed for the reaction of isopropyl iodide with phenylvinylsulfone under the optimal conditions in Table 1 (entry 13). The charge–time graph is shown in Fig. 2 and shows a relatively smooth transfer of charge from the start of the reaction to the point where no more sulfone was observed.

We have calculated that for a 1.2 mmol reaction scale (1.44 mmol of alkyl iodide), around 300 C of charge was passed which corresponds to no more than two moles of electrons per mole of alkyl iodide. This is extraordinarily efficient in terms of the amount of electricity used. Given that we know that a small quantity of oxygen is required for a successful reaction, two



Table 2 Exploring the reaction scope

Entry	Halide	Acceptor	Product	Yield ^a , %
1				100
2				82
3				60
4				95 ^b
5				98
6				21 ^c
7				90
8				98
9				96
10				98
11				95
12				99

^a Isolated yield. ^b 3.0 equivalents of iodide employed. ^c Unoptimized.

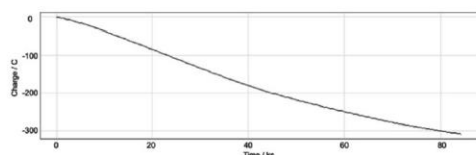
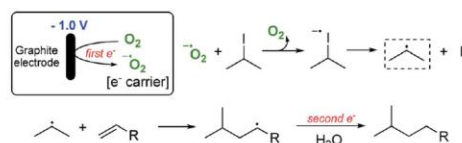


Fig. 2 Charge transferred over the course of the reaction.

general pathways are envisaged to explain the observed reactivity. The first and simplest of these is outlined in Scheme 2.

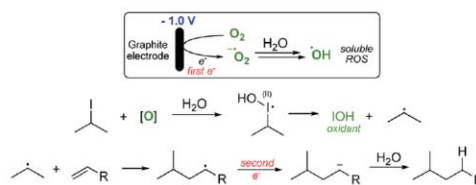
Pathway 1 involves initial reduction of O₂ to generate superoxide which then acts as an electron carrier, transferring the electron to σ* of the C–I bond and liberating O₂ which is



Scheme 2 Proposed electron-transfer pathway 'pathway 1'.

therefore, formally catalytic. This leads to collapse of the subsequent radical anion and the release of the required carbon-centred radical. Pathway 2 (shown in Scheme 3) on the other hand involves initial reduction of O₂ to give a reactive species capable of activating an alkyl iodide, presumably by oxidation. Fragmentation of the unstable I(II) species then occurs to yield the alkyl radical.

With regard to pathway 1, we concluded that this pathway was unlikely to be in operation. Two observations led us to this conclusion; firstly, as mentioned above, cyclic voltammetry of isopropyl iodide (see ESI†) demonstrated that the alkyl halide is not reduced within the redox window of the solvent so it is unlikely that superoxide (which is relatively easily generated) will be a sufficiently powerful reducing agent to deliver an electron to σ* of the C–I bond to effect homolysis. Secondly, entry 3 in Table 1 shows that water is an essential component for successful reaction, again suggesting that more reactive oxygen species are formed as depicted in pathway 2 (Scheme 3). We also considered the possibility that under the acidic conditions employed, the reduction of molecular oxygen to give hydrogen peroxide could also be occurring and therefore this reactive oxygen species could be implicated in the process. In order to ascertain if this was the case, we also performed the reaction in the absence of oxygen but with hydrogen peroxide present. No terminal product was observed in this case. Furthermore, we also examined the addition of iron(II) sulfate to the reaction medium in order to catalyse the formation of hydroxyl radicals from any putative hydrogen peroxide in the solution (the Fenton reaction)²⁵ in the hope that this might accelerate the rate of these reactions. No effect was observed on the reaction and consequently we concluded that hydrogen peroxide was unlikely to be a major player in the main reaction process, although it is possible that traces of H₂O₂ generated *via* initial reduction of aerial O₂ are responsible for initiation of the process.



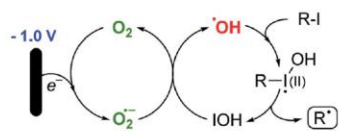
Scheme 3 Proposed 'redox-relay' pathway 2'.

Given the observations outlined above, we believe that pathway 2 is more likely, with the generation of the highly reactive hydroxyl radical as the species responsible for the reaction turnover. Initially we assumed that the iodides were simply being oxidised to give the I(III) iodanes which then undergo reduction to unstable I(II) species that fragment to yield IOH and the alkyl radical. However, given that the reaction is also applicable to some alkyl bromides (entry 7, Table 2), this seems unlikely, since hypervalent bromine reagents are extremely difficult to access under mild oxidative conditions and consequently are not commonly employed in organic synthesis.^{16–18} As such, we needed to consider an alternative reactive species that might be promoting the reaction pathway. As the only likely reactive species capable of activating both bromides and iodides in our solution, we suspected that the hydroxyl radical might be fulfilling this function.

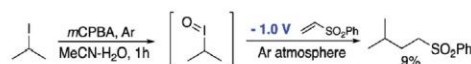
Such a pathway is appealing because the hydroxyl radical is known to be sufficiently reactive to activate organic halides^{19,20} and the differing efficiencies between alkyl bromides and iodides can be easily explained by the accessibility of the lone pairs of the relevant halogen. Furthermore, it is known (particularly in biological systems) that the superoxide radical (or, since these reactions are generally performed under acidic conditions, the hydroperoxyl radical – pK_a 4.88)²¹ reacts with hypohalous acids and hydrogen peroxide to yield hydroxyl radicals.²² A system therefore exists where the alkyl halide is continually activated to form alkyl radicals *via* the two interlocking cycles outlined in Scheme 4.

It is noteworthy that when pure methanol (a known hydroxyl radical scavenger)²³ is used as the reaction solvent (Table 1, entry 1), no reaction is observed until a significant amount of water is added as a co-solvent (Table 1, entry 2). Even then, the reaction rate is significantly attenuated, and the yield falls far short of the optimised conditions. More detailed mechanistic studies will follow.

An obvious question if such a redox relay pathway involving a mutually cooperative interaction between hypohalous acid and superoxide is the fact that hypohalous acid is not present at the beginning of the reaction to initiate the process, how is the reaction initiated? Given that only a trace of the hydroxyl radical is needed to be generated before the redox relay pathway outlined in Scheme 4 can then take over, it is possible that trace amounts of hydrogen peroxide could be formed and then react with superoxide in the uncatalyzed (and slow) Haber–Weiss reaction.²⁴ Alternatively, trace amounts of iodide present in the alkyl halide starting materials could also be responsible since H_2O_2 and iodide under acidic conditions has been suggested as



Scheme 4 Proposed reactive species in the redox relay pathway.



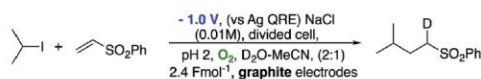
Scheme 5 An intermediate I(III) iodane is unlikely to be a major intermediate.

a source of hydroxyl radicals in iodine-based chemical oscillators.²⁵

In order to further support the mechanistic proposal outlined in pathway 2 and the involvement of a transient hypervalent iodine species, we attempted to emulate the initial oxidation of the alkyl iodide to the iodane species with a classical oxidant in the absence of O_2 followed by exposure of that species to the reducing potential that would allow the radical reaction to occur. Knowing that alkyl iodides can be oxidised to I(III) iodanes by *mCPBA* we accordingly stirred the peracid with isopropyl iodide in an inert atmosphere for 1 h before applying a reducing potential and the addition of phenyl vinyl sulfone. After 18 h, only 9% of the required product was obtained (Scheme 5). The fact that the yield is so poor given that *mCPBA* would be expected to completely oxidise this alkyl iodide to the iodane suggests that the I(III) species is not a major intermediate in the reactive pathway. Interestingly however, others have noted that aryl peracids are sources of the hydroxyl radical^{26,27} and this may explain the low level of conversion observed here.

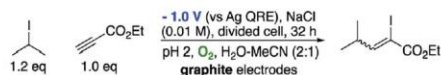
We also wished to demonstrate that the intermediate radical (A in Scheme 3) is reduced by an electron transfer step resulting in an anion which is then quenched by a proton from the aqueous reaction medium rather than a radical hydrogen atom transfer step (most likely from acetonitrile). This was easily achieved by performing the reaction in a D_2O -MeCN mixture as shown in Scheme 6. Performing the reaction in this way led to deuterium incorporation adjacent to the sulfonyl group. To check that the alkyl sulfone was not simply undergoing exchange after the reaction had occurred, we also subjected the undeuterated alkyl sulfone to the reaction conditions for 72 h. No deuterium incorporation was observed.

Now reasonably convinced by our proposed mechanism, we wished to gain more insight into the key electron transfer steps occurring within the pathway. Given that we have already established that only two electrons are ‘consumed’ during the reaction (*i.e.* $2.4 F mol^{-1}$) per mole of iodide, and noting that excess O_2 did not improve (and in fact attenuated) the reaction, we suspected that only a sub-stoichiometric amount of O_2 was required to catalyse the reaction. This was easily demonstrated by again performing the reaction in an inert atmosphere (Ar) and observing that no reaction occurred until a small amount of air (1 mL, *ca.* 0.2 mL O_2) was injected into the system. This



Scheme 6 Demonstration that protonation of a sulfonyl anion occurs from the aqueous medium.





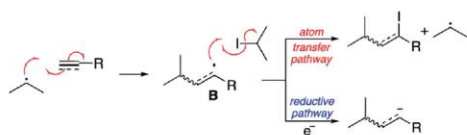
Scheme 7 Intermolecular atom-transfer process.

corresponds to approximately 0.0083 mmol of O₂ or 0.57 mol%. Once this had occurred the reaction proceeded smoothly to completion in 20 h, demonstrating that oxygen is only required in extremely low quantities and suggesting that it is likely to be the mediator in the process.

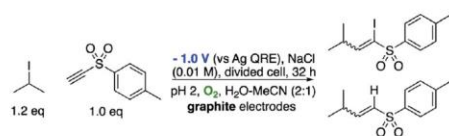
With some understanding of the reaction mechanism and some excellent results (both inter and intramolecular examples) employing alkenes, we were keen to test our methodology with alkynes to discover if they would be suitable partners for intermolecular radical reactions. Consequently, we employed our optimised conditions from Table 1, replacing the alkene acceptor with ethyl propiolate (Scheme 7).

To our surprise, we isolated not the expected reduced addition product, but the addition product as the α -iodo alkene as a 1.2 : 1 mixture of *E* and *Z* isomers. The electrochemical conditions appear to have promoted the atom transfer radical addition (ATRA) reaction in this case. The results are consistent with the experiments of Curran, who achieved the same transformation employing heat and bis-tributyl tin.²⁸ Presumably the mechanism outlined in Scheme 8 is in operation.

We have attributed this observation to the stability of the intermediate radical **B**. In our previous reactions with alkenes the intermediate radical is directly resonance stabilised by the adjacent electron withdrawing group. In the example outlined in Scheme 8 however, the intermediate will be a highly reactive vinyl radical not directly stabilised by the adjacent ester. As such, presumably the rate of iodine atom abstraction is significantly faster than reduction to give a similarly unstabilised vinyl anion. Support for this hypothesis is observed when 4-methylphenyl ethynyl



Scheme 8 Proposed mechanistic pathways.

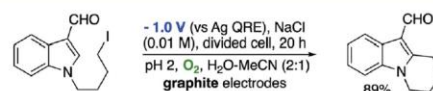


Scheme 9 Competitive atom-transfer vs. reduction pathways.

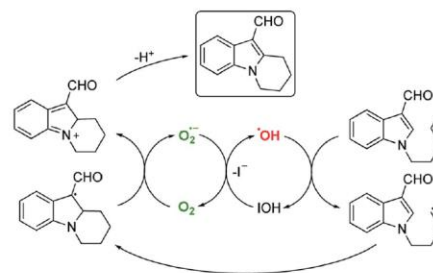
sulfone is employed as the reacting partner (Scheme 9). The product of this reaction is a mixture of the atom transfer reaction and reduction. This is explained by the fact that although still highly reactive, both the vinyl radical and anion obtain some degree of stabilisation *via* $n-\sigma^*$ interactions between the radical or anion and the C-S σ^* orbital.^{29,30} As such in this case, both pathways are competitive in terms of rate.

Finally, with such encouraging intermolecular radical processes in hand we also wanted to examine if our conditions could be applied to redox-neutral intramolecular cyclisations to aromatic systems. Accordingly, we prepared 1-(4-iodobutyl)-1*H*-indole-3-carbaldehyde. Pleasingly, exposure of this molecule to our conditions led to the cyclised, oxidised system in excellent yield (Scheme 10).

Although it is tempting to assume that the oxidative cyclisation would require an excess of molecular oxygen to deliver the observed product, we did not perform this reaction under such conditions but rather using the optimised procedure outlined in Table 1. The rate and efficiency also seemed to be comparable (or better) than the other examples in Table 2 suggesting that adventitious aerial oxygen was not responsible for this observation. In 1991 Bowman suggested a pseudo S_{RN}1 process to explain this phenomenon for tin mediated cyclisations to aryl systems in the absence of any other oxidising agent, where the radical resulting from cyclisation is a powerful single electron donor capable of activating another molecule of iodide.³¹ This explanation was also favoured by Moody for the Bu₃SnH mediated cyclisation of the same frameworks as those outlined in Scheme 10.³² For our system following electrochemical initiation, this would lead to a self-perpetuating combination of three different cycles leading to the oxidised product as illustrated in Scheme 11.



Scheme 10 Redox-neutral cyclisation.



Scheme 11 Likely pathway for redox-neutral cyclisation.



Conclusions

In conclusion, we have described a new electrochemical approach to performing radical reactions, (particularly intermolecular radical reactions) between alkyl iodides and a variety of alkene and alkyne acceptors. The conditions employed are environmentally benign and the yield and efficiency of the reaction often exceeds the classical method employing tin reagents. We have described the reaction mechanism in terms of a 'redox relay' sequence initiated by molecular oxygen. Our work here will provide a framework for the further development of this chemistry to reach other examples where tin reagents were considered the 'gold-standard' for radical reactions.

Conflicts of interest

There are no conflicts of interest to declare.

Acknowledgements

We wish to thank the Leverhulme Trust (RPG-2019-183) for generous financial support of our programme. The authors also gratefully acknowledge Dr D. Macmillan and Dr K. Karu for mass spectrometry and Dr A. Aliev for NMR support.

Notes and references

- G. J. Rowlands, *Annu. Rep. Prog. Chem., Sect. B: Org. Chem.*, 2011, **107**, 19–33.
- P. Renaud and M. P. Sibi, *Radicals in Organic Synthesis*, Wiley-VCH, Weinheim, Germany, 2001, vol. 1 and 2.
- P. A. Baguley and J. C. Walton, *Angew. Chem., Int. Ed.*, 1998, **37**, 3072–3082.
- J. D. Nguyen, E. M. D'Amato, J. M. R. Narayanan and C. R. J. Stephenson, *Nat. Chem.*, 2012, **4**, 854–859.
- B. Schweitzer-Chaput, M. A. Horwitz, E. de Pedro Beato and P. Melchiorre, *Nat. Chem.*, 2019, **11**, 129–135.
- For a review see: M. H. Shaw, J. Twilton and D. W. C. MacMillan, *J. Org. Chem.*, 2016, **81**, 6898–6926.
- E. J. Horn, B. R. Rosen and P. S. Baran, *ACS Cent. Sci.*, 2016, **2**, 302–308.
- C. A. Paddon, F. L. Bhatti, T. J. Donohoe and R. G. Compton, *J. Phys. Org. Chem.*, 2007, **20**, 115–121.
- J. A. Cleary, M. S. Mubarak, K. L. Vieira, M. R. Anderson and D. G. Peters, *J. Electroanal. Chem. Interfacial Electrochem.*, 1986, **198**, 107–124.
- B. Giese, J. A. González-Gómez and T. Witzel, *Angew. Chem., Int. Ed. Engl.*, 1984, **23**, 69–70.
- A. Studer, S. Amerin, F. Schleth and T. Schulte, *J. Am. Chem. Soc.*, 2003, **125**, 5726–5733.
- S. Caddick, J. D. Wilden, H. D. Bush, S. J. Wadman and D. B. Judd, *Org. Lett.*, 2002, **4**, 2549–2551.
- H. Miyabe, M. Ueda, A. Nishimura and T. Naito, *Org. Lett.*, 2002, **4**, 131–134.
- O. Edetanlen-Elliot, R. J. Fitzmaurice, J. D. Wilden and S. Caddick, *Tetrahedron Lett.*, 2007, **48**, 8926–8929.
- W. H. Koppenol, *Free Radical Biol. Med.*, 1993, **15**, 645–651.
- M. Ochiai, Y. Nishi, S. Goto, M. Shiro and H. J. Frohn, *J. Am. Chem. Soc.*, 2003, **125**, 15304–15305.
- M. Ochiai, Y. Nishi, S. Goto, M. Shiro and H. J. Frohn, *Angew. Chem., Int. Ed.*, 2005, **44**, 406–409.
- M. Ochiai, K. Miyamoto, T. Kaneaki, S. Hayashi and W. Nakanishi, *Science*, 2011, **332**, 448–451.
- U. Brühlmann, H. Büchler, F. Marchetti and R. E. Bühler, *Chem. Phys. Lett.*, 1973, **21**, 412–414.
- H. Mohan and K.-D. Asmus, *J. Chem. Soc., Perkin Trans. 1*, 1987, 1795–1800.
- M. Hayyan, M. A. Hashim and I. M. Alnashef, *Chem. Rev.*, 2016, **116**, 3029–3085.
- L. P. Candeias, K. B. Patel, M. R. L. Stratford and P. Wardman, *FEBS Lett.*, 1993, **333**, 151–153.
- V. Můčka, P. Bláha, V. Čuba and J. Červenák, *Int. J. Radiat. Biol.*, 2013, **89**, 1045–1052.
- W. H. H. Koppenol, *Redox Rep.*, 2001, **6**, 229–234.
- D. R. Stanisavljev, M. C. Milenković, M. D. Mojović and A. D. Popović-Bijelić, *J. Phys. Chem. A*, 2011, **115**, 2247–2249.
- T. Katsumi and S. Osamu, *Bull. Chem. Soc. Jpn.*, 1962, **35**, 1678–1683.
- A. Bravo, H.-R. Bjorsvik, F. Fontana, F. Minisci and A. Serri, *J. Org. Chem.*, 1996, **61**, 9409–9416.
- D. P. Curran and D. Kim, *Tetrahedron*, 1991, **47**, 6171–6188.
- S. Wolfe, A. Stolow and L. A. Lajohn, *Tetrahedron Lett.*, 1983, **24**, 4071–4074.
- D. A. Bors and A. J. Streitwieser, *J. Am. Chem. Soc.*, 1986, **108**, 1397–1404.
- W. R. Bowman, H. Heaney and B. M. Jordan, *Tetrahedron*, 1991, **47**, 10119–10128.
- C. J. Moody and C. L. Norton, *Tetrahedron Lett.*, 1995, **36**, 9051–9052.





Cite this: DOI: 10.1039/d1cc03019a

Received 8th June 2021
Accepted 26th July 2021

DOI: 10.1039/d1cc03019a

rsc.li/chemcomm

Mechanistic studies of reactive oxygen species mediated electrochemical radical reactions of alkyl iodides†

Tsz-Kan Ma,* Diyuan Li[†] and Jonathan D. Wilden[†]*

Mechanistic studies of a reactive oxygen species mediated electrochemical radical reaction of alkyl iodides are described. Hydroxyl radicals and ozone are identified to be the active species involved in the formation of alkyl radicals under mildly reducing potential (−1.0 V vs. Ag QRE) in buffered acidic conditions (pH 3.6).

Carbon-centered radicals are important synthetic intermediates in organic synthesis. To date, the generation of alkyl radicals heavily relies on the homolytic cleavage of labile carbon-halogen (C-X) bonds. In particular, *n*-tributyltin hydride and azobisisobutyronitrile (AIBN) mediated radical chain reaction of alkyl halides is the dominant approach to produce predictable C-centered radicals chemoselectively under mild conditions.¹ Although organotin reagents have been proven to be extremely versatile to construct carbon-carbon (C-C) bonds, the substantial toxicity of organotin compounds has limited their large-scale applications. To circumvent this issue, alternative tin-free radical chain reaction initiators such as organoboranes and thiols have been employed but their efficiency and scope are often limited.^{2,3}

Recent advances in photocatalysed processes provides alternative approaches to generate C-centered radicals, representing a significant step to move away from using any toxic organotin reagents.⁴ On the other hand, synthetic organic electrochemistry has also gained popularity as an alternative method to manipulate organic compounds *via* direct addition or removal of electrons to generate reactive radical species.⁵ However, direct electrochemical activation of alkyl halides *via* reduction has limited synthetic utility due to the requirement of highly reducing potentials.

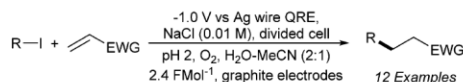
Recently, our group has developed a highly efficient methodology to activate alkyl iodides with the use of air and electricity as the promoters (Scheme 1).⁶ The classic Giese reaction could be carried out electrochemically under mildly reducing

conditions (−1.0 V vs. Ag QRE) in semi-aqueous media with inexpensive graphite electrodes. Molecular oxygen is selectively activated to mediate the radical reactions of alkyl iodides. Herein, we report results of our studies into the mechanism of this intriguing and novel reaction sequence.

We first sought to determine the active initiator derived from molecular oxygen which starts the reaction sequence. According to our previous studies, the presence of molecular oxygen and water is essential for the reaction to occur.⁶ We originally postulated that hydroxyl radicals were involved in the activation of the iodide, however, subsequent experiments have suggested that an alternative mediator must also be involved. Accordingly, we wondered if the agent was ozone. To test our hypothesis that ozone could be the oxidant to activate the alkyl iodide, a sample of neat isopropyl iodide was subjected to a constant stream of ozone and it quickly turned brown. After that, this sample was exposed to a reducing potential (constant potential, 1.0 V vs. Ag wire quasi-reference electrode, graphite rod working electrode, divided cell) in an acidic acetonitrile-water solution (pH 2) containing phenyl vinyl sulfone under an inert atmosphere saturated with argon (Scheme 2). Gratifyingly, the ozonised alkyl iodide was fully consumed and reacted with phenyl vinyl sulfone to give the corresponding alkyl sulfone (74%). It is postulated that ozonation of isopropyl iodide produced an unstable trioxide intermediate, which decomposes into the corresponding alkyl radical, IO[•] radical and molecular oxygen to initiate the radical reaction.^{7,8} The proposed trioxide intermediate is analogous to the reaction between aqueous ozone with halide anions as well as alkanes.^{7–10} The necessity of molecular oxygen and water in the reaction vessel could be explained by the requirement of ozone production electro-catalytically. The formation of

Department of Chemistry, University College London, 20 Gordon Street, London, WC1H 0AJ, UK. E-mail: j.wilden@ucl.ac.uk

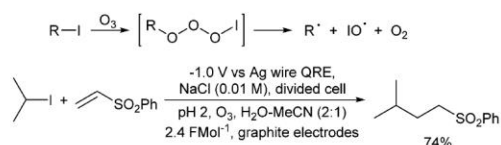
† Electronic supplementary information (ESI) available. See DOI: 10.1039/d1cc03019a



Scheme 1 Electrochemical Giese reaction.



Communication

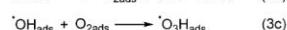
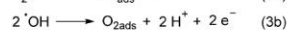
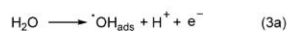


Scheme 2 Reaction between ozonised alkyl iodide and phenyl vinyl sulfone.

ozone relies on the reaction between adsorbed hydroxyl free radicals and molecular oxygen at the anode (eqn (3a)–(3d)) as direct oxidation of water to ozone requires a much higher potential ($E^\circ = 1.51$ V) and is unlikely to occur under the operating potential (Scheme 3).¹¹ To further validate this hypothesis, excess ethyl vinyl ether was added to the anodic chamber to quench the ozone generated from the anode where another sample of isopropyl iodide and phenyl vinyl sulfone were subjected to the standard conditions in the cathodic chamber. Indeed, addition of ethyl vinyl ether has completely terminated the reaction and the substrates are fully recovered. In addition, subjecting anethole to the reaction condition at the anodic chamber resulted in the formation of the corresponding 4-methoxybenzaldehyde (2%) and 1-(4-methoxyphenyl)propane-1,2-diol (30%).

The electrochemical radical reaction of alkyl iodide could also be extended to intramolecular reductive cyclisation (Table 1). When alkyl iodide **1** was subjected to a mild reducing potential (constant potential, 1.0 V vs. Ag wire quasi-reference electrode, graphite rod working electrode, divided cell) in an acidified MeCN-H₂O (1:1, pH 1) solution, it was reductively cyclised into the corresponding pyrrolidine **2** (31%) with *N*-allyltosylamide **3** (23%) as a by-product (Table 1, entry 1). *N*-Allyltosylamide **3** is likely to be produced *via* β -elimination from an anionic intermediate, terminated by the abstraction of the hydrogen atom from the solvent.¹² The effect of pH was also examined by adjusting the pH of the solvent with various buffer solutions. It was found that optimal conversion occurred (Table 1, entry 2) at pH 3.6 and no reaction occurred at pH 7.

To further investigate the role of reactive oxygen species in the reaction, sodium terephthalate was used as the molecular fluorescence probe for the detection of hydroxyl radicals.¹³ Sodium terephthalate is a non-fluorescent compound that would react with hydroxyl radicals to form a fluorescent aromatic hydroxylated product, namely sodium 2-hydroxyterephthalate, that is known to show a characteristic emission at 430 nm.¹⁴ Therefore, sodium terephthalate was introduced to the reaction mixture under different conditions to detect the presence of hydroxyl radicals.

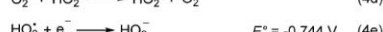
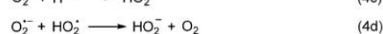
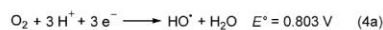


Scheme 3 Electro-catalytic ozone production.

Table 1 Reductive cyclisation of alkyl iodide **1**

Entry	Solvent	pH	Time, h	2 , ^a %	3 , ^a %
1	MeCN-H ₂ O (1:1)	1 ^b	24	31	23
2	MeCN-H ₂ O (1:1)	3.6 ^c	6	40	37
3	MeCN-H ₂ O (1:1)	5.7 ^c	24	Trace	33
4	MeCN-H ₂ O (1:1)	7 ^d	24	N/R ^e	N/R ^e

^a Isolated yield. ^b pH adjusted with HCl. ^c pH adjusted with acetate buffer. ^d pH adjusted with phosphate buffer. ^e Alkyl iodide **1** was fully recovered.



Scheme 4 Formation of reactive oxygen species.

First, a classic Fenton reaction was carried out in the presence of this molecular probe to validate this approach.¹⁵ An aliquot of the reaction mixture was extracted, and the fluorescence emission was recorded. By comparing that emission spectrum (Fig. 1a, blue curve) with the emission spectrum of sodium terephthalate (Fig. 1a, black curve), hydroxyl radicals were detected, giving rise to the intense fluorescence emission at 430 nm. By applying this technique to the cathodic chamber of the reaction vessel where radical cyclisation of alkyl iodide **1** occurred, the same emission was observed (Fig. 1a, red curve), confirming the presence of hydroxyl radicals in the reaction mixture.

With this encouraging result in hand, the focus was switched to examine the origin of hydroxyl radicals in the reaction vessel (Fig. 1b). Sodium terephthalate was added to a solution of acetonitrile-water (pH 3.6) with sodium chloride as the electrolyte and exposed to a mild reducing potential (constant potential, 1.0 V vs. Ag wire quasi-reference electrode, graphite rod working electrode, divided cell). It is observed that hydroxyl radicals are present at both the anodic and cathodic chambers, but they are more concentrated at the cathodic chambers relatively. The relative low concentration of hydroxyl radicals at the anodic chamber is consistent with the fact that only small amount of adhered hydroxyl radicals are generated at the anode to facilitate the electro-catalytic ozone generation process.¹⁶ The formation of hydroxyl radicals at the cathodic chamber is possible *via* various one-electron redox reactions (eqn (4a)–(4g)) (Scheme 4) under the operating potential.^{17–19} The operative reactions generate oxygenic



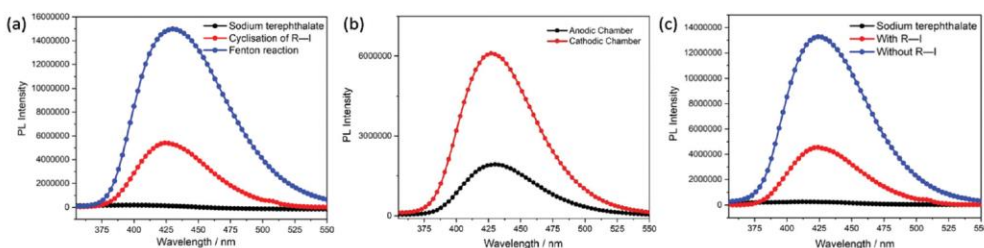


Fig. 1 Emission spectra of sodium 2-hydroxyterephthalate under different reaction conditions.

radicals which would lead to the formation of hydrogen peroxide and homolysed to form hydroxyl radicals. This would also indicate that a buffered acidic solvent system would be essential for the steady formation of hydroxyl radicals at the cathodic chamber to facilitate the radical reactions of alkyl iodides. Moreover, a low pH environment would also inhibit the auto-decomposition of hydrogen peroxide, another reactive oxygen species that could homolyse into hydroxyl radicals. At higher pH, the decomposition of hydrogen peroxide into molecular oxygen and water would dominate, limiting the supply of hydroxyl radicals and, therefore, lead to no reactivity.²⁰

Lastly, the effect of alkyl iodide on the consumption of hydroxyl radicals was examined. Control experiments have shown that the relative concentration of hydroxyl radicals decreases when alkyl iodide **1** is present (Fig. 1c) and indicated that hydroxyl radicals are involved directly in facilitating the radical cyclisation of alkyl iodide **1**.

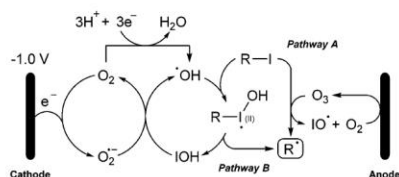
Following with the results of these experiments, we propose the following mechanism for the generation of alkyl radicals (Scheme 5). Two productive reaction pathways are responsible for the oxidation of alkyl iodide. The reaction is initiated by the generation of ozone at the anode *via* an electro-catalytic process and the resulting ozone is reacted with the alkyl iodide in the cathodic chamber, by slow diffusion in the closed divided cell *via* the pressure equalizer channel as well as the semiporous sintered glass divider. Reaction between ozone and alkyl iodide generated an unstable trioxide intermediate that subsequently fragment into the corresponding alkyl radical, IO[•] radical and molecular oxygen. The generated IO[•] radicals lead to the accumulation of hypoiodous acid that is known to react with superoxide radicals to yield highly reactive hydroxyl radicals to oxidise more alkyl iodides into the corresponding unstable I(II)

species that fragment to yield hypoiodous acid and alkyl radicals.²¹ As a result, alkyl iodides could be activated by both productive pathways. Furthermore, additional redox reactions of molecular oxygen and hydrogen peroxide would also supply more hydroxyl radicals to facilitate the radical reaction of alkyl iodides.

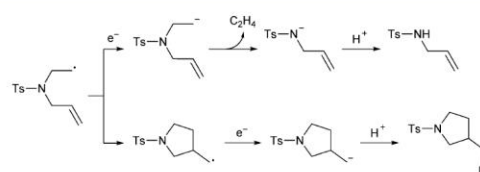
The reactivity of alkyl iodide **1** could be rationalised as follows (Scheme 6): once the primary radical is formed, there are two competing reaction pathways, which lead to the formation of pyrrolidine and *N*-allyltsylamide. When the primary alkyl radical is reduced by the electrode, the resulting anion would then undergo rapid elimination to produce ethene and an anionic intermediate, which could be protonated to give *N*-allyltsylamide. Another pathway involves the reaction of the primary radical with the allyl group *via* an intramolecular pathway to give a cyclised primary radical intermediate, which can then be reduced by the electrode to the corresponding anion to be protonated and form the pyrrolidine.

In conclusion, these experimental results indicate that under the standard electrochemical conditions, alkyl iodide are first ozonolysed to yield an unstable intermediate that fragments into the corresponding alkyl and IO radicals as well as molecular oxygen. This activates a superoxide radicals and hypoiodous acid mediated 'redox relay' reaction sequence to oxidise more alkyl iodides into the corresponding unstable I(II) species to produce more alkyl radicals. The use of sodium terephthalate as a fluorescence molecular probe provided insight to the role of hydroxyl radicals in this reaction sequence. Further studies on other radical reactions with this electrochemical approach are ongoing in our laboratory.

We wish to thank the Leverhulme Trust (RPG-2019-183) for generous financial support of our programme. The authors also



Scheme 5 Proposed reaction mechanism for the generation of alkyl radicals.



Scheme 6 Reductive cyclisation of alkyl iodide **1**.



gratefully acknowledge Dr D. MacMillan and Dr K. Karu for mass spectrometry and Dr A. Aliev for NMR support.

Conflicts of interest

There are no conflicts to declare.

Notes and references

- 1 G. J. Rowlands, *Annu. Rep. Prog. Chem., Sect. B: Org. Chem.*, 2011, **107**, 19–33.
- 2 V. Darmency and P. Renaud, *Radicals in Synthesis I*, Springer-Verlag, Berlin/Heidelberg, 2006, vol. 263, pp. 71–106.
- 3 A. Studer and S. Amrein, *Synthesis*, 2002, 835–849.
- 4 S. Crespi and M. Fagnoni, *Chem. Rev.*, 2020, **120**, 9790–9833.
- 5 (a) M. Yan, Y. Kawamata and P. S. Baran, *Chem. Rev.*, 2017, **117**, 13230–13319; (b) D. Pollok and S. R. Waldvogel, *Chem. Sci.*, 2020, **11**, 12386–12400.
- 6 D. Li, T.-K. Ma, R. J. Scott and J. D. Wilden, *Chem. Sci.*, 2020, **11**, 5333–5338.
- 7 Y. Sakamoto, A. Yabushita, M. Kawasaki and S. Enami, *J. Phys. Chem. A*, 2009, **113**, 7707–7713.
- 8 T. M. Hellman and G. A. Hamilton, *J. Am. Chem. Soc.*, 1974, **96**, 1530–1535.
- 9 S. W. Hunt, M. Roeselová, W. Wang, L. M. Wingen, E. M. Knipping, D. J. Tobias, D. Dabdub and B. J. Finlayson-Pitts, *J. Phys. Chem. A*, 2004, **108**, 11559–11572.
- 10 Q. Liu, L. M. Schurter, C. E. Muller, S. Aloisio, J. S. Francisco and D. W. Margerum, *Inorg. Chem.*, 2001, **40**, 4436–4442.
- 11 Y.-H. Wang and Q.-Y. Chen, *Int. J. Electrochem.*, 2013, **2013**, 1–7.
- 12 A. Hosomi, M. Hojo, J. Yoshizawa, Y. Funahashi, R. Okada, S. Nakamura and J. Tateiwa, *Heterocycles*, 1998, **49**, 85.
- 13 A. Gomes, E. Fernandes and J. L. F. C. Lima, *J. Biochem. Biophys. Methods*, 2005, **65**, 45–80.
- 14 B. Tang, L. Zhang and Y. Geng, *Talanta*, 2005, **65**, 769–775.
- 15 H. J. H. Fenton, *J. Chem. Soc., Trans.*, 1894, **65**, 899–910.
- 16 Y.-H. Wang and Q.-Y. Chen, *Int. J. Electrochem.*, 2013, **2013**, 1–7.
- 17 J.-M. Noël, A. Latus, C. Lagrost, E. Volanschi and P. Hapiot, *J. Am. Chem. Soc.*, 2012, **134**, 2835–2841.
- 18 M. H. Shao, P. Liu and R. R. Adzic, *J. Am. Chem. Soc.*, 2006, **128**, 7408–7409.
- 19 S. C. Perry, D. Pangotra, L. Vieira, L. I. Csepei, V. Sieber, L. Wang, C. Ponce de León and F. C. Walsh, *Nat. Rev. Chem.*, 2019, **3**, 442–458.
- 20 L. Szpyrkowicz, C. Juzzolino and S. N. Kaul, *Water Res.*, 2001, **35**, 2129–2136.
- 21 L. P. Candeias, K. B. Patel, M. R. L. Stratford and P. Wardman, *FEBS Lett.*, 1993, **333**, 151–153.

